

**PHASE REDISTRIBUTION AND SEPARATION OF GAS-
LIQUID FLOWS IN AN EQUAL-SIDED IMPACTING TEE
JUNCTION WITH A HORIZONTAL INLET AND
INCLINED OUTLETS**

by

Moftah A. Mohamed

A Thesis submitted to the Faculty of Graduate Studies
The University of Manitoba
in Partial Fulfillment of the Requirements for the Degree of

DOCTOR OF PHILOSOPHY

Department of Mechanical and Manufacturing Engineering
University of Manitoba
Winnipeg, Manitoba

Copyright© 2012 by Moftah A. Mohamed

*I dedicate this work
To my dad and my mom
My wonderful sons, Anas and reda
and to my wonderful daughters, Nour and Huda*

*Finally, I reserve the biggest thank you for my Wife, Karima,
who has supported me throughout this adventure and
continues to be an unending source of love and support.*

ABSTRACT

Phase-redistribution and full-phase separation data were generated for two-phase (air-water) flow splitting at an equal-sided impacting tee junction with a horizontal inlet and inclined outlets. The flow loop incorporated a tee junction machined in an acrylic block with the three sides having an equal diameter of 13.5 ± 0.1 mm I.D. Both sets of experiments were conducted at a nominal pressure (P_s) of 200 kPa (abs) and near-ambient temperature (T_s).

The operating conditions for the phase-redistribution experiments were as follows: inlet superficial liquid velocities (J_{L1}) ranging from 0.01 to 0.18 m/s, inlet qualities (x_1) ranging from 0.1 to 0.9, mass split ratios (W_3/W_1) from 0 to 1.0, and outlet inclination angles ranging from horizontal to vertical. These inlet conditions corresponded to inlet flow regimes of stratified, wavy, and annular. Phase-redistribution data revealed that the redistribution of phases depended on the inlet conditions, the mass split ratio at the junction, and the inclination angle of the outlets. The magnitude of the inclination effect was dependent on the inlet flow regime. The phase redistribution in stratified flow was very sensitive to the outlet angle and full separation could be achieved at angles as low as 0.7° . Wavy flow was less sensitive to the outlet angle and annular flow was even less sensitive to the outlet angle.

The capability of a single impacting tee junction to perform as a full phase separator has been examined. Experimental data were obtained for the limiting inlet conditions under which full separation was attainable at various outlet inclinations (θ) of 2.5° , 7.5° ,

15°, 30°, 60°, 75°, and 90°. Full separation data have shown that a single impacting tee junction can perform as a full-phase separator for some inlet conditions. Flow phenomena near the limiting conditions were observed and a simple correlation based on the similarity between these flow phenomena and the phenomenon of liquid entrainment in small upward branches was developed. This correlation was capable of accurate prediction of the data in terms of magnitude and trend.

ACKNOWLEDGEMENTS

I would first like to express my gratitude to my supervisors Prof. H. M. Soliman and Prof. G. E. Sims. Their insight and guidance proved invaluable in the pursuit of new ideas and in the completion of this thesis.

My appreciation also goes to the technical staff, Mr. John Finken and Mr. Irwin Penner for their expertise and help in constructing the test facility.

Many thanks also go to my teachers, friend, and colleagues; I make special mention of Amr Elazhary, who has been an invaluable help throughout.

The financial support provided by the Natural Sciences and Engineering Research Council of Canada (NSERC), the Post Graduate Scholarship funded by the Libyan government, Teaching Assistantships awarded by the Department of Mechanical and the Manufacturing Engineering, and lectureships awarded by the International College of Manitoba at the University of Manitoba are gratefully acknowledged.

TABLE OF CONTENTS

ABSTRACT.....	iii
ACKNOWLEDGMENTS.....	v
TABLE OF CONTENTS.....	vi
LIST OF FIGURES.....	viii
LIST OF TABLES.....	xi
NOMENCLATURE.....	xiii
1. INTRODUCTION.....	1
2. LITERATURE REVIEW.....	8
2.1 Overview.....	8
2.2 Phase Redistribution in Branching Tee Junctions	9
2.2.1 Horizontal Equal-Sided Junctions.....	9
2.2.2 Horizontal Junctions with an Inclined Branch.....	13
2.2.3 The Use of Branching Junctions as a Phase Separator.....	19
2.3 Phase Redistribution in Impacting Tee Junctions.....	22
2.3.1 Horizontal Equal-Sided Junctions.....	22
2.3.2 Junctions with a Vertical Upward Inlet.....	32
2.4 Conclusion Remarks.....	34
3. EXPERIMENTAL TEST FACILITY AND PROCEDURE	36
3.1 Introduction.....	36
3.2 Experimental Test Facility.....	36
3.2.1 Air-Water Loop.....	36
3.2.2 Test Section.....	40
3.2.3 Lifting and Rotating Mechanisms.....	42
3.2.4 Mixer	44
3.2.5 Separation Tanks.....	44
3.2.6 Instrumentation.....	47
3.3 Phase-Redistribution Experiments	51
3.3.1 Experimental Procedure.....	51
3.3.2 Reduction of Phase Distribution Data.....	53
3.4 Full-Separation Experiments.....	54
3.4.1 Experimental Procedure.....	54
3.4.2 Recording of Full-Separation Data.....	55
3.5 Effect of Outlet Length.....	56

3.5.1	Introduction.....	56
3.5.2	Procedure for Phase-Redistribution Experiments with Short Outlets	57
3.5.2	Procedure for Full-Separation Experiments with Short Outlets.....	58
4.	RESULTS AND DISCUSSION.....	59
4.1	Data Range.....	59
4.2	Measurement Uncertainty.....	63
4.3	Test Loop Symmetry and Reliability.....	64
4.4	Phase-Redistribution Data.....	67
4.4.1	Overview.....	67
4.4.2	Data of the Stratified Flow Regime	67
4.4.3	Data of the Wavy Flow Regime	69
4.4.4	Data of the Annular Flow Regime.....	71
4.4.5	Discussion of the Phase-Split Mechanism.....	74
4.5	Observed Flow Regimes in the Outlets.....	78
4.6	Full Phase Separation.....	83
4.6.1	Full-Separation Data.....	83
4.6.2	Visual Observation of Flow Phenomena.....	83
4.6.3	Correlation of Full-Separation Data.....	89
4.7	Tee Junction with Short Outlets.....	95
4.7.1	Phase-Redistribution Data.....	95
4.7.2	Full-Separation Data	97
5.	CONCLUSIONS AND RECOMMENDATIONS.....	99
5.1	Conclusions	99
5.2	Recommendations for Future Work.....	100
	REFERENCES.....	102
	APPENDICES	
A.	CALIBRATION OF THE MEASURING DEVICES.....	112
B.	PHASE-REDISTRIBUTION AND FULL-SEPARATION DATA.....	124
C.	EXPERIMENTAL UNCERTAINTY.....	162

LIST OF FIGURES

Figure	Description	Page
1.1	Relevant parameters for two-phase flow in an impacting tee junction with a horizontal inlet and inclined outlets.....	4
1.2	Schematic representation of how phase-redistribution data of an impacting tee junction are presented (a) horizontal inlet and horizontal outlets, (b) horizontal inlet and inclined outlets.....	6
3.1	Schematic diagram of the test loop.....	37
3.2	Test loop with a horizontal junction.....	38
3.3	Test loop with an inclined junction.....	38
3.4	Top view of the test section.....	41
3.5	Schematic diagram of the lifting and rotating mechanisms where the system appears in the horizontal position.....	43
3.6	Schematic of the two-phase mixer; slightly modified from El-Shaboury (2005).....	45
3.7	Details of a separation tank; slightly modified from El-Shaboury (2005).....	46
3.8	Tee-junction with short outlets.....	58
4.1	Inlet conditions for phase-redistribution experiments plotted on the Mandhane et al. (1974) flow-regime map.....	61
4.2	Illustration of test-loop symmetry for data groups St1, Wa2, and An3 with a horizontal inlet and horizontal outlets.....	65
4.3	Comparison between the present data of St1, Wa2, and An2 and similar data from El-Shaboury (2005) at $P_s = 150$ kPa.....	66
4.4	Phase-redistribution data for stratified flow (St1).....	68
4.5	Phase-redistribution data for stratified flow (St2).....	68
4.6	Phase-redistribution data for wavy flow (Wa1).....	70
4.7	Phase-redistribution data for wavy flow (Wa2).....	70
4.8	Phase-redistribution data for annular flow (An1).....	72
4.9	Phase-redistribution data for annular flow (An2).....	72
4.10	Phase-redistribution data for annular flow (An3).....	73

4.11	Effect of J_{G1} on the phase split at $J_{L1} = 0.04$ m/s and $\theta = 5.0^\circ$	76
4.12	Effect of J_{G1} on the phase split at $J_{L1} = 0.04$ m/s and $\theta = 45.0^\circ$	76
4.13	Effect of J_{L1} on the phase split at $J_{G1} = 40$ m/s and $\theta = 30.0^\circ$	77
4.14	Effect of J_{L1} on the phase split at $J_{G1} = 10$ m/s and $\theta = 30.0^\circ$	77
4.15	Comparison between the observed flow regimes in Outlet 3 at 5° downward inclination and the map of Shoham (1982).....	79
4.16	Comparison between the observed flow regimes in Outlet 3 at 30° downward inclination and the map of Shoham (1982).....	80
4.17	Comparison between the observed flow regimes in Outlet 3 at 90° downward inclination and the map of Shoham (1982).....	80
4.18	Comparison between the observed flow regimes in Outlet 2 at 5° upward inclination and the map of Shoham (1982).....	81
4.19	Comparison between the observed flow regimes in Outlet 2 at 30° upward inclination and the map of Shoham (1982).....	82
4.20	Comparison between the observed flow regimes in Outlet 2 at 90° upward inclination and the map of Shoham (1982).....	82
4.21	Limiting conditions for full separation at various outlet inclinations plotted on the flow-regime map of Mandhane et al. (1974).....	84
4.22(a)	Observed flow phenomena at $\theta = 7.5^\circ$, $J_{L1} = 0.05$ m/s, and $J_{G1} = 1.6$ m/s (Type A before entrainment).....	85
4.22(b)	Observed flow phenomena at $\theta = 7.5^\circ$, $J_{L1} = 0.05$ m/s, and $J_{G1} = 1.75$ m/s (Type A after entrainment).....	86
4.23(a)	Observed flow phenomena at $\theta = 90^\circ$, $J_{L1} = 0.025$ m/s, and $J_{G1} = 5.1$ m/s (Type B before entrainment).....	86
4.23(b)	Observed flow phenomena at $\theta = 90^\circ$, $J_{L1} = 0.025$ m/s, and $J_{G1} = 5.6$ m/s (Type B after entrainment).....	87
4.24(a)	Observed flow phenomena at $\theta = 90^\circ$, $J_{L1} = 0.13$ m/s, and $J_{G1} = 0.5$ m/s (Type C full separation before ntrainment).....	88
4.24(b)	Observed flow phenomena at $\theta = 90^\circ$, $J_{L1} = 0.17$ m/s, and $J_{G1} = 0.5$ m/s (Type C churning region in Side 2 before entrainment).....	88
4.25	Relevant parameters for liquid entrainment in upward branches	90
4.26	Comparison between the data of Franca and Lahey (1992) and the model of Taitel and Dukler (1976).....	92
4.27	Values of C_1 in Eq. (4.1) with $C_2 = 0.4$	92
4.28	Comparison between the experimental data and the predictions from Eq. (1) with $C_2 = 0.4$ and C_1 from Fig. 4.27.....	93
4.29	Quantitative comparison between experimental and predicted values of	

	J_{G1} at the same J_{L1}	94
4.30	Comparison between phase-redistribution data from (St1) obtained with long outlets and data obtained with short outlets.....	95
4.31	Comparison between phase-redistribution data from (Wa2) obtained with long outlets and data obtained with short outlets.....	96
4.32	Comparison between phase-redistribution data from (An2) obtained with long outlets and data obtained with short outlets.....	96
4.33	Full-separation data with short outlets plotted on the Mandhane et al. (1974) flow-regime map	98

LIST OF TABLES

Table Number	Description	Page
2.1	References on phase redistribution in equal-sided branching tee junctions with a horizontal inlet and horizontal outlets.....	10
2.2	References on phase redistribution in branching junctions with a horizontal inlet and inclined branch.....	14
2.3	References on phase-redistribution in impacting junctions with a horizontal inlet and horizontal outlets.....	23
2.4	References on phase redistribution in impacting junctions with a vertical upward inlet and horizontal outlets.....	33
3.1	Specifications and duty of the air-flow-measurement instruments.....	48
3.2	Specifications and duty of the water-flow-measurement instruments...	49
3.3	Specifications and duty of the pressure-measurement instruments.....	50
4.1	Ranges of operating conditions for phase-redistribution experiments...	60
4.2	Ranges of operating conditions for full-separation experiments.....	62
A1.1	Calibration data of pressure gauge No.1.....	113
A1.2	Calibration data of pressure gauge No. 2.....	113
A1.3	Calibration data of pressure gauge No. 3.....	113
A1.4	Calibration data of pressure gauge No. 4.....	113
A1.5	Calibration data of pressure gauge No. 5.....	114
A1.6	Calibration data of pressure gauge No. 6.....	114
A1.7	Calibration data of pressure gauge No. 7.....	114
A1.8	Calibration data of pressure gauge No. 8.....	114
A2.1	Calibration data of air rotameter AI-1.....	117
A2.2	Calibration data of air rotameter AI-2.....	117
A2.3	Calibration data of air rotameter AI-3.....	117
A2.4	Calibration data of air rotameter AO2-1.....	117
A2.5	Calibration data of air rotameter AO2-2.....	118
A2.6	Calibration data of air rotameter AO2-3.....	118
A2.7	Calibration data of air rotameter AO2-4.....	118
A2.8	Calibration data of air rotameter AO3-1.....	118
A2.9	Calibration data of air rotameter AO3-2.....	119

A2.10	Calibration data of air rotameter AO3-3.....	119
A2.11	Calibration data of air rotameter AO3-4.....	119
A2.12	Calibration data of water rotameter WI-1.....	119
A2.13	Calibration data of water rotameter WI-2.....	120
A2.14	Calibration data of water rotameter WI-3.....	120
A2.15	Calibration data of water rotameter WO2-1.....	120
A2.16	Calibration data of water rotameter WO2-2.....	120
A2.17	Calibration data of water rotameter WO2-3.....	121
A2.18	Calibration data of water rotameter WO2-4.....	121
A2.19	Calibration data of water rotameter WO3-1.....	121
A2.20	Calibration data of water rotameter WO3-2.....	121
A2.21	Calibration data of water rotameter WO3-3.....	122
A2.22	Calibration data of water rotameter WO3-4.....	122
A3.1	Calibration data of the air thermocouples.....	122
A3.2	Calibration data of the water thermocouples.....	123
B1	Phase-redistribution data.....	124
B2	Phase-redistribution mass-flow rate data.....	142
B3	Full-separation data.....	157
C1	Uncertainty intervals for phase-redistribution data.....	163
C2	Uncertainty intervals for full-separation data.....	173

NOMENCLATURE

Symbol	Description	Units
A	Cross-sectional area of the pipe	m^2
C_1	Constant in the full-separation correlations	-
C_2	Constant in the full-separation correlations	-
D	Diameter	m
F_{G3}	Fraction of inlet gas exiting through Outlet 3 ($= W_{G3}/W_{G1}$)	-
F_{L3}	Fraction of inlet liquid exiting through Outlet 3 ($= W_{L3}/W_{L1}$)	-
Fr_G	Gas Frude number	-
g	Gravitational acceleration	m/s^2
h_G	Gas height in the inlet pipe	m
J_G	Superficial gas velocity	m/s
J_L	Superficial liquid velocity	m/s
P_s	Test-section pressure	Pa
T_s	Temperature at the tee junction inlet	$^{\circ}C$
W	Total mass-flow rate	kg/s
W_G	Gas mass-flow rate	kg/s
W_L	Liquid mass-flow rate	kg/s
x_i	Quality, $i = 1, 2,$ and 3	-
α	Void fraction	-
μ_G	Gas viscosity	$Pa.s$
μ_L	Liquid viscosity	$Pa.s$
ρ_G	Gas density	kg/m^3
ρ_L	Liquid density	kg/m^3
θ	Outlet angle of inclination	-
Subscripts		
1	Inlet	
2	Outlet 2	
3	Outlet 3	

CHAPTER 1

INTRODUCTION

Two-phase flow passing through tee junctions is relevant to many industrial systems including power, chemical processes, nuclear energy, and hydrocarbon production industries. Tee junctions are often a necessary feature in the networks used to distribute two-phase flow in these industrial facilities. These junctions are constructed from off-the-shelf piping components. They require no moving parts, no periodic adjustments, and little or no maintenance throughout their life cycle. Junctions may be used either to combine two inlet streams into one outlet stream (combining tees) or to divide one inlet stream into two outlet streams (dividing tees). For the case of impacting tees, the three sides of the junction may have different orientations between two limiting positions: vertically upward and vertically downward. In the present investigation, the focus is on an impacting tee junction with a horizontal inlet and inclined outlets over the entire range from horizontal to vertical.

When two phases flowing in a pipe encounter a dividing tee junction, almost inevitable maldistribution of the phases takes place between the outlets. This unpredictable nature of splitting of the two phases between the junction outlets can have a major effect on the behavior of equipment downstream from the junction. Severe maldistribution of the phases can lead to all of the liquid flowing into one outlet while in other conditions all the gas may flow into the same outlet. One example of this is the route preference of liquid condensate during what is called enhanced oil recovery (EOR), where steam is used to lower the viscosity of residual oil in the reservoir. Steam from the

main supply station is distributed to all injection points via tees. External cooling and pressure drop along the pipe network causes the appearance of two-phase flow. The flow of all steam condensate in one direction after passing through a tee junction reduces the effectiveness of the oil recovery performance. A similar effect was reported by Oranje (1973), who investigated the route preference of liquid condensate during the transport of natural gas in natural-gas transportation pipeline networks.

Apart from the cases where phase maldistribution in tee junctions is a design problem, there are examples where this phenomenon has been used to advantage. In a wide range of industrial processes where two-phase flow occurs there is a need to separate the different phases. Traditionally, this is done with large vessels using gravity as the means of separation. Gravity separators are large in size with the associated problems of weight and high operating costs. Research has indicated that pipe junctions may provide a possible alternative. Azzopardi et al. (2002) demonstrated the use of a tee-junction-based separator that has operated successfully within an operational plant. The problem faced by the plant operator was that only part of the liquid from the reactor flashed to vapor after passing through a valve. Therefore the flow reaching the distillation column was a mixture of liquid and vapor, reducing the column efficiency. A tee junction was installed and used as a partial phase separator allowing the liquid-rich stream and gas-rich stream to be fed into different points of the distillation column. The standard solution to this problem would be to install a gravity separator. This would be expensive and require a large space to install.

Bos and du Chatinier (1987) reviewed some of the applications in which simple tee junctions are used for gas-liquid separation in the so called multi-bottle slug catchers used

in offshore oil and gas production where a two-phase flow is divided in a series of tee junctions into a number of large-diameter pipes at small downward inclination. Each pipe contains a tee junction with one vertically upward outlet used to withdraw the majority of gas. All gas outlets are combined together in a manifold, and a similar arrangement is made for the liquid.

The division of two-phase flow in tee junctions depends on many variables including: junction geometry (i.e., equal-sided, reduced-size arm, symmetric or asymmetric), junction orientation (horizontal or inclined), inlet conditions (inlet flow rate and inlet quality), mass split ratio between the two outlets, system pressure, system temperature, and the properties of the fluids involved. The large number of influencing parameters has contributed to the fact that no general method is available to predict the phase redistribution under all possible operating conditions.

Figure 1.1 shows a schematic diagram of an equal-sided impacting tee junction with a horizontal inlet, and outlets inclined at an angle θ from the horizontal. Superscripts 1, 2, and 3 are used throughout to represent quantities in the inlet, Outlet 2, and Outlet 3 respectively. Outlet 2 is the outlet where the flow is in the upward direction and the Outlet 3 is the outlet where the flow is in the downward direction. A two-phase mixture enters through the inlet side with a gas mass flow rate W_{G1} and a liquid mass flow rate W_{L1} . The total inlet mass flow rate is W_1 , where $W_1 = W_{G1} + W_{L1}$, and the inlet quality is x_1 , where $x_1 = W_{G1}/W_1$. The inlet mass flow rate (W_1) is divided at the junction into two streams with mass flow rates W_2 and W_3 , where $W_1 = W_2 + W_3$. The flow in Outlet 2 consists of a gas component with a mass flow rate W_{G2} and a liquid component with a mass flow rate W_{L2} and thus, $W_2 = W_{G2} + W_{L2}$. The quality in Outlet 2 is x_2 , where $x_2 = W_{G2}/W_2$. Similarly, the

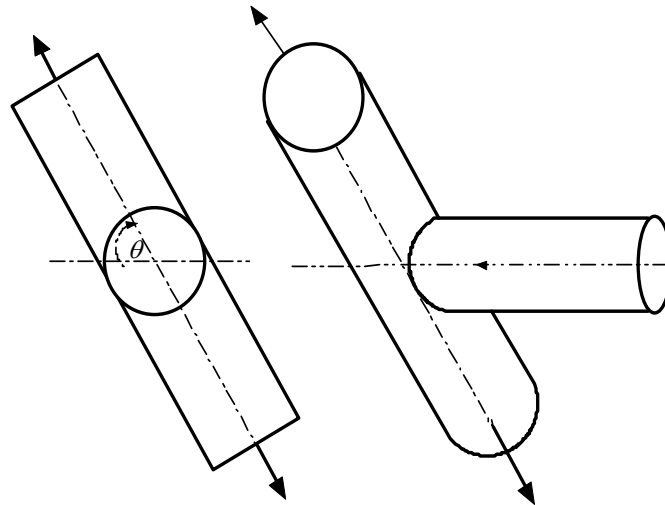
flow in Outlet 3 consists of a gas component with a mass flow rate W_{G3} and a liquid component with a mass flow rate W_{L3} with $W_3 = W_{G3} + W_{L3}$. The quality in Outlet 3 is x_3 , where $x_3 = W_{G3}/W_3$. The following parameters will be used in presenting the phase-redistribution data in this investigation;

$$\text{Overall mass split ratio } W_R = W_3/W_1 \quad (1.1)$$

$$\text{Gas mass split ratio } F_{G3} = W_{G3}/W_{G1} \quad (1.2)$$

$$\text{Liquid mass split ratio } F_{L3} = W_{L3}/W_{L1} \quad (1.3)$$

Outlet 2 mass flow rate (W_2)
 Outlet 2 quality (x_2)
 Outlet 2 diameter (D_2)



Inlet mass flow rate (W_1)
 Inlet quality (x_1)
 Inlet diameter (D_1)

Outlet 3 mass flow rate (W_3)
 Outlet 3 quality (x_3)
 Outlet 3 diameter (D_3)

Fig. 1.1 Relevant parameters for two-phase flow in an impacting tee junction with a horizontal inlet and inclined outlets

Figure 1.2(a) is an example of how the phase-distribution data for a tee junction with a horizontal inlet and horizontal outlets can be illustrated. The 45° line ACE represents the equal-phase-split line, i.e., the mixtures in the three sides of the junction have the same qualities. Geometric symmetry of the outlets implies that all phase separation data lines (or curves) must pass through center point C where both F_{G3} and F_{L3} have a value of 0.5. To satisfy the mass balance, the second part of the data line that lies after the center point should be an inverted mirror image of the data line that lies before the center point. Figure 2.1(a) contains some of the possible data lines. The shape of the data line depends on the inlet conditions. All the data must start at point A (0,0). As the extraction ratio W_3/W_1 increases, there are two limiting conditions represented by lines AB and AD. For line AB, only gas is diverted into Outlet 3 while for line AD, only liquid is diverted into Outlet 3. Data may fall anywhere between the lines AB and AD. When the data line approaches the point B or the point D, the data automatically have to pass through point C that has an $F_{G3} = 0.5$ and an $F_{L3} = 0.5$. The data may exist only within the two squares ABCD and CFEG and no data can exist in the other two squares.

Figure 1.2 (b) shows an example of how the phase-redistribution data for an impacting tee junction with a horizontal inlet and inclined outlets can be illustrated. As θ increases, the tendency of the liquid phase to flow into Outlet 3 increases. This can be attributed to the gravitational effect. The data line will move to the upper side of the diagram away from that data line of the horizontal case. Geometric symmetry no longer exists and consequently, the data lines do not pass through the center point C. A further increase of the angle of inclination may lead to the point of total separation of phases. At this point, the total inlet gas mass flow rate flows through Outlet 2 and the total inlet

liquid mass flow rate flows through Outlet 3 (i.e., $F_{G3} = 0$ at $F_{L3} = 1$). The main question is to know the combination of inlet conditions, and outlet inclination angles that ensure total phase separation.

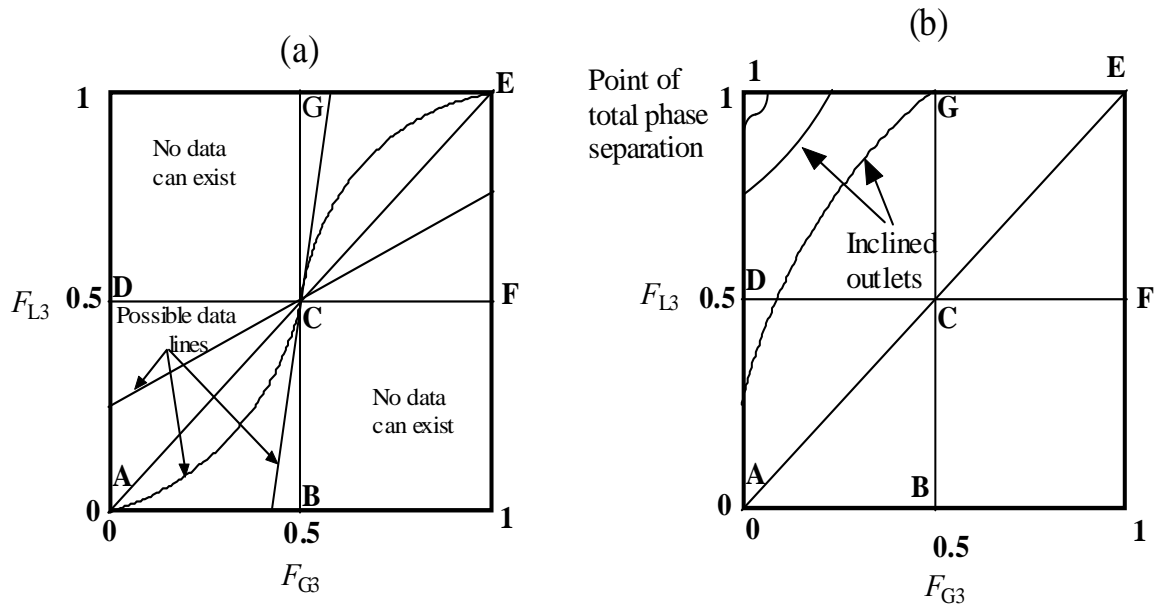


Fig. 1.2 Schematic representation of how phase-redistribution data of an impacting tee junction are presented (a) horizontal inlet and horizontal outlets, (b) horizontal inlet and inclined outlets.

A reasonable amount of information has already been reported in the literature for the flow split at tee junctions. Most of the work in the past was directed to the geometry of branching tees with much fewer publications on impacting tee junctions. Most of the previous researchers on impacting tee junctions have concentrated on impacting tee junctions with a horizontal inlet and horizontal outlets. Although impacting tee junctions with inclined outlets are in use, publications considering the inclination effect cannot (to

the best of the author's knowledge) be found in the open literature. To date, although the use of impacting tee junctions is common in pipeline networks, the possibilities of using them as a partial or perfect phase separator has not been investigated thoroughly in the open literature. The available data on the use of junctions as separators have dealt mainly with branching tees. For the limited inlet conditions tested using branching junctions, it was proposed that the separation was not perfect and junctions should be incorporated as partial phase separators in a more intensive separation system. It will be shown below that full separation of phases using an impacting junction with inclined outlets, for limited inlet conditions, is possible. Therefore, it is the objective of this work to expand the state of knowledge on two-phase flow in an impacting tee junction by considering parameters affecting the two-phase flow that have not been studied before. The following is a list of the specific objectives of this experimental investigation.

1. To determine experimentally the effect of the outlet inclinations on two-phase flow (air-water) splitting at an impacting tee junction covering a wide range of inlet conditions, inclination angles ranging from horizontal to vertical, and the whole range of mass split ratios from 0 to 1.
2. To determine experimentally the capability of a single impacting tee junction with a horizontal inlet and inclined outlets to perform as a full phase separator.
3. To develop a correlation for prediction of the limiting inlet conditions of J_{G1} and J_{L1} at various inclination angles at which full separation of the phases is attainable.

CHAPTER 2

LITERATURE REVIEW

2.1 Overview

Two-phase flow through dividing tee junctions is most often characterized by the maldistribution of phases between the two outlets. This maldistribution of phases is of technical concern because of its effect on the equipment downstream from the junction. However, this phenomenon can be utilized as a useful tool to build compact and inexpensive separators of gas–liquid mixtures (Azzopardi, 1993). Phase redistribution and phase separation are two topics of fundamental interest to research in two-phase flow. The work in this thesis considers the two aspects of the problem and deals exclusively with two-phase flow in impacting tee junctions with a horizontal inlet and inclined outlets.

A considerable amount of research has been done on two-phase flow in dividing tee junctions. Comprehensive reviews, most notably by Lahey (1986), Muller and Reimann (1991), Azzopardi and Hervieu (1994), and Azzopardi (1999) can be found in the literature. The latest identifies about 70 references of experimental and/or theoretical investigations on phase redistribution at tee junctions. The large number of investigations is evidence of the importance and complexity of the problem. Most of this research was directed to the geometry of branching tees. By contrast, a much smaller number of studies has been reported on the geometry of impacting tee junctions. Therefore, this review examines the progression of the knowledge in branching and impacting tee junctions in order to benefit from what is already known in these two areas. It should be noted that

regardless of similarity and common objectives, branching and impacting tee junction are treated almost independently in the literature.

2.2 Phase Redistribution in Branching Tee Junctions

As there has been so much research activity investigating the many aspects that affect the phase redistribution at branching junctions, only the relevant investigations will be cited in this review. Consequently, the review will be limited to:

1. Horizontal equal-sided junctions.
2. Horizontal junctions with an inclined branch.
3. The use of branching tee junctions as a phase separator.

2.2.1 Horizontal Equal-Sided Junctions

A large numbers of investigations on two-phase flow in branching tee junctions with horizontal main and branch sides can be found in the literature. Some of the experimental and/or theoretical investigations were reported by Saba and Lahey (1984), Azzopardi et al. (1988), Azzopardi and Memory (1989), Arirachakaran (1990), Buell et al. (1994), Rubel et al. (1994), Roberts et al. (1995), Stacey et al. (2000), Rea and Azzopardi (2001), Wren et al. (2005), Das et al. (2005), and Yang and Azzopardi (2007). Most of the previous data are for air-water flow at low pressure; however, a few studies exist for steam-water flow and liquid-liquid flow. Much of the research on the fully horizontal equal-sided junctions has been coupled with investigations on the effect of a reduced branch diameter. Some examples of that are the work of Shoham et al. (1989), Azzopardi et al. (1990), Ballyk et al. (1991), Walters et al. (1998), Van Gorp et al. (2001), and Pandey et al. (2006). Since there is such a wealth of literature, only a sample of the recent publications will be

reviewed in detail. The selected references are considered according to the type of inlet flow regime approaching the junction. The different pipe diameters, junction pressure, and mass extraction ratios used in each of the studies are indicated in Table 2.1. It should be noted that all pressures stated in this thesis are absolute pressure.

Table 2.1 References on phase redistribution in equal-sided branching tee junctions with a horizontal inlet and horizontal outlets

Author(s)	D_1 (mm)	Test fluid	P_s (bar)	J_{G1} (m/s)	J_{L1} (m/s)	W_3/W_1	Inlet flow regime
Buell et al. (1994)	37.6	Air-Water	1.5	2-40	0.002-0.2	0.1-0.9	St, Wa, Sl, An
Stacey et al. (2000)	5	Air-Water	1.5	15-20	0.11-0.19	0.0-1.0	An
Rea and Azzopardi (2001)	127	Air-Water	1.0	4-30	0.04-0.558	0.0-1.0	St
Wren et al. (2005)	5	Air-Water	1.48	1.14, 1.82, 2.28, 4.56	0.093, 0.166, 0.313	0.02-0.98	Sl

An = **Annular**, Sl = **Slug**, St = **Stratified**, Wa = **Wavy**

Buell et al. (1994) reported experimental data on phase redistribution and pressure drop for air-water mixtures at a horizontal, equal-sided (37.6-mm I.D.) branching tee junction. Their results demonstrated that, in general, uneven phase redistribution existed at the junction. Increasing inlet superficial liquid velocity J_{L1} at constant inlet superficial gas velocity J_{G1} , resulted in increasing preference of the gas to exit through the branch. They explained this trend using the idea that was suggested by Azzopardi et al. (1988) whereby an increase in J_{L1} results in an increase in the average axial momentum of the liquid phase, thus reducing the probability of the liquid to enter the branch. At constant J_{L1} and various values of J_{G1} , the phase-redistribution data did not produce a consistent trend due to the complications associated with the flow-regime transitions encountered with changing J_{G1} .

Stacey et al. (2000) presented phase-redistribution data of annular flow at an equal-sided tee junction of 5-mm I.D. The purpose of their investigation was to compare their results with data obtained from junctions of other diameters. Their data showed that increasing the inlet superficial liquid velocity J_{L1} at constant gas inlet J_{G1} resulted in a small but clear gas preference to exit through the branch. This trend agreed with that observed by Buell et al. (1994). A similar trend for annular flow was observed by Azzopardi and Memory (1989) who suggested an explanation for this trend based on the level of liquid entrainment in the gas flow in the pipe core. They proposed that the fraction of liquid diverted into the branch comes mainly from the wall liquid film. Therefore, decreasing the liquid flow rate decreases the liquid droplet entrained in the gas flow which would then increase the liquid level in the wall film. As a result, an increase in the fraction of liquid diverted into the branch is expected. Stacey et al. also noted that changing the inlet superficial gas velocity J_{G1} at constant liquid inlet velocity J_{L1} , had only a minor effect on the phase redistribution.

Rea and Azzopardi (2001) reported experimental results for a large 127-mm I.D. branching tee junction with inlet velocities from 0.04 to 0.558 m/s for the liquid and 4 to 30 m/s for the gas phase. In addition to phase redistribution, they have reported experimental measurements of liquid height and void fraction values. Although the points of higher liquid superficial velocities appear to be in the annular and slug regions on the flow-regime maps, they were observed to be in the stratified-flow region with a very thin film at the top of the pipe in some cases. One explanation to that is the length of the inlet pipe (56 pipe diameter) used in these experiments was not enough to allow for slug development. Their phase-redistribution results showed little variation with gas inlet flow

rates over the ranges studied. Similar observations were made by Stacey et al. (2000). The results at low inlet liquid flow rates showed no signs of liquid preference to exit through the branch as have been previously suggested by other researchers like Buell et al. (1994). Their explanation was that those higher tendencies of liquid to exit through the branch were for lower inlet flow rates than the lowest flow rates used in their experiments. Moreover, other researchers used smaller junction diameters than 127 mm. Rea and Azzopardi phase-redistribution results, when plotted on F_{G3} versus F_{L3} diagram, were classified into three regions: an initial region at the lowest gas mass extraction ratios of steep slope, a central region of moderate slope, and a third region of steep slope at the highest gas mass-split ratios. Rea and Azzopardi used their phase-redistribution data to test the predictive ability of several phase-redistribution models. They found that the model of Shoham et al. (1987) was the most promising one. The model prediction of the fraction of liquid diverted into the branch at any given gas mass split ratio, though it followed the trend of the data, always predicted lower values. Moreover, the model failed to give reasonable results at high liquid flow rates.

Wren et al. (2005) presented phase-redistribution data of air-water flow using a 5-mm I.D. tee junction with all pipes in the horizontal plane. The experiments were confined to the slug-flow regime for four inlet gas superficial velocities of 1.14, 1.82, 2.28, and 4.56 m/s, and three inlet liquid superficial velocities of 0.093, 0.166, and 0.313 m/s. The pressure at the tee junction was maintained at 148 kPa. In all experiments, phase-redistribution data lines were seen to lie just below the even phase-redistribution line on a F_{G3} versus F_{L3} diagram. For the condition tested and at high mass-split ratios, increasing the inlet superficial liquid velocity J_{L1} at constant gas inlet J_{G1} showed a

limited increase in gas preference to enter the branch. Increasing the inlet superficial gas velocity J_{G1} at constant liquid inlet velocity J_{L1} , resulted in a small but clear preference of the liquid to enter the branch. When their phase-redistribution data were compared with the data taken from the annular-flow regime by Stacey et al. (2000), a significant difference between the two sets of data was observed. More liquid entered the branch in annular flow at small mass-split ratios and less liquid entered the branch at high mass split ratios. When their data were compared to the data taken for slug flow by Arirachakaran (1990) who used a larger junction of 50-mm I.D., close agreement was found for medium mass split ratios with both data lines lying close to the equal phase-redistribution lines. Large disagreements were observed at high mass-split ratios with a larger tendency of the gas to enter the branch for large diameter junctions.

2.2.2 Horizontal Junctions with an Inclined Branch

Much of the research on branching junctions with an inclined branch has been coupled with investigations on the effect of a reduced branch diameter. Some of the experimental and/or theoretical investigations of phase redistribution with inclined branches were reported by Hong (1978), Seeger et al. (1986), Reimann et al. (1988), Ballyk et al. (1991), Azzopardi and Smith (1992), Peng et al. (1993), Penmatcha et al. (1996), Marti and Shoham (1997), Peng et al. (1998), Ottens et al. (1999), and Wren (2001). The majority of published material deals with the case of vertical upward and vertical downward branches.

Table 2.2 lists some of the references on phase redistribution at branching tee junctions where the effect of the branch inclination has been investigated. The references

were selected to highlight the effect of inlet flow regimes and various inclination angles from near horizontal to vertical. The inlet flow conditions, junction diameters, branch-to-inlet diameter ratio and junction pressure used in each of the studies are indicated in Table 2.2. By convention, an angle of 0° represents a fully horizontal tee junction, positive angles indicate that the branch is raised above the horizontal and negative angles indicate downward inclinations of the branch.

Table 2.2 References on phase redistribution in branching junctions with a horizontal inlet and inclined branch

Author(s)	Branch Orientation	D_1 (mm)	Diameter Ratio	Test Fluids	P_s (bar)	J_{G1} (m/s)	J_{L1} (m/s)	Inlet Flow Regime
Hong (1978)	$0^\circ, \pm 45^\circ, \pm 90^\circ$	9.5	1.0	Air-Water	1.2, 1.6	9.1-42.7	0.0023-0.047	Wa, An
Penmatcha et al. (1996)	$+35^\circ, +20^\circ, +10^\circ, +5^\circ, +1^\circ, 0^\circ, -5^\circ, -10^\circ, -25^\circ, -40^\circ, -60^\circ$	50.8	1.0	Air-Water	3.0	6.1	0.0051, 0.015, 0.03, 0.059	St, Wa
Marti and Shoham (1997)	$+20^\circ, +10^\circ, +5^\circ, +1^\circ, 0^\circ, -5^\circ, -10^\circ, -25^\circ, -40^\circ, -60^\circ$	50.8	0.5, 1.0	Air-Water	3.0	6.1	0.0051, 0.015, 0.03, 0.059	St, Wa
Ottens et al. (1999)	$0^\circ, +0.1^\circ, +0.25^\circ, +0.5^\circ$	51	1.0	Air-Water	1.0	5-14	0.0009-0.014	St

An = **Annular**, St = **Stratified**, Wa = **Wavy**

Hong (1987) presented phase-distribution data for air-water two-phase flow using an equal-sided (9.5-mm I.D.) tee junction with a horizontal inlet and branch inclinations ranging from vertical upward to vertical downward. The inlet quality varied between 25% and 97%. At each inlet superficial gas velocity (J_{G1}), the inlet superficial liquid velocity (J_{L1}) was varied between 0.0023 and 0.047 m/s. These conditions corresponded to wavy and annular flow in the inlet. For the horizontal branch, most of the data lines lie below the equal-phase-split line when plotted on a F_{G3} versus F_{L3} diagram with visible preference of

the liquid to enter the branch. At fixed J_{G1} , an increase in J_{L1} resulted in an increase in gas preference to exit through the branch; however, this trend was reversed at small gas mass-split ratios of less than 0.1. At a fixed J_{L1} , an increase in the J_{G1} resulted in an increase in liquid preference to exit through the branch. Hong concluded that the inlet flow regime had no clear effect on the phase distribution. For the inclined case, Hong presented only one set of data for gas inlet superficial velocity of 27.4 m/s, inlet liquid superficial velocity of 0.023 m/s and branch inclination varying from vertical upward to vertical downward. The results indicate that inclining the branch had a significant effect on the phase-redistribution data as compared to the horizontal case. When the branch was inclined at $+90^\circ$, the data line moved toward the equal-phase-redistribution line on a F_{G3} versus F_{L3} diagram with an increased tendency of the gas to enter the branch as compared to the horizontal case. With an upward inclined branch at $+90^\circ$, a significant amount of gas of about 20% has to be diverted before any liquid is extracted. Moving the branch downward to -90° increased the tendency of the liquid phase to exit through the branch. Partial phase separation was achieved with 100% of the liquid phase entering the branch with 40% of the gas removed with it. Hong suggested that gravity is the main force leading to more liquid flowing into the branch when it faces down.

Penmatcha et al. (1996) provided both experimental and theoretical data for phase-redistribution of air-water two-phase flow in a junction of 50.8-mm I.D. Although their work was limited only to stratified flows it involved rotating the branch around the main horizontal pipe from angles of $+35^\circ$ above the horizontal to -60° below it. The inlet superficial gas velocity was fixed at 6.1 m/s and the liquid superficial velocity was set at 0.0051, 0.015, 0.03, and 0.059 m/s. These inlet conditions corresponded to inlet flow

regimes of stratified and wavy flows. For the case of a horizontal branch, their results agreed with the general trend observed by other researchers in which increasing J_{L1} at constant J_{G1} , resulted in an increased preference of gas to enter the branch. For the cases of downward inclination, their data showed a trend similar to that observed by Hong (1987). The greater the inclination angle, the greater the fraction of liquid diverted into the branch. For the inlet conditions tested, rotating the branch downward at an angle of -60° was enough to achieve partial phase separation with 100% of the liquid phase being removed through the branch. For the cases of upward inclination, a significant amount of gas had to be diverted into the branch before any liquid flowed into the branch. For an angle of $+5^\circ$, the onset of liquid flow into the branch did not occur until the fraction of the gas diverted into the branch was $F_{G3} \approx 0.5$. This number increased dramatically to about 0.8 at the higher angle of $+35^\circ$. However, once the liquid started to flow into the branch, only a small increase in gas flow was needed to divert the majority of liquid into the branch. Beyond the onset of liquid flow point, the liquid height at the junction increased sharply, as the liquid momentum decreased, and more liquid was diverted into the branch. Their data showed that for small inclinations the preference of liquid to enter the branch decreased as the liquid inlet flow increased. That effect on the phase redistribution became relatively small as the inclination angle exceeded $+5^\circ$. Penmatcha et al. (1996) used the dividing-streamlines model of Shoham et al. (1987) as the base for their theoretical work. The model was able to predict the general trend of data but it tended to over predict the fraction of liquid diverted into the branch for a given fraction of gas diverted.

Marti and Shoham (1997) extended the work of Penmatcha et al. (1996) to include the effects of reducing the branch diameter. Comparisons between the two sets of data for the horizontal branch showed that for low inlet liquid mass flow rate, the fraction of liquid entering the branch was less for the reduced junction as compared to the regular one. For higher liquid mass-flow rates, both cases had an almost equal liquid fraction being diverted to the branch at a given gas mass-split ratio. They have suggested that the reduction in the branch diameter reduced the axial distance at the mouth of the branch available for liquid diversion to occur as the branch opening became smaller. As a result, the time available for liquid to flow into the branch instead of continuing to flow into the run side was also reduced. The other reason is the elevation difference between the bottom of the inlet pipe and the branch opening. In the case of a reduced branch, the liquid flowing at the bottom of the pipe needs to 'climb-up' the wall to flow into the branch opening in order to be diverted into the branch. As a result, more liquid by-passes the branch opening of the reduced junction and continues along the run side. For high gas mass-split ratio, the inlet-to-branch pressure drop in the case of a reduced branch is higher than that of a regular junction. As a result the gas velocity in the reduced branch increases significantly for the same gas fraction diverted into the branch. Higher gas velocity in the smaller diameter pipe draws more liquid into the reduced branch when compared to a regular tee junction system. For downward branches, the results showed that gravity acted in favor of the liquid to flow into the branch in the case of regular and reduced tee. Although this effect was observed in both cases, it was more pronounced at low inlet liquid mass flow rates for the case of regular tee junctions. In general, less liquid was diverted into the reduced branch at low gas-split ratios. For higher gas mass-split ratios,

reduced and regular junctions had an almost equal liquid fraction entering the branch at a given gas mass split ratio. This can be explained as before for the fully horizontal case. At low gas mass-split ratios, the reduced travel time for liquid and liquid axial momentum are the determining factors, while at high gas mass-split rates the pressure drop becomes the dominant factor in determining the amount of liquid diverted into the branch. For the case of upward inclined branch, the results suggested that more liquid was diverted into the branch for the reduced branch junction at low gas split ratios as compared to the regular tee. The explanation for this was that the reduced tee had a higher pressure drop, due to the higher gas velocities within the smaller cross-section. However, as the gas mass split was increased the amount of liquid diverted into the branch, for a particular gas fraction becomes essentially equal for both junctions. High mass split ratio resulted in a combined effect by pressure drop, gravity, and inertia forces which appear to be equal for both regular and reduced junctions. As was noted by Penmatcha et al. (1996), a significant amount of gas had to be diverted into the branch before any liquid started to flow with it. For an angle of $+20^\circ$, the onset of liquid flow into the branch did not occur until 50% of the gas was diverted into the branch. Their results indicated that the redistribution of phases tended to become independent of the inlet liquid velocities as the upward inclination angle exceeded $+5^\circ$. Marti and Shoham extended the model of Penmatcha et al. (1996) to include the effects of reducing the branch diameter. The model produced reasonable agreement with the experimental data.

Ottens et al. (1999) reported phase-redistribution data on air-water flow with small liquid holdup through an equal-sided tee junction with a diameter of 51-mm I.D. and small branch inclination in the upward direction of up to 0.5° . The experiments were

performed under atmospheric pressure, near-ambient temperature, inlet superficial gas velocities of 5 to 14 m/s, and inlet superficial liquid velocities of 0.0009 to 0.014 m/s. Their results indicated that a small branch inclination angle from the horizontal, in their case less than 0.5° , can have a significant influence on the phase redistribution of gas-liquid flows. A significant amount of gas has to be diverted into the branch before any liquid is extracted with it. The liquid take-off point varied with the inclination angle. For example, at an inclination angle of 0.1° this point was observed at approximately $F_{G3} \approx 0.15$, while at an inclination angle of 0.5° this point was observed at approximately $F_{G3} \approx 0.5$. Similar observations were reported by Penmatcha et al. (1996) and Hong (1978).

Ottens et al. (1999) also studied the effect of liquid viscosity on phase redistribution. That was done by comparing the results of the air-water mixture with those of two air-water-glycerol mixtures where the viscosities of the water-glycerol were 3 and 6 times the viscosity of water. The results corresponded to $J_{G1} = 12$ m/s, and $\theta = 0.25^\circ$. It was found that liquid did not flow into the branch until about 40% of gas was extracted. At $F_{L3} < 0.4$, the viscosity has a small effect on F_{G3} , while for $F_{L3} > 0.4$, the viscosity had a significant effect on the phase redistribution with F_{G3} decreasing as the viscosity increased.

2.2.3 The Use of Branching Junctions as a Phase Separator

Using a tee junction as a phase separator has advantages over conventional separators because of the junction's simple geometry, low cost, compact size, and minimal maintenance requirements. Azzopardi (1993) reviewed the applications in which simple tee junctions were used for gas-liquid separation. All the tees considered in that

study were of the branching type with a horizontal main pipe and a vertical upward or a vertical downward branch. The geometry and flow parameters affecting the phase redistribution at the junction were reviewed. It was concluded that branching tees can be used for primary separation (with partial separation in most instances); however, it was cautioned that changes in the inlet conditions can severely affect the phase split at the junction. Later, Azzopardi et al. (2002) demonstrated the use of a tee-junction-based separator in a chemical plant. For an inlet condition of annular flow, the separation performance was found to depend on the fraction of liquid entrained as droplets and the distribution of liquid film thickness around the circumference of the inlet pipe. In order to improve the separation performance, Wren and Azzopardi (2004) considered the performance of a separating system consisting of two branching tee junctions arranged in series. The first junction had a horizontal main pipe and a vertically upward branch and the second junction had a horizontal inlet and a vertically downward branch. The second junction was either equal sided or reduced with a branch-to-main diameter ratio of 0.6. Inlet regimes of semi-annular and stratified flow were used in the experiments. They suggested a criterion of less than 10% by volume of liquid exiting with the gas stream and less than 10% by volume of gas exiting with the liquid stream for junction to be considered as a viable phase separator. It was possible to collect a gas-rich stream from both the upward branch and the main pipe and a liquid-rich stream from the downward branch. The inclusion of the reduced tee was found to improve the phase separation of the system and made it possible to achieve one part of the separation criterion of less than 10% liquid in the gas stream. However, such a design did not resolve the problem of higher than 10% gas content in the downward arm containing the liquid-rich stream.

Baker et al. (2007) used the same separator system of Wren and Azzopardi and added control valves on two of the three outlets of the separator in order to enhance the performance. One of these valves was installed on the downward branch and was used to automatically control the liquid level in that branch, while the second valve was installed on the main outlet and operated manually to maximize the liquid flow in the downward branch. Experiments were performed using stratified and slug inlet flow regimes of air-kerosene mixtures. It was demonstrated that the separator system was capable of producing a gas-free liquid stream and a gas-rich stream with less than 10% liquid by volume over a wide range of inlet conditions.

To the best of the author's knowledge, the utilization of impacting tees as phase separators has not been investigated yet in the open literature. It is the objective of this study to determine experimentally the inlet conditions under which full separation of phases is attainable and to support these results by a physically-based correlation.

2.3 Phase Redistribution in Impacting Tee Junctions

Reviews of the available literature on impacting tee junctions were given by Azzopardi (1999) and El-Shaboury et al. (2001). All previous investigations were directed to the geometry of equal-sided junctions. The majority of the previous work corresponds to junctions with a horizontal inlet and horizontal outlets. However, a few publications were directed to the junction orientation of vertical inlet and horizontal outlets. A careful examination of the literature revealed that publications considering inclined outlets and the use of impacting tee junctions as a phase separator cannot (to the best of the author's knowledge) be found in the open literature. As a consequence, a serious lack in

knowledge exists in these two particular areas. The rest of this review examines the progression of knowledge in the following areas:

1. Horizontal equal-sided impacting junctions.
2. Impacting junctions with a vertical inlet.

2.3.1 Horizontal Equal-Sided Junctions

Table 2.3 gives a summary of previously published experimental work on two-phase flow through equal-sided impacting junctions with a horizontal inlet and horizontal outlets. The table includes impacting tees and impacting wyes. Most of the previous work corresponds to air-water flows at low pressure; however, limited work has been done for wet-steam, R-11 two-phase flows, and two-phase air-solid mixture of micro-glass and millet flow.

One of the earliest works relevant to the present study was that of Hong (1978). He reported phase-redistribution data using air-water flow through a horizontal impacting tee junction of 9.5-mm I.D. Data were obtained for one set of inlet conditions of superficial gas velocity 27.4 m/s, and superficial liquid velocity of 0.0235 m/s. These inlet conditions corresponded to annular flow with an inlet quality of 0.62. The results showed that the flow emerging from both outlets had the same quality as the inlet except for $W_3/W_1 < 0.15$ and $W_3/W_1 > 0.85$. It was suggested by other researchers that Hong's data may have been affected by strong surface-tension forces due to the small tube diameter.

Hwang (1986) published phase-redistribution data for a 38-mm I.D. horizontal junction. Measurements were taken for air-water flows through a 90° tee and a 45° wye at various inlet conditions. The system pressure ranged between 130 and 200 kPa. Three

Table 2.3 References on phase-redistribution in impacting junctions with a horizontal inlet and horizontal outlets

Author(s)	Angle Between Inlet and Outlet 3	D_1 (mm)	Test Fluids	P_s (bar)	J_{G1} (m/s)	J_{L1} (m/s)	W_3/W_1	Inlet Flow Regime
Hong (1978)	90°	9.5	Air-Water	1.22	27.4	0.0235	0.0-1.0	An
Hwang (1986)	45°, 90°	38	Air-Water	1.3 – 2.0	1.5-6.5	1.35-2.539	0.02-0.93	Bu-St
Chien and Rubel (1992)	90°	50.8	Steam-Water	28.6 - 42.4	12-40	0.033-0.283	0.2-0.5	An, An-Mt
Ottens et al. (1995)	90°	29.5	Air-Water	1	15.8	0.00063-0.03	0.0-1.0	Wa
Hong and Griston (1995)	90°	19, 50, 100	Air-Water	1	4.6-22.86	0.045-1.35	0.05-0.95	An-Mt, St
Fujii et al. (1995)	90°	10	Nitrogen-Water	1	0.03-12	0.05-0.5	0.0-1.0	An, Pl, Sl, St, Wa
Fujii et al. (1996)	30°, 60°, 90°	10.5	Air-Water	1	0.1-7.0	0.05-0.5	0.0-1.0	An, Pl
Asano et al. (1997)	30°, 60°, 90°	10	R-11 (Saturated mixture)	1	0.07-19	0.03-0.55	0.0-1.0	Pl, Sl
Asano et al. (2001)	30°, 60°, 90°	10.5	Air-Water	1	0.1-7.0	0.05-0.5	0.0-1.0	An, Pl, Sl, St
El-Shaboury (2005)	90°	37.8	Air-Water	1.5	0.5-40	0.01-0.18	0.5	St, Wa, An
Guangbin et al (2010)	10°, 15°, 20°, 30°	32	Air – Micro-glass, millet	1	14 - 21	-		homogenous suspension

An = Annular, An-Mt = Annular-Mist, Bu = Bubbly, Bu-St = Bubbly-Stratified, Ch = Churn, Pl = Plug, Sl = Slug, St = Stratified, St-Wa = Stratified-Wavy, Wa = Wavy.

inlet mass fluxes (1350, 2050, and 2700 kg/m².s) were considered with very low inlet qualities of 0.002, 0.003, and 0.004. These inlet conditions corresponded to a bubbly-stratified inlet flow regime. Phase-redistribution data were acquired over a wide range of extraction ratios ranging from 0.02 to 0.93 and shown on a diagram of quality ratio x_3/x_1 against mass-split ratio W_3/W_1 diagram. For the impacting tee, no gas flow was observed through Outlet 3 until the mass split ratio reached a value between 0.3 and 0.4. The quality ratio x_3/x_1 in this zone was equal to zero, that is, only liquid was diverted into Outlet 3. However in the range of $0.4 < W_3/W_1 < 0.6$, a mixture of gas and liquid was observed in Outlet 3. As expected, equal phase separation was observed at $W_3/W_1 = 0.5$. For $W_3/W_1 > 0.6$, partial phase separation (i.e, $W_{G1} = W_{G3}$) occurred where all the gas was diverted into Outlet 3. These results indicate that an impacting tee junction can operate like a fluidic switch for the conditions tested. The trend of Hwang's data is quite different from that obtained by Hong (1978). It was suggested later by Hwang et al. (1989) that Hong's data may have been affected by strong surface-tension forces due to the small tube diameter and the hydrostatic head of the fluid in the pipes leading to the phase separators. For the impacting wye, the zone at which a mixture of gas and liquid was observed in Outlet 3 occurred at approximately $0.03 < W_3/W_1 < 0.25$. The condition of equal phase redistribution was obtained for the 45° wye junction at $W_3/W_1 < 0.5$. These trends were explained by the fact that liquid-phase inertia was much larger than that of the gas phase, making it more difficult for liquid to enter Outlet 3.

Chien and Rubel (1992) presented phase distribution data of wet steam during annular flow through a 50.8-mm I.D. horizontal impacting junction. The system pressure ranged between 28.6 and 42.4 bars, inlet steam quality ranging from 0.2 to 0.8, the vapor

extraction ratio ranging from 0.2 to 0.5, and the inlet superficial vapor velocity ranged from 12 to 40 m/s, which gave annular and annular-mist inlet flow regimes. The purpose of their study was to investigate the effects of inlet quality, inlet velocity, mass-split ratio and system pressure on the phase redistribution of the steam as it passes through the junction. Their results showed that for a given inlet quality, the mass-split ratio is a key factor affecting the quality at the outlets. The data showed that the outlet steam qualities were always different from the inlet quality if the vapour extraction ratio was not equal to 0.5. The value of x_3/x_1 deviated more from one as the vapor extraction ratio deviated from 0.5. For a constant mass-split ratio, the steam quality ratio became closer to one as the steam inlet quality increased. Inlet steam pressure and inlet vapor velocity were not found to have a significant effect on the data.

Ottens et al. (1995) conducted an experimental investigation of air-water flow through an impacting tee junction with a diameter of 29.5-mm I.D., atmospheric pressure and ambient temperature. Phase-redistribution data were reported for a fixed superficial gas velocity of 15.8 m/s and superficial liquid velocities of 0.00063, 0.00302, 0.012, and 0.03 m/s. These inlet conditions corresponded to inlet qualities ranging between 0.38 and 0.97. Phase-redistribution data were acquired over a wide range of extraction ratios from 0.0 to 1.0 and the results were plotted on diagrams of gas extraction ratio F_{G3} against liquid extraction ratio F_{L3} . At the highest inlet quality tested, the data showed a clear preference of gas to enter Outlet 3 with no liquid diverted up to a certain gas extraction ratio value (F_{G3} of around 0.45). This was followed by a region in which a mixture of liquid and gas were diverted into Outlet 3. At $F_{G3} = 0.5$ the qualities at the inlet and both outlets were equal, as expected. For gas extraction ratios above a certain value (around

0.55), all the liquid was diverted into Outlet 3. As the inlet quality decreases, the value of F_{G3} at which liquid started to flow into Outlet 3 (liquid take-off point) decreased and the phase-redistribution lines moved toward the equal phase-split line. At the lowest inlet quality of 0.38, no gas was diverted into Outlet 3 up to a certain liquid extraction ratio (F_{L3} of around 0.2) and for liquid extraction ratios above a certain value (around 0.8), all the gas was diverted into Outlet 3. This trend of data at low qualities agrees with the trend obtained by Hwang et al. (1986).

Hong and Griston (1995) presented phase-redistribution data for low-inlet quality two-phase (air-water) flow through horizontal impacting junctions. They also developed an empirical method to predict phase redistribution. Experiments were conducted using a 19-mm I.D. impacting tee. The inlet conditions were: inlet superficial gas velocities between 4.6 and 22.86 m/s, liquid volume fractions ranging from 0.01 to 0.06, and near atmospheric pressure. The inlet conditions tested corresponded to inlet qualities between 0.018 and 0.19. Phase-redistribution data were acquired over a wide range of extraction ratios ranging from 0.05 to 0.95 and plotted on diagrams of gas extraction ratio F_{G3} against liquid extraction ratio F_{L3} . At the lowest liquid volume fraction tested (0.01m/s), and the lowest gas inlet superficial velocity (4.6 m/s), phase-redistribution data followed the equal phase-split line over the entire range of the extraction ratio. Increasing the gas inlet superficial velocity at a constant volume fraction of 0.01 resulted in an effect such that no gas flow was observed through Outlet 3 until the mass-split ratio reached a value between 0.15 and 0.3. This trend agrees with previous observations by Hwang (1986) and Ottens et al. (1995). As the liquid volume fraction increased (or the inlet quality decreased) the data lines deviated from the equal phase-split line in a clockwise direction.

The same trend was observed by Ottens et al. (1995). At the highest liquid volume fraction tested, increasing the gas inlet superficial velocity had a very limited or no effect on the phase-redistribution data and the data lines approached a near horizontal line passing through the point $F_{L3} = F_{G3} = 0.5$.

Hong and Griston also conducted field tests to study the effect of junction diameters on phase redistribution using two different nominal diameters of 50 and 100 mm. They also tested different types of insert devices in order to determine the one that increases the extraction-ratio range over which even phase splitting can be obtained. Field tests were conducted with inlet superficial gas velocities between 1.48 and 21.44 m/s, liquid volume fractions ranging from 0.007 to 0.145. The data for the normal 50-mm diameter tee showed that uneven phase redistribution occurred once the vapor mass split deviated from 0.5. The data also showed clear preference of liquid to enter into Outlet 3 at vapor mass-split ratio of less than 0.5. For the junction of 100-mm diameter, the data showed that the liquid and vapor phases split proportionately to each outlet for nearly the entire range of test conditions. The same data were obtained with a modified tee design using inserts (nozzle and vanes) downstream of the junction. Some of these inserts increased the range of mass-split ratio for which equal-quality split occurred, while others were not successful.

Fujii et al. (1995) reported phase-redistribution data for nitrogen-water flow through a 10-mm I.D. horizontal impacting tee. The purpose of their study was to investigate the effect of inlet conditions on phase redistribution. The inlet flow conditions were: liquid superficial velocities of 0.05 to 0.5 m/s, gas superficial velocities of 0.03 to 12 m/s, and junction pressure of 1.0 bar. These conditions corresponded to inlet flow regimes of plug,

slug, annular, stratified, and wavy flows. Phase-redistribution data were acquired over the entire range of mass-split ratios from 0.0 to 1.0 and the results were plotted on diagrams of quality ratio x_3/x_1 against mass-split ratio W_3/W_1 . Experiments were also conducted under microgravity to investigate the capability of an impacting tee junction as a phase separator for two-phase flow thermal control systems in space applications. These two-phase systems have been proposed to replace the single-phase systems used already in space ships because of their compactness and reduced weight. For most of the slug, plug, and annular inlet flow regimes data, no gas flow was observed through Outlet 3 up to a certain gas extraction ratio (W_3/W_1 of about 0.3). On increasing the mass split, a mixture of liquid and gas started to flow into Outlet 3 up to $W_3/W_1 \approx 0.7$. This was followed by a zone that extended up to the end of the extraction-ratio range in which all the gas was diverted into Outlet 3. As expected, at the point of $F_{G3} = 0.5$ the qualities at the inlet and both outlets were equal. For plug flow, the results indicated that increasing the inlet gas velocity at a fixed high inlet liquid velocity (i.e., 0.5 m/s) had little effect on the phase-redistribution data. The trend of the results under different inlet gas velocities was nearly the same both quantitatively and qualitatively. At low inlet liquid velocity (i.e., 0.2 m/s), increasing the inlet gas velocity failed to produce a clear trend of data. As the inlet gas velocity increased, there was an initial decrease in liquid tendency to enter Outlet 3. With a further increase in inlet gas velocity, the trend reversed. For slug and annular flows, the gas velocity had little effect on phase redistribution. For annular flow, increasing the inlet liquid velocity at constant gas velocity resulted in a trend similar to that mentioned above except for the case of liquid superficial velocities less than 0.15 m/s. Gas and liquid always appeared in Outlet 3 no matter what was the value of the extraction ratio. For

stratified and wavy flows, the data failed to produce a clear trend. A mixture of gas and liquid were diverted into the two outlets for all values of mass-split ratio. In general, their results followed the general trend observed by Hwang (1986), Ottens et al. (1995), and Hong and Griston (1995). They have concluded that phase redistribution is strongly affected by the inlet flow regime and the effect of inlet liquid velocity on phase redistribution became greater with increasing inlet gas velocity.

Fujii et al. (1996) reported phase-redistribution data for air-water flow through a horizontal tee and wyes of 10.5-mm I.D. The inlet conditions tested corresponded to annular and plug inlet flow regime. No gas flow was observed through Outlet 3 up to a certain gas extraction ratio (W_3/W_1 of less than 0.5). As expected, at the point of $F_{G3} = 0.5$ the qualities at the inlet and both outlets were equal. On increasing the mass split, a mixture of liquid and gas started to flow into Outlet 3 up to $W_3/W_1 \approx 0.6$. This was followed by a zone that extended up to the end of the extraction-ratio range in which all the gas was diverted into Outlet 3. This is consistent with the results obtained by Hwang (1986), Ottens et al. (1995), Hong and Griston (1995), and Fujii et al. (1995). For impacting wyes, similar data trends to those observed with impacting tee. Decreasing the angle between the inlet and Outlet 3 resulted in an increase of zone at which all the gas was diverted into Outlet 3. This trend of data agreed with the trend obtained by Hwang et al. (1986).

Asano et al. (1997) reported phase-redistribution data for two-phase one-component Refrigerant R-11 flow through horizontal impacting tees and impacting wye of 10-mm I.D. The inlet conditions of gas inlet superficial velocity of 0.07 to 19 m/s and inlet liquid superficial velocity of 0.03 to 0.55 m/s corresponded to an inlet quality

ranging from 0.001 to 0.3. Phase-redistribution results of Refrigerant R-11 followed the same trend of those of air-water results obtained by Hwang (1986), Ottens et al. (1995), Hong and Griston (1995), and Fujii et al. (1995). The only differences were the value of “gas take-off point” at which the gas started to flow into Outlet 3. That value for R-11 was higher than that for air-water.

In a later work, Asano et al. (2001) have also reported phase-redistribution data for air-water flow through a horizontal impacting tee and two impacting wyes of 30°, and 60° at normal gravity and microgravity. The experiments were conducted with a 10.5-mm I.D. junction set in a horizontal plane. Air and water were used as the working fluids with inlet liquid superficial velocities of 0.05 to 0.5 m/s and gas superficial velocities of 0.1 to 7.0 m/s. These inlet conditions corresponded to stratified, slug, plug, and annular flows. The data showed a similar trend to that previously observed by other researchers. For the impacting tee, at low inlet qualities, the results followed the same trend obtained by Hwang (1986), Ottens et al. (1995), Hong and Griston (1995), and Fujii et al. (1995). Again, the value of the “gas take-off point” which is the value of W_3/W_1 at which gas starts to be diverted into outlet 3 was the only difference. Using the wye junctions at similar inlet conditions, the value of W_3/W_1 at the gas take-off point increased by decreasing the angle between the inlet and the outlets. For the impacting tee, about 25% of the water could be extracted from the inlet two-phase flow at $J_{L1} = 0.5$ m/s, quality = 0.0166 and $J_{G1} = 7.0$ m/s before any gas flowed into the outlet. For the wye junction with an angle between the inlet and the outlets of 30° and under similar inlet conditions, about 82% of liquid could be extracted by the time gas started to divert into the outlet.

El-Shaboury (2005) reported phase-redistribution and pressure-drop data for air-water flow through an impacting tee junction of 37.8-mm I.D with horizontal inlet and horizontal outlets. He also developed predictive equations for calculating the phase redistribution and pressure drop. The operating conditions were: system pressure of about 150 kPa, near ambient temperature, inlet superficial gas velocities ranging between 0.5 and 40 m/s, inlet superficial liquid velocities ranging between 0.0026 and 0.18 m/s, and extraction ratios (W_3/W_1) between 0 and 1. These inlet conditions corresponded to inlet flow regimes of stratified, wavy, and annular. His phase-redistribution data were compared to data from previous studies (Ottens et al., 1995; Hong and Griston, 1995; Azzopardi et al., 1986a) under similar inlet conditions. Very good agreement in trend and magnitude was found in these comparisons. He concluded that, in general, an even phase split is obtained only at the point $F_{L3} = F_{G3} = 0.5$. The effect of varying J_{G1} at fixed J_{L1} caused the phase-redistribution data line (or curve) to move around the point (0.5, 0.5) on an F_{L3} versus F_{G3} diagram in an anti-clockwise direction. This effect is the exact opposite of the effect of increasing J_{L1} at a fixed J_{G1} . These observations are consistent with those made by previous researchers for horizontal impacting junctions.

Guangbin et al. (2010) have reported phase-redistribution characteristics of gas–solid two-phase flow using horizontal wye junctions with one outlet fixed at an angle of 15° from the inlet and one adjustable outlet of 15° , 20° , and 30° from the inlet. The three sides of the junction had an equal diameter of 32-mm I.D. Micro-glass bead and millet particles with similar diameter and different solid density were used in this experimental system. The air inlet velocity was between 14 and 21 m/s. The inlet flow regime was classified as homogenous suspension flow style. It was observed that when the angle between the

changeable outlet and the main pipe increased, the solids mass ratio flowing in the changeable outlet decreased. Decreasing the inlet gas velocity reduced the solids mass ratio flowing into of the changeable outlet. The solids distribution was mainly decided by the angles between the branches and the main pipe. For the same branch angle, the trend of solids distribution curves, to the selected solids materials, were similar. Micro-glass beads with larger solid density had more stable solid-distribution curves with increased inlet gas velocity.

2.3.2 Junctions with a Vertical Upward Inlet

Table 2.4 gives a summary of previously published work on two-phase flow through equal-sided impacting junctions with a vertical inlet and horizontal outlets. Azzopardi et al. (1986a) reported phase-redistribution data for air-water flow through a 31.8-mm I.D. impacting tee with a vertical inlet and horizontal outlets. Inlet conditions were: liquid mass flow rate of 0.0252 and 0.0630 kg/s, gas mass flow rate ranging from 0.0157 to 0.0346 kg/s and junction pressure of 170 kPa. These inlet conditions corresponded to the annular-flow regime with inlet qualities ranging between 0.21 and 0.58. The data exhibited a trend similar to that observed using junctions with a horizontal inlet and horizontal outlets. The results showed that for mass-split ratios less than 0.5, there was a tendency of the liquid to exit through Outlet 3. For mass-split ratios higher than 0.5, the data were an inverted mirror image of the low-mass-split-ratio data. Azzopardi et al. (1986b) also used the same junction to report phase- redistribution data for air-water churn flow. The liquid superficial velocities varied from 0.08 to 0.8 m/s and the gas superficial velocities varied from 1.61 to 4.02 m/s. The pressure at the junction

was maintained at 1.7 bar. The trend in the results was very similar to those obtained by Azzopardi et al. (1986a) for annular flow.

Table 2.4 References on phase redistribution in impacting junctions with a vertical upward inlet and horizontal outlets

Author(s)	D_1 (mm)	Test Fluids	P_s (bar)	J_{G1} (m/s)	J_{L1} (m/s)	W_3/W_1	Inlet Flow Regime
Azzopardi et al. (1986a)	31.8	Air-Water	1.7	10.4-21.9	0.032-0.079	0.0-1.0	An
Azzopardi et al. (1986b)	31.8	Air-Water	1.7	1.61-4.02	0.08-0.8	0.0-1.0	Ch
Wang and Shoji (2002)	15	Air-Water	1	0.09-7.08	0.09-0.19	0.0-1.0	Ch
Wang et al. (2003)	15	Air-Water	1	0.03-9.4	0.09-0.47	0.0-1.0	An , Bu, Ch

Wang and Shoji (2002) investigated the fluctuation characteristics of two-phase churn flow splitting in an equal-sided impacting tee junction (15-mm I.D.) with a vertical inlet and horizontal outlets. Inlet conditions were: inlet gas velocities ranging between 0.09 and 7.08 m/s, inlet liquid velocities ranging between 0.09 and 0.19 m/s, atmospheric pressure, room temperature, and mass-split ratios from 0 to 1.0. Their phase-redistribution data followed the typical trend similar to that observed by Azzopardi (1986b). The root-mean-square analysis (RMS) was applied to the differential pressure signals. The chaos dynamic method of power spectral density (PSD) was also employed to reveal their peculiar features in the frequency domain as well. It was found that increasing the inlet gas superficial velocity or inlet liquid superficial velocity resulted in higher intensity fluctuation of both pressure drop and mass-split ratio.

Wang et al. (2003) expanded the work of Wang and Shoji (2002) to bubbly, churn, and annular inlet flow regimes. Several methods used in chaos dynamics were employed to analyze the differential pressure fluctuations of two-phase flow with the aim of showing the two-phase behavior splitting at the junction. Experiments were conducted with air-water mixtures using a 15-mm I.D. tee junction with a vertical inlet and horizontal outlets. Inlet conditions were: inlet gas velocities ranging between 0.03 and 9.4 m/s, inlet liquid velocities ranging between 0.09 and 0.47 m/s, atmospheric pressure, room temperature, and mass extraction ratio of 0.0-1.0. The averaged data for phase redistribution and pressure drop were not reported in these two investigations. Their results suggested that chaotic behavior exists and that two-phase flow splitting at impacting tees is a complicated nonlinear dynamic system by analysis on time series of differential pressure.

2.4 Conclusion Remarks

After a careful examination of the literature, the following conclusions can be drawn:

1. There has been significant research interest on two-phase flow in junctions (branching wyes and tees and impacting wyes and tees).
2. Much more work was done on branching junctions than impacting junctions.
3. The only configurations used in impacting junctions were junctions with a horizontal inlet and horizontal outlets or a vertical inlet and horizontal outlets.
4. To date, and to the best of the author's knowledge, publications considering the effects of outlet inclination and the use of an impacting junction as a phase separator

cannot be found in the open literature. The present investigation is the first study that considers the effect of outlet inclination on phase redistribution and the potential of using a single impacting tee junction as a total phase separator.

CHAPTER 3

EXPERIMENTAL TEST FACILITY AND PROCEDURES

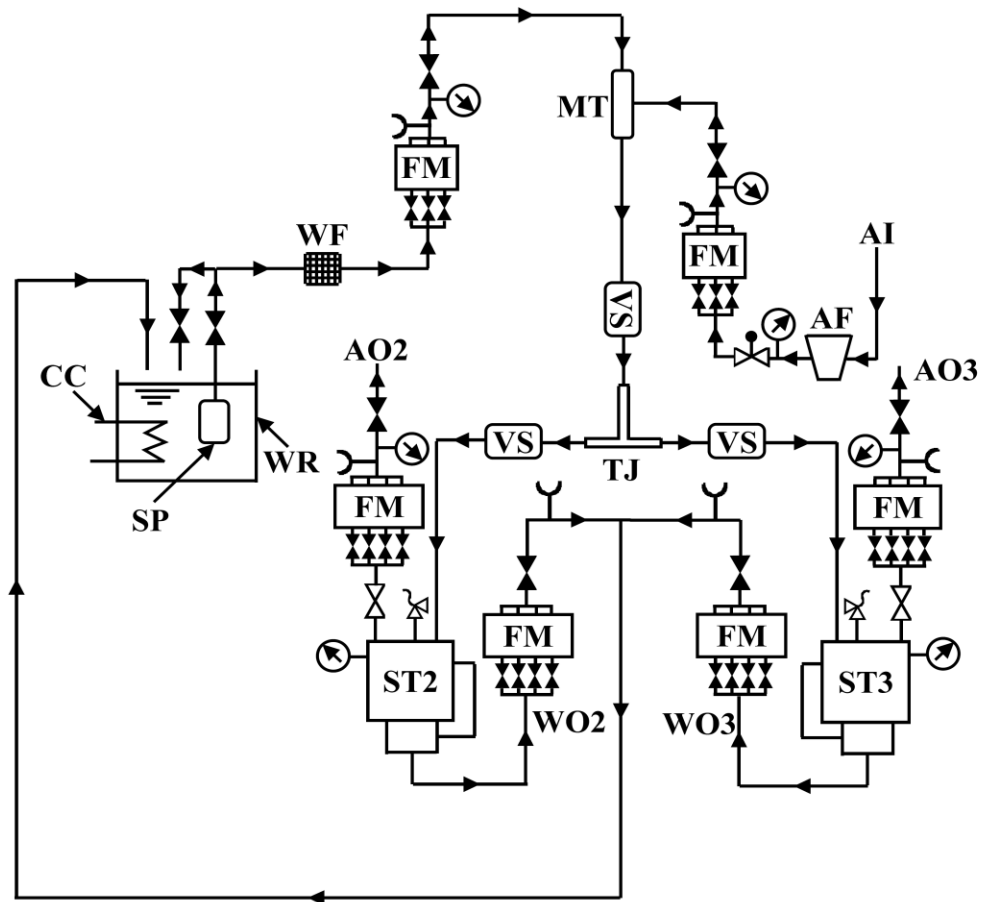
3.1 Introduction.

The present experimental investigation has two objectives: the first one is to determine the effects of outlet inclination on the phase redistribution of air-water flow passing through an impacting tee junction. The second objective is to determine the separation capabilities of a single impacting tee junction with a horizontal inlet and inclined outlets. The test facility constructed to achieve these objectives has several features similar to those used by other researchers to study phase redistribution in horizontal tee junctions. The major distinctive feature of this facility is the ability to incline the two outlets from horizontal to vertical.

3.2 Experimental Test Facility

3.2.1 Air-Water Loop

The apparatus used in the experiments is illustrated schematically in Fig. 3.1 and actual photographs are shown in Figs. 3.2 and 3.3. Air was drawn from the main supply line through an intake section which contains an air filter and pressure controller to clean and control the air pressure, respectively. The inlet air flow rate (W_{G1}) to the mixer was controlled using throttling valves and metered using one of three calibrated



Symbol	Description	Symbol	Description
AF	Air filter	WF	Water filter
AI	Air inlet	WO	Water outlet
AO	Air outlet	WR	Water reservoir
CC	Cooling coil	⊗	Valve
FM	Flow meter	⊗	Control valve
MT	Mixing tee	⊕	Pressure controller
SP	Submersible pump	⊗	Pressure gauge
ST	Separation tank	⊕	Thermocouple
TJ	Tee junction	⊗	Safety valve

Fig. 3.1 Schematic diagram of the test loop



Fig. 3.2 Test loop with a horizontal junction



Fig. 3.3 Test loop with an inclined junction

rotameters with overlapping ranges. Both air temperature and pressure readings were recorded using a thermocouple and a pressure gauge, respectively. Distilled water was drawn from the storage tank by means of a submersible pump. The desirable water mass flow rate and pressure were adjusted using a bypass line around the pump. The water flow rate (W_{L1}) was metered by one of three calibrated rotameters with overlapping ranges. Water temperature and pressure were recorded in a similar manner to that of the air. The temperature of the water was held steady during the experiment by a cooling coil immersed in the water tank. Water was then injected into the air stream inside the mixer through a perforated copper tube.

The two-phase air-water mixture was then discharged from the mixer through a straight length of approximately 62 tube diameters of copper tubing to allow the mixture flow to be fully developed before it entered the visual section. The visual section (15 tube diameters in length) was constructed from an acrylic block and used to identify the inlet flow regime. Another length of approximately 32 tube diameters was allowed before the mixture entered the cross-section where the inlet of the junction meets the outlets. Each outlet leading to its respective separation tank consisted of a length of approximately 56 tube diameters followed by a visual section (15 tube diameters in length) used to identify the outlet flow regimes, and approximately a length of 10 tube diameters downstream of the visual section. The air-water two-phase flow emerging from each outlet was directed to its respective separation tank where the mixtures were separated and then metered. The two outlets were connected to their respective separation tanks using flexible tygon tubes of 13.5-mm I.D. Water flow leaving the bottom of each separation tank was metered using four rotameters with overlapping ranges and so giving W_{L2} and W_{L3} . The

outlet water temperatures were then measured using thermocouples and the two water outlets were joined giving a single return line to the storage tank. A similar arrangement was made for the air emerging from the top of the separation tanks. The air from each of the separation tanks passed through a throttling valve; the two valves together allowed control of separation tank pressure and mass flow split W_3/W_1 . Each air flow rate was measured using a combination of four calibrated rotameters with overlapping ranges used for individual measurement of gas flow rate at both outlets, W_{G2} and W_{G3} . Both air outlets were then manifolded together with exhaust to the room. Extreme care was taken in order to ensure that the entire test facility (up to the separation tanks) was symmetric around the inlet centerline.

3.2.2 Test Section

Figure 3.4 shows a schematic diagram of the test section and the adjoining parts. The entire test section including the mixer, visual sections, the tee junction, and the copper tubing connecting these components were mounted on a rigid frame made of aluminum T-beam sections. The inlet part of the test section leading to the junction runs perpendicular to the two outlets on top the aluminum frame. A survey theodolite (AN 20, Wild Heerbrugg, Lewis instrument Limited) was used to ensure the horizontality of the aluminum frame and the inlet side of the test section. Care was taken to ensure that the axes of the tee junction, inlet visual section, and copper tubing connecting them together were in the same horizontal plane. Another quick procedure was used to confirm the horizontality of the system using a differential water level. A digital inclinometer was used to read the inclination angle of the outlets. The inclination has a resolution of $\pm 0.1^\circ$. The following is a brief description of the test-section parts.

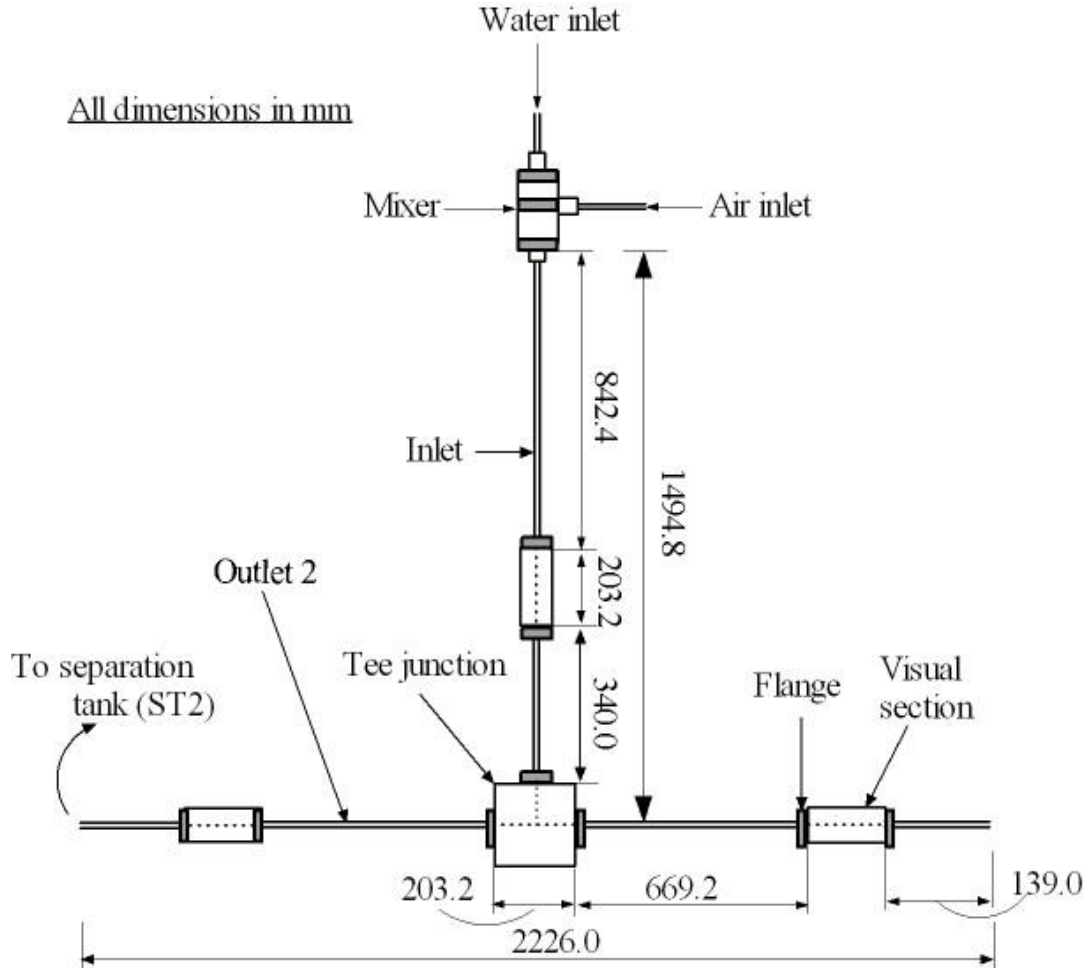


Fig. 3.4 Top view of the test section

Tee junction

The tee junction used in this experiment was machined in a $203.2 \times 179.0 \times 86.2$ mm acrylic resin block. Two perpendicular bores of 13.5 ± 0.1 mm in diameter were drilled into the acrylic block to form the tee junction. The inside of the junction where the two bores met was carefully machined with square edges so as to eliminate the radius of curvature as a possible variable in the experimental work. This was also

needed to ensure consistency with other research laboratories. A single pressure tap was installed close to the junction and used to monitor the junction pressure. The junction block was provided with flanges at the three ends in order to connect the junction with the rest of the test section. These flanges were soldered to the copper tubing and bolted to the acrylic block. Care was taken to ensure that the holes drilled in the junction acrylic and the copper tubing was of the same inside diameter and that the centerline of the copper and acrylic were aligned.

Visual sections

Three visual sections were incorporated in the inlet and the two outlets. The main purpose of these sections was to identify both the inlet and outlet flow regimes. Each of the three visual sections on the inlet and outlet sides was machined in a $203.2 \times 90 \times 76.2$ mm acrylic block. Care was taken to ensure that the inside diameter of the holes drilled into the visual sections were identical to the inside diameter of the copper tubing before and after the visual section. Each visual section was provided with two flanges so as to connect it with the copper tubing, and O-rings were used for sealing. Extreme care was taken to ensure alignment and coaxiality between the visual sections and the rest of the test section as explained in a previous section.

3.2.3 Lifting and Rotating Mechanisms

The lifting mechanism is shown schematically in Fig. 3.5. The lifting mechanism consisted of two gears connected to a stationary (base) frame along which a steel rack connected to a moving frame that can slide vertically. The aluminum frame with the test

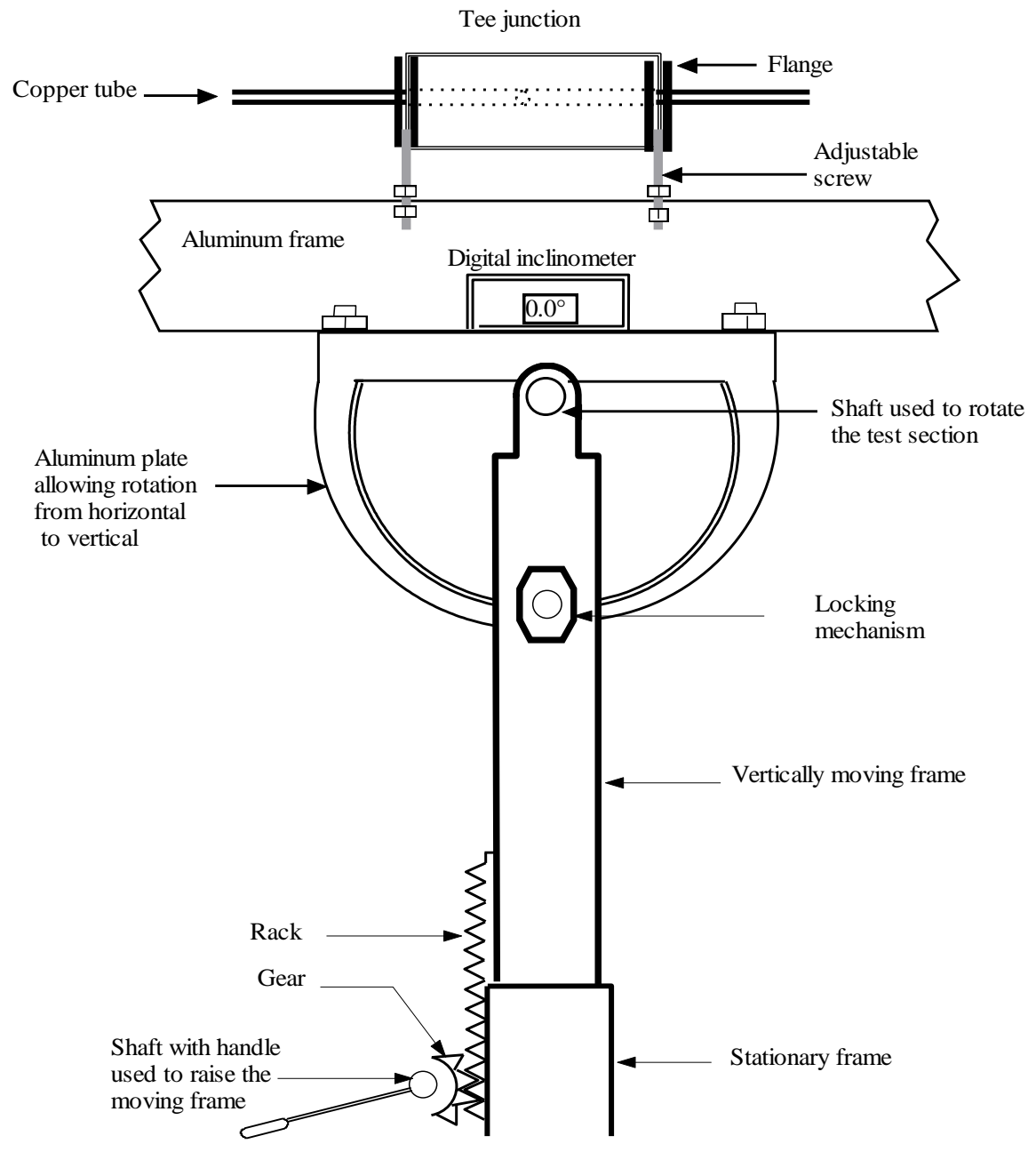


Fig. 3.5 Schematic diagram of the lifting and rotating mechanisms where the system appears in the horizontal position

section on top of it was mounted on top of the vertically moving frame using a rotating stainless steel shaft. The height of the test section was adjusted so that Outlet 2 could be drained into the separation tank. This was done by turning the gears manually lifting the test section to the desired height. The two outlets were inclined to the desired angle manually by rotating the test-section shaft around its axis. The aluminum frame was locked in place by means of a bolt and a nut once the desired angle of inclination was achieved. The base frame was mounted on adjustable wheels used as an additional means to ensure the horizontality of the test section.

3.2.4 Mixer

The entire mixer was made of copper tubing and fittings soldered together as shown in Fig. 3.6. A perforated tube (holes 1.6 mm in diameter) of 12.7-mm I.D. was fitted inside a larger tube of 51-mm I.D. and used to inject water into the air stream coming to the mixer through the larger tube. The two-phase mixture emerging from the mixer was directed into the inlet tube (13.5-mm I.D.) and allowed to become fully developed before entering the tee junction.

3.2.5 Separation Tanks

The two separation tanks were identical in design. Both were made of Type 304 stainless steel Sch. 40 pipe sections. Figure 3.7 shows a schematic diagram of the tank including detailed dimensions and location of the nozzle, the three baffles, the two abrupt changes in cross-sectional area, sight glass, pressure gauge, and safety valve. The two-phase mixture entering the top of the separation tank was separated by means of

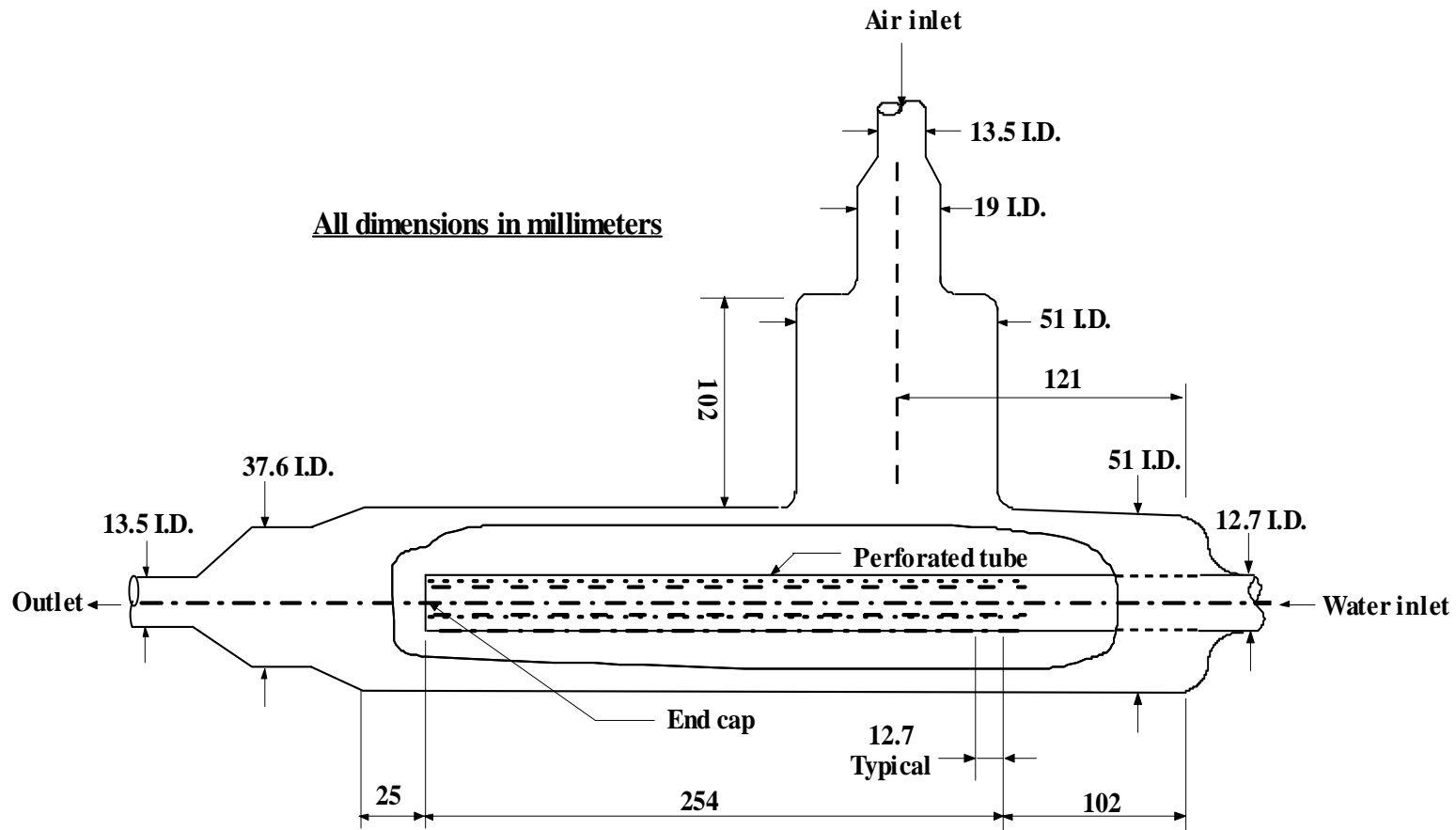


Fig. 3.6 Schematic of the two-phase mixer; slightly modified from El-Shaboury (2005)

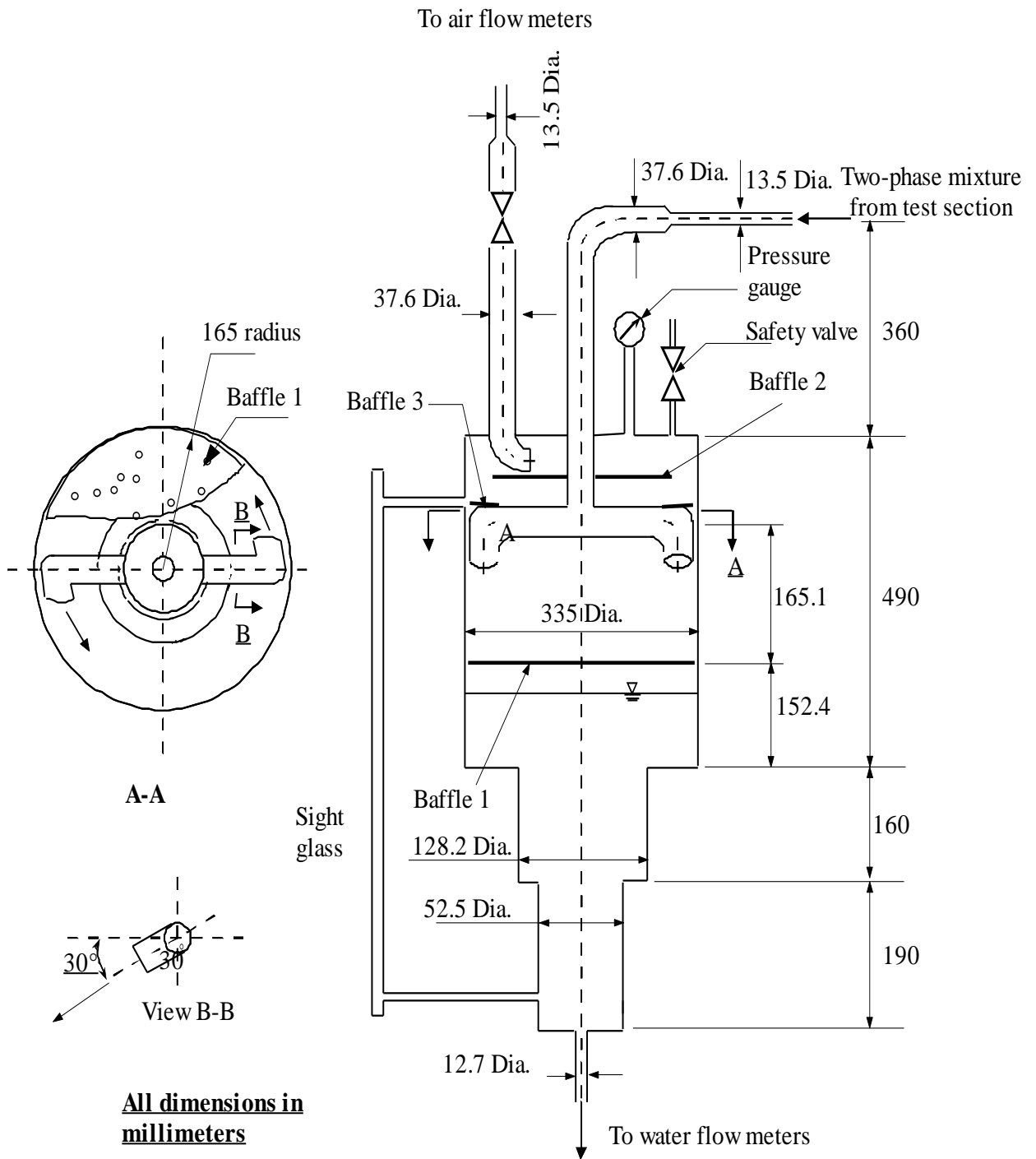


Fig. 3.7 Details of the separation tank; slightly modified from El-Shaboury (2005)

centrifugal action. Water exiting the bottom of the tank drained downward and air exited from the top of the tank. Perforated stainless steel baffles were used to prevent the air exiting the top of the tank from entraining water droplets. The sections of different cross-sectional area allowed for sensitive control of the water level, depending on the flow rate, the smallest cross sectional area being associated with the smallest flow rate. A pressure gauge and a safety valve set at 735 kPa were installed on the tank top blind flange. All fittings connecting the tanks to the copper tubing were dielectric unions to eliminate rusting of the joints and contamination of the distilled water. It should be mentioned that both the mixer and the separation tanks used in the present investigation were those described in detail by El-Shaboury (2005).

3.2.6 Instrumentation

Several, carefully calibrated, instruments were used in this study to measure and control different variables in the flow loop. These variables include the pressure, mass flow rate, angle of inclination, and temperature. Tables 3.1 to 3.3 list the specification and duties of each instrument used in the flow loop. The pressures at the inlet air rotameters, inlet water rotameters, tee junction, separation tanks, and the two air outlets rotameters were measured using pressure gauges. The pressure gauges were calibrated with a dead-weight tester. The results of these calibrations are presented in Tables A1.1 through A1.8 of Appendix A. A feedback pressure controller (Fisher 4160K series) and a regulator were used to maintain a steady pressure of the air coming from the main supply line. Needle valves were installed upstream and downstream of the rotameter to control the flow rate through them. The temperature of air and water was measured at

Table 3.1 Specifications and duty of the air-flow-measurement instruments

Instrument	Specification	Measured variable
Rotameter AI-1	Brooks rotameter, Model: 1355EZ186 Range: 6.47-64.7 SLPM Float type: Ball – st. steel	Flow rate of inlet air (Side 1)
Rotameter AI-2	Brooks rotameter; Model: 1307EZ80 Range: 38.1-381 SLPM Float type: Conventional – st. steel	Flow rate of inlet air (Side 1)
Rotameter AI-3	Brooks rotameter, Model: 1307EZ84 Range: 200-2004 SLPM Float type: Conventional – st. steel	Flow rate of inlet air (Side 1)
Rotameter AO2-1	Brooks rotameter, Model: 1355EZ184 Range: 0.87-8.68 SLPM Float type: Ball – Sapphire	Flow rate of Outlet 2 air (Side 2)
Rotameter AO2-2	Brooks rotameter, Model: 1355EZ186 Range: 6.47-64.7 SLPM Float type: Ball – st. steel	Flow rate of Outlet 2 air (Side 2)
Rotameter AO2-3	Brooks rotameter, Model: 1307EZ80 Range: 38.1-381 SLPM Float type: Conventional – st. steel	Flow rate of Outlet 2 air (Side 2)
Rotameter AO2-4	Brooks rotameter, Model: 1307EZ84 Range: 200-2004 SLPM Float type: Conventional – st. steel	Flow rate of Outlet 2 air (Side 2)
Rotameter AO3-1	Brooks rotameter Model: 1114DG41AEHAA Range: 0.86-8.6 SLPM Float type: Ball– Glass	Flow rate of Outlet 3 air (Side 3)
Rotameter AO3-2	Brooks rotameter, Model: 1307EZ186 Range: 4.64-46.4 SLPM Float type: Ball – sapphire	Flow rate of Outlet 3 air (Side 3)
Rotameter AO3-3	Brooks rotameter, Model: 1307EZ80 Range: 38.1-381 SLPM Float type: Conventional – st. steel	Flow rate of Outlet 3 air (Side 3)
Rotameter AO3-4	Brooks rotameter, Model: 1307EZ79 Range: 72.9-729 SLPM Float type: Conventional – st. steel	Flow rate of Outlet 3 air (Side 3)

Table 3.2 Specifications and duty of the water-flow-measurement instruments

Instrument	Specification	Measured variable
Rotameter WI-1	Brooks rotameter, Model: 1355EZ183, Range: 8.54-85.4 cm ³ /min Float type: Ball – sapphire	Flow rate of inlet water (Side 1)
Rotameter WI-2	Brooks rotameter, Model: 1355EZ182, Range: 49.14-491.4 cm ³ /min Float type: Ball – st. steel	Flow rate of inlet water (Side 1)
Rotameter WI-3	Brooks rotameter, Model: 1307EZ81, Range: 250-2955 cm ³ /min Float type: Conventional – st. steel	Flow rate of inlet water (Side 1)
Rotameter WO2-1	Brooks rotameter Model: 1114DC91BDHAA Range: 1.0-10.0 cm ³ /min Float type: Ball – sapphire	Flow rate of Outlet 2 water (Side 2)
Rotameter WO2-2	Brooks rotameter Model: 1114DC71BDHAA Range: 7.45-74.5 cm ³ /min Float type: Ball – sapphire	Flow rate of Outlet 2 water (Side 2)
Rotameter WO2-3	Brooks rotameter Model: 1114DG41BDHAA Range: 48.5-485 cm ³ /min Float type: Ball – st. steel	Flow rate of Outlet 2 water (Side 2)
Rotameter WO2-4	Brooks rotameter Model: 1114DJ41BDHAA Range: 295-2950 cm ³ /min Float type: Conventional – st. steel	Flow rate of Outlet 2 water (Side 2)
Rotameter WO3-1	Brooks rotameter Model: 1114DC91BDHAA Range: 1.0-10.0 cm ³ /min Float type: Ball – Sapphire	Flow rate of Outlet 3 water (Side 3)
Rotameter WO3-2	Brooks rotameter Model: 1114DC71BDHAA Range: 7.45-74.5 cm ³ /min Float type: Ball – Sapphire	Flow rate of Outlet 3 water (Side 3)
Rotameter WO3-3	Brooks rotameter Model: 1114DG41BDHAA Range: 48.5-485 cm ³ /min Float type: Ball – st. steel	Flow rate of Outlet 3 water (Side 3)
Rotameter WO3-4	Brooks rotameter: Model: 1114DJ41BDHAA Range: 295-2950 cm ³ /min Float type: Conventional – st. steel	Flow rate of Outlet 3 water (Side 3)

Table 3.3 Specifications and duty of the pressure-measurement instruments

Instrument	Specification	Measured variable
Pressure gauge No.1	Marshall town Bourdon gauge Range: 0-689.8 kPa	Before pressure controller
Pressure gauge No.2	USG Bourdon gauge Range: (0-1100 kPa	After the pressure controller
Pressure gauge No.3	USG Bourdon gauge Range: 0-689.8 kPa	Pressure of the air at the inlet rotameters
Pressure gauge No.4	Ashcroft gauge Range: 0-413.9 kPa	Pressure of the water at the inlet rotameters
Pressure gauge No.5	Wika Bourdon gauge Range: 0-413.9 kPa	Pressure at the tee junction inlet (Side1)
Pressure gauge No.6	Marshall town Bourdon gauge Range: 0-413.9 kPa	Pressure in the separation tank of Outlet 2
Pressure gauge No.7	Marshall town Bourdon gauge Range: 0-413.9 kPa	Pressure in the separation tank of Outlet 3
Pressure gauge No.8	USG Bourdon gauge: Range; 0-689.8 kPa	Pressure of the air at the rotameters (Outlet 2)
Pressure gauge No.9	USG Bourdon gauge Range: 0-689.8 kPa	Pressure of air at the rotameters (Outlet 3)

six different locations using iron-constantan thermocouples. The thermocouples were calibrated at the ice and room temperature using precision thermometers with a discrimination of 0.1°C. The difference between the thermocouple reading and the thermometer reading was within ± 0.5 °C. A digital protractor (Pro 3600 digital protractor, Angle Sensor Technology) with a resolution of 0.1° was used to measure the outlet angle of inclination. The protractor was attached to the middle of the front side of the aluminum frame close to the junction.

Air and water flow rates were measured using rotameters with different capacities to allow for individual measurements. All rotameters were calibrated and the calibrations were compared against the manufacturers' values. In the working ranges, the calibrations for the rotameters were typically within $\pm 2\%$ (air) and $\pm 3\%$ (water) of the manufacturers' values. The in-house calibration values of the measuring instruments were used in the data analysis. Linear interpolation between any two consecutive points was used in the case of air and water rotameters as well as pressure gauges. The calibration results for the air and water rotameters are given in Tables A2.1 to A2.22 of Appendix A.

3.3 Phase-Redistribution Experiments

3.3.1 Experimental Procedure

The testing procedure was designed to examine the effect of outlet inclination on the two-phase (air-water) phase redistribution at an impacting tee junction. After the test section was set at the desired outlet inclination angle, the following numbered steps were followed in performing the tests. Reference should be made to Fig. 3.1.

1. The barometric pressure and ambient temperature were recorded.
2. The inlet and discharge valves at the separation tanks were left fully open.
3. The valve to the air supply line was gradually opened. The outlet pressure of the pressure controller was set at approximately 172 kPa-g (25 psig).
4. The control valve for the appropriate air inlet was selected and completely opened. The control valve located after the air inlet rotameters was adjusted to give the desired air inlet flow rate. The appropriate air outlets control valves were selected and adjusted simultaneously to give the desired junction pressure of 2.0 bar (abs).

5. The water inlet control valve was partially opened and the by-pass valve was fully opened.
6. The proper water inlet rotameter valve was fully opened and the water pump was switched on.
7. The control valve located after the water inlet rotameters was adjusted according to the desired water flow rate.
8. When the water level in the separation tanks reached a level at which it could be monitored easily, the appropriate outlet water rotameters were activated and the appropriate outlet control valves were adjusted to keep a steady level in the separation tanks.
9. The cooling water for the water storage tank was turned on. The test water flowing to the test section was kept at approximately 20 to 24°C.
10. The correct test-section pressure of 2.0 bar (abs) was maintained by continuously adjusting the air outlet's control valves. The water level in the separation tanks was kept steady by adjusting the outlet water flow rate using the water outlet's control valves. This iterative procedure was needed to achieve exactly the desired test conditions of inlet flow rate, test-section pressure, correct mass-split ratio and steady water level in the separation tanks.
11. With the desired test section pressure, desired inlet flow rate, and with a steady level of liquid in the separation tanks, the mass-split ratio W_3/W_1 was checked. If different from the desired value, it was adjusted using the air outlet's control valves. Adjustments were done to correct the mass-split ratio in a way such that the correct inlet mass flow rate and correct test-section pressure were maintained.

The water level in the separation tanks was kept steady once again by adjusting the outlet water using the control valves. If needed, this iterative procedure was carried out again until the desired operating conditions were completely achieved.

The time needed to achieve about 15 min of steady-state operation depended on the inlet flow regime and value of mass-split ratio (W_3/W_1); this time was between 45 and 60 min. During the steady-state period, the following parameters had to remain unchanged for at least 15 to 20 min before recording any phase-redistribution data.

- a. Inlet test section pressure.
- b. Inlet and outlet mass flow rate of both air and water.
- c. Water level in the separation tanks.
- d. The air and water pressure and temperature throughout the system.

Two other parameters were monitored after the recording of the phase-redistribution data; these were: the mass balances of both air and water. The percentage deviation between the inlet flow rate and the sum of the two outlet flow rates for each phase was called the mass-balance error. For both phases, this mass balance error never exceeded 3.1% throughout the entire experiments.

3.3.2 Reduction of Phase-Redistribution Data

Recorded values of W_{G1} , W_{L1} , W_{G2} , W_{L2} , W_{G3} , and W_{L3} were used to calculate the following parameters:

1. The total inlet, Outlet 2, and Outlet 3 mass flow rates were calculated by

$$W_1 = W_{G1} + W_{L1}, \quad (3.1)$$

$$W_2 = W_{G2} + W_{L2}, \quad (3.2)$$

and
$$W_3 = W_{G3} + W_{L3}. \quad (3.3)$$

2. The inlet, Outlet 2, and Outlet 3 qualities were calculated by

$$x_1 = W_{G1} / W_1, \quad (3.4)$$

$$x_2 = W_{G2} / W_2, \quad (3.5)$$

and
$$x_3 = W_{G3} / W_3. \quad (3.6)$$

3. The fraction of total inlet gas entering Outlet 3 and the fraction of total inlet liquid entering Outlet 3 were calculated by

$$F_{G3} = W_{G3} / W_{G1}, \quad (3.7)$$

and
$$F_{L3} = W_{L3} / W_{L1}. \quad (3.8)$$

4. The ratio of Outlet 3 to inlet quality, x_3/x_1 , was calculated.

5. The density of inlet air was calculated by

$$\rho_{G1} = P_s / (0.287(T_s+273.15)). \quad (3.9)$$

6. The gas inlet superficial velocity and liquid inlet superficial velocity were calculated by

$$J_{G1} = W_{G1} / \rho_{G1} (\pi/4 D^2), \quad (3.10)$$

and
$$J_{L1} = W_{L1} / \rho_{L1} (\pi/4 D^2). \quad (3.11)$$

3.4 Full-Separation Experiments

3.4.1 Experimental Procedure

The testing procedure was designed to determine the limiting inlet conditions for which the impacting tee junction can perform as a full separator at various inclination angles of the outlets. All experiments were conducted at a steady test-section pressure of

$P_s = 2$ bar (abs) and ambient temperature. The angles of inclination that were employed in the experiments were $\theta = 2.5^\circ, 7.5^\circ, 15^\circ, 30^\circ, 60^\circ, 75^\circ,$ and 90° .

For each inclination angle, the air outlet valve for Side 3 of the junction and the water outlet valve for Side 2 were closed. Air and water inlet flows were induced at rates that gave full separation (i.e., $W_{G2} = W_{G1}$ and $W_{L3} = W_{L1}$). The liquid flow out from the separation tank connected to Outlet 3 was adjusted to maintain a steady liquid level in the separation tank throughout the experiment. For experiments with $J_{G1} < 1$ m/s, the value of W_{L1} was increased very slowly (at a rate of about 1% per minute) while maintaining steady values of J_{G1} and P_s . This procedure continued until a critical condition was reached where the liquid began being entrained in the upward gas stream. This condition was characterized by the continuous flow of a liquid stream or liquid drops from the air-water interface at the junction to the separation tank connected to Side 2. The onset of this critical condition was determined visually through the clear acrylic test section, the visual section on Side 2, and the clear Tygon tubing connecting Side 2 with its separation tank. For experiments with $J_{G1} > 1$ m/s, the value of W_{G1} was increased slowly while maintaining W_{L1} and P_s constant until the critical condition of liquid entrainment in Side 2 was reached. The full-separation data reported later correspond to the inlet conditions (J_{L1} and J_{G1}) immediately before the onset of liquid entrainment at each inclination angle θ .

3.4.2 Recording of Full-Separation Data

The operating conditions immediately before the onset of liquid entrainment in Side 2 were recorded. These data consisted of the following parameters:

1. The atmospheric pressure.
2. The absolute test-section pressure, P_s , in Pa.

3. Inlet air temperature T_s , in °C.
4. Angle of inclination, θ .
5. Air and water inlet mass flow rates, W_{G1} and W_{L1} , in kg/s, respectively, from which J_{G1} and J_{L1} were calculated.
6. The percentages of air and water mass-balance errors.

3.5 Effect of Outlet Length

3.5.1 Introduction

It should be noted that the total length of each outlet, which does not include the tygon tube connecting the outlet to the separation tank, was 1.113 m, as shown in Fig. 3.2. Early observations during the phase-redistribution experiments showed that under certain conditions, a stationary layer of liquid was formed to a certain length in Side 2, but no liquid flowed into the separation tank of Outlet 2. By increasing the gas flow rate or reducing the inclinations angle, the liquid eventually flowed into the separation tank.

Similar observations were made during the full-separation experiments. It was observed that at certain inlet conditions, i.e., $60^\circ \leq \theta \leq 90^\circ$ and $J_{G1} < 3$ m/s, and near the limiting condition of full separation, the inlet flow regime approaching the junction was either slug or plug. As the liquid phase started to entrain in the gas flow in Side 2, a churning zone of gas and liquid formed at the lower part of Outlet 2 near the junction extending to a certain length in Side 2. Full separation existed and no flow of liquid was observed into the separation tank of Outlet 2. Changing the inlet conditions by a small increase in J_{L1} or J_{G1} beyond this point, a limiting condition was reached whereby liquid was pulled up by the gas flow all the way through Side 2.

These observations indicate that, under such conditions the length of the outlet may have an effect on both phase-redistribution and full-separation data. Necessary modifications of the test rig were made and experimental tests were carried out to study such effects. The tests involved repeating some of the phase-redistribution data groups while the effect of outlet length was examined for the entire sets of data for full separation.

3.5.2 Procedure for Phase-Redistribution Experiments with Short Outlets

Outlets

The testing procedure was designed to examine the effect of outlet length on the two-phase (air-water) phase redistribution at an impacting tee junction. The experiments were done after reducing the length of each outlet to about 17.8 tube diameters as shown in Fig. 3.8. Phase-redistribution data were acquired only for part of the inlet conditions tested using long outlets. The inlet conditions tested with short outlets were selected to highlight the effect of inlet flow regimes and various inclination angles.

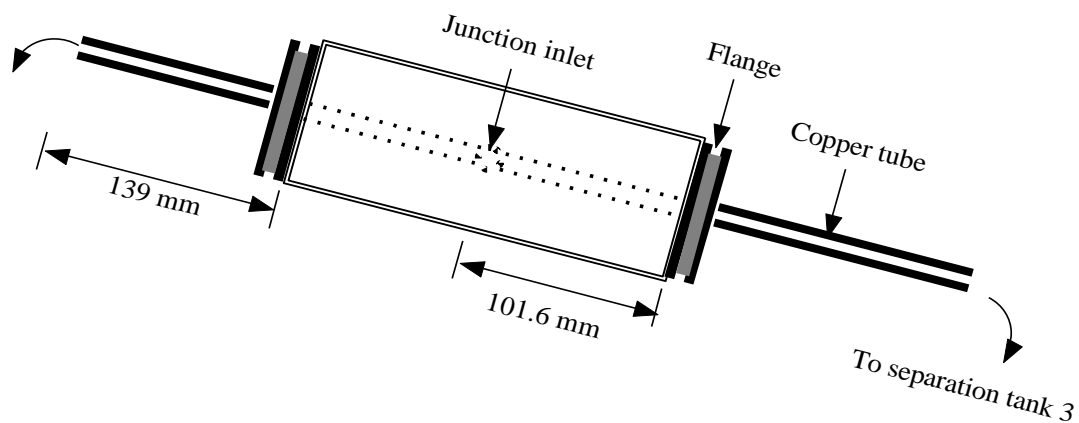


Fig. 3.8 Tee-junction with short outlets

The inlet conditions tested included stratified, wavy, and annular inlet flow regimes. Details of the data range tested with short outlets are given in Chapter 4. Experimental procedures consisted of steps identical to those used during the experiment with long outlets. Data were recorded and used to calculate phase-redistribution parameters. Results were plotted in F_{G3} versus F_{L3} and compared to those obtained from experiments with long outlets.

3.5.3 Procedure for Full-Separation Experiments with Short Outlets

Since it was difficult to discern the flow beyond the transparent part of the test, it was decided to use only the length of the transparent part of the test section to determine whether full separation occurred or not. The full-separation data obtained for short outlets at any given value of θ correspond to values of J_{G1} and J_{L1} immediately after the liquid in Outlet 2 passed the transparent part of the test section. Full-separation experiments were acquired for the whole range tested using long outlets. The procedure followed in these experiments was identical to that used in the experiments with long outlets. The split mechanism and the flow characteristics at the three sides of the junction were visually observed. The visual observations were expected to help understand the split mechanism and in turn to aid in developing a correlation capable of predicting the limiting conditions for full separation.

A Sony HD 1080 video camera was positioned just in front of the test section and video footage was then recorded and analyzed. For each set of inlet flow conditions, the video footage was analyzed in order to observe qualitatively the mechanism of the flow split at the junction and to inspect visually the upward flow as it passed the clear part of the test section.

CHAPTER 4

RESULTS AND DISCUSSION

4.1 Data Range

The present experimental investigation consists of two components: phase-redistribution experiments and full-separation experiments. The phase-redistribution data generated in this experimental investigation consist of seven “data sets”. Each data set corresponded to a fixed combination of J_{G1} and J_{L1} , fixed test section pressure and temperature. Each data set consisted of a number of “data groups”. Each data group corresponded to a fixed inclination angle θ and consisted of a number of data points. Each data point corresponded to a fixed mass split ratio W_3/W_1 between 0 and 1. The range of angles of inclination tested varied with the inlet flow conditions and ranged from horizontal to less than 1.0° for some inlet conditions to a range from horizontal to vertical for other inlet conditions.

The number of angles of inclination that was tested for each inlet condition was between 4 and 7 angles. The total number of data groups for all data sets and all inclination angles was 40 data groups. Seven of those groups were performed with a tee junction with a horizontal inlet and horizontal outlets. The whole range of W_3/W_1 was covered in each data group. The total number of data points for all inlet conditions and all angles of inclination was 390 data points with 28 more data points generated for repeatability purposes. The nominal test-section pressure was 200 kPa (abs) \pm 2.0 kPa, while the junction temperature was $22^\circ\text{C} \pm 2.0^\circ\text{C}$ throughout the investigation. Overall mass balances were performed individually on both the air and water streams. The mass-

balance errors were defined as the percentage deviation between the inlet flow rate of a specific phase and the sum of its two outlet flow rates. The mass balance error is positive when the sum of the two outlets flow rates is greater than the inlet flow rate and vice versa. The air mass-balance error was within $\pm 2.3\%$ and the water mass-balance error was within $\pm 3.1\%$. The largest deviation of both air and water mass balance occurred at the lowest J_{G1} or J_{L1} . Table 4.1 shows the range of operating conditions for the two-phase test runs for the tee junction with both horizontal and inclined outlets while Tables B1 and B2 in Appendix B give the complete set of phase-redistribution data and mass flow rates, respectively.

Table 4.1 Ranges of operating conditions for phase-redistribution experiments

Total number of data points	390
Inlet flow regimes	Stratified, wavy, and annular
Mass-split ratio, W_3/W_1	0.0 – 1.0
Angle of inclination, θ	Horizontal to vertical
Inlet superficial gas velocity, J_{G1} , in m/s	2.0 - 40
Inlet superficial liquid velocity, J_{L1} , in m/s	0.01 – 0.18
Test-section pressure, P_s , in kPa (abs)	200 ± 2.0
Temperature, in $^{\circ}\text{C}$	22 ± 2.0
Inlet quality, x_1	0.1 – 0.9
Air-mass balance errors, in %	Within ± 2.3
Water-mass balance errors, in %	Within ± 3.1

Figure 4.1 shows the nominal J_{G1} and J_{L1} for the 7 inlet conditions plotted on the Mandhane et al. (1974) flow-regime map. The boundaries shown are typical for systems

with low pressure, air-water flows, and small diameter pipes (less than 51 mm). The actual values of J_{G1} and J_{L1} during the experimental investigation for all data points were kept within $\pm 1.0\%$ of the nominal values. The labeling of the seven data sets in Fig. 4.1 is according to the observed inlet flow regimes. The three major flow regimes (stratified (St), wavy (Wa), and annular (An)) were identified using the description given in Mandhane et al. (1974). Very good agreement can be seen between the visually observed inlet flow regimes and the flow regimes predicted by the map.

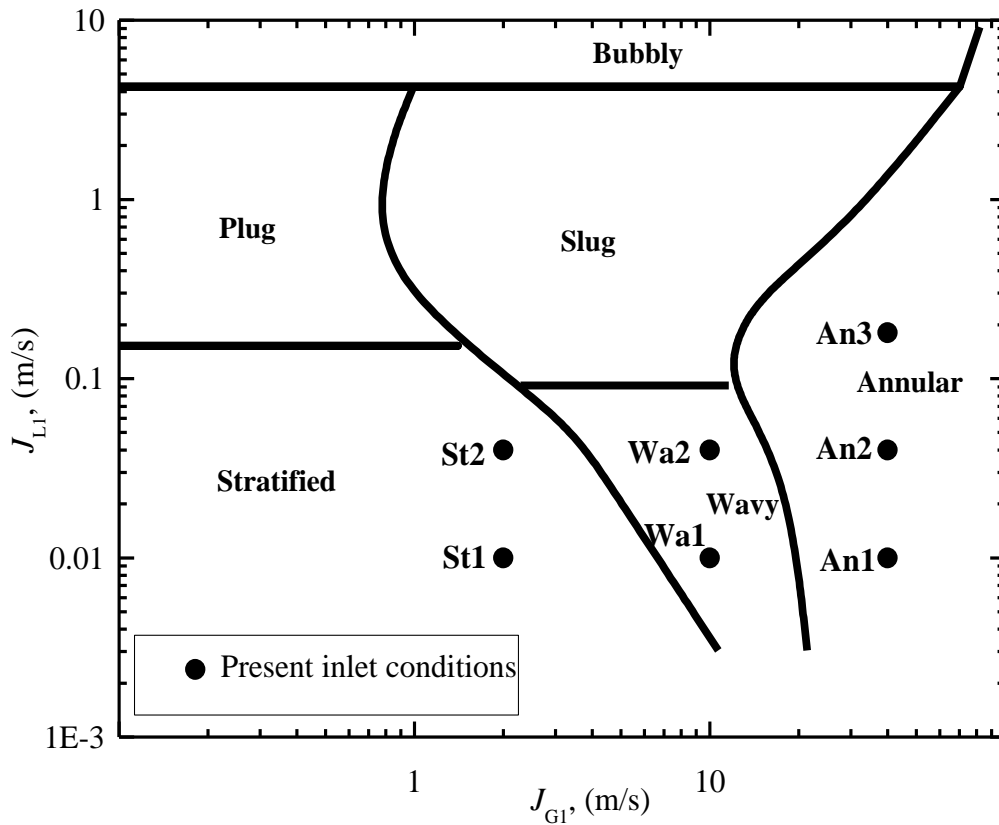


Fig. 4.1 Inlet conditions for phase-redistribution experiments plotted on the Mandhane et al. (1974) flow-regime map

The full-separation data generated in this experimental investigation consist of seven data groups. Each data group corresponded to a fixed angle of inclination. The angles of inclination that were employed in this investigation were inclination angles θ of 2.5°, 7.5°, 15°, 30°, 60°, 75°, and 90°. For each angle, the limiting values of J_{G1} , and J_{L1} , for full separation were determined. The air-mass balance error was within $\pm 3.9\%$ for 84% of the data; these data corresponded to $J_{G1} > 0.2$ m/s. The water mass-balance error was within $\pm 7.0\%$ for 84% of the data; these data corresponded to $J_{L1} > 0.0025$ m/s. At any data point, full separation was initially obtained in the junction at sufficiently low values of J_{G1} and J_{L1} with all the gas flowing into Side 2 and all the liquid flowing into Side 3. Starting from this condition and gradually increasing either J_{G1} or J_{L1} , limiting values of the inlet conditions were reached whereby liquid started to flow into Side 2. Table 4.2 shows the range of operating condition for the full-separation test runs while Table B3 in Appendix B gives the complete set of full-separation data.

Table 4.2 Ranges of operation conditions for full-separation experiments.

Total number of data points	80
Inlet flow regimes	Stratified, wavy, slug, and plug
Angle of inclination, θ	2.5° to 90°
Inlet superficial gas velocities, J_{G1} , in m/s	0.1 – 13.5
Inlet superficial liquid velocities, J_{L1} , in m/s	0.001 – 0.25
Test-section pressure, P_S , in kPa (abs)	200 \pm 2.0
Temperature, in °C	22 \pm 2.0
Inlet quality, x_1	0.00096 – 0.96
Air-mass balance errors, in %	Within ± 3.9 for $J_{G1} > 0.2$ m/s
Water-mass balance errors, in %	Within ± 7.0 for $J_{L1} > 0.0025$ m/s

4.2 Measurement Uncertainty

An uncertainty analysis was conducted for both the phase-redistribution and full separation data. The analysis was based on the method outlined by Moffat (1988). All uncertainties given in the current study are meant to accommodate: discrimination uncertainties in the measuring instruments, the error in fitting an equation (for computer data reduction) to the calibration data, the accuracy of the calibrating devices, and unsteadiness in the process. A summary of the analysis is given here and a complete set of results is given in Appendix C.

The pressure gauges were calibrated using a deadweight tester, thermocouples (at the ice point and room temperature) using thermometers with a discrimination of 0.05°C , gas rotameters using wet-test meters and venturi meters (in turn the calibration of which are traceable to NIST standards), and liquid rotameters using a weigh-and-time method. In the working ranges, the calibrations of the rotameters were typically within $\pm 2\%$ (air) and $\pm 3\%$ (water) of the manufacturers' values. For all experiments, the uncertainties in θ , D , P_s , and T_s (throughout the flow loop) were found to be within $\pm 0.1^{\circ}$, $\pm 1.5\%$, $\pm 1.8\%$, and $\pm 0.2^{\circ}\text{C}$, respectively.

For phase-redistribution experiments, the inlet flow rates of liquid (W_{L1}) and gas (W_{G1}), and the inlet quality (x_1) the uncertainties were found to be within $\pm 2.8\%$, $\pm 3.8\%$, and $\pm 4.1\%$, respectively. Higher uncertainties were found in the outlet flow rates because of their smaller values relative to the inlet. For W_{L2} the uncertainty was within $\pm 5\%$ for 84% of the data and within $\pm 10\%$ for the remaining data, for W_{L3} the uncertainty was within $\pm 4\%$ for 95% of the data and within $\pm 8.5\%$ for the remaining data, for W_{G2} the uncertainty was within $\pm 6\%$ for 92% of the data and within $\pm 8.9\%$ for the remaining data,

and for W_{G3} the uncertainty was within $\pm 6\%$ for 75% of the data and within $\pm 9.4\%$ for the remaining data. The uncertainty in the inlet superficial velocities of liquid (J_{L1}) and gas (J_{G1}) were found to be within $\pm 4.1\%$ and $\pm 6.4\%$, respectively. Finally, the important parameters used in plotting the phase-distribution data, F_{L3} and F_{G3} , had uncertainties within $\pm 4\%$ for 84% of the data and within $\pm 8.6\%$ for the remaining data for F_{L3} , and uncertainties within $\pm 7\%$ for 83% of the data and within $\pm 10\%$ for the remaining data for F_{G3} . Table C1 in Appendix C gives detailed results of the uncertainty measurements for the phase-redistribution data.

For full-separation experiments, overall mass balances were performed individually on both the air and water streams. For data points with $J_{G1} \leq 0.2$ m/s, the inlet gas flow rate was too small to be measured within the acceptable range (10% of the scale) of the smallest rotameter. The outlet air flow rate leaving Side 2 was measured by the appropriate rotameter and assumed to be equal to the inlet flow rate. The air mass balance was not considered in these cases. For data with $J_{G1} > 0.2$ m/s, the air mass-balance error was within $\pm 3.9\%$. The water mass-balance error was within $\pm 7.0\%$ for 84% of the data; these data corresponded to $J_{L1} > 0.0025$ m/s. The uncertainties in W_{G1} and W_{L1} were found to be within $\pm 7.7\%$ and $\pm 3.0\%$, respectively (data points with $J_{G1} \leq 0.2$ m/s and $J_{L1} \leq 0.0025$ m/s were not included). The uncertainties in J_{G1} and J_{L1} were found to be within $\pm 9.3\%$ and $\pm 4.2\%$, respectively (data points with $J_{G1} \leq 0.2$ m/s and $J_{L1} \leq 0.0025$ m/s were not included). Table C2 in appendix C gives the complete set of uncertainty measurement for the full-separation data.

4.3 Test Loop Symmetry and Reliability

Before the testing began, the adequateness of the test loop had to be proven by

ensuring both its symmetry and its ability to reproduce published data under similar conditions. Phase-redistribution data for inlet conditions ST1, Wa2, and An3 were generated over the full range of mass-split ratios with $\theta = 0^\circ$ and $P_s = 200$ kPa. The symmetry of an equal-sided impacting tee junction require that all data lines should pass through the point $F_{G3} = F_{L3} = 0.5$. Also, in order to satisfy the mass balance, the two parts of the curve before and after the 0.5 point should be an inverted mirror image of each other. Figure 4.2 shows that the data lines of the conducted experiments obey the expected behavior imposed by symmetry. Such results indicate that the test loop is symmetric around the inlet centerline.

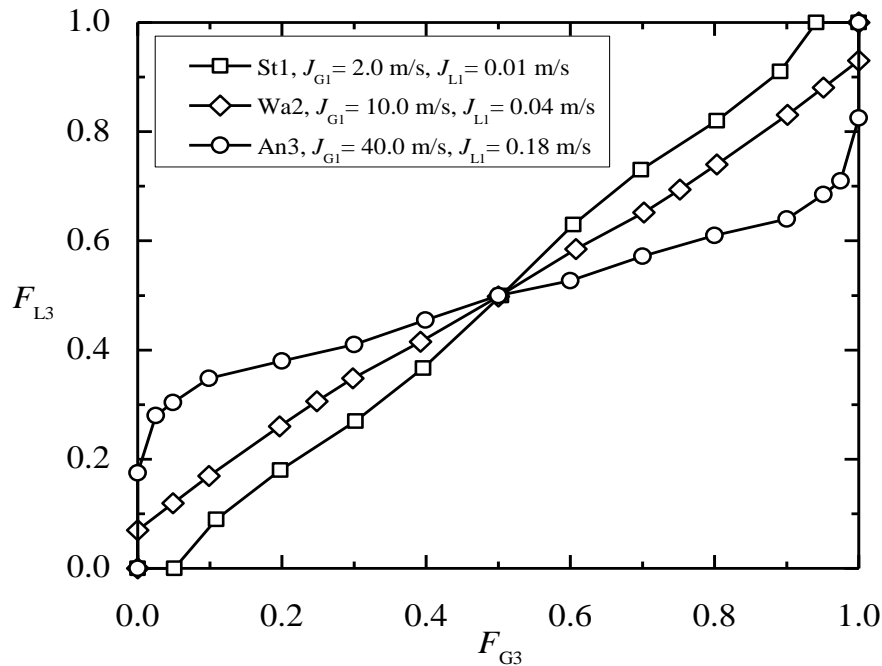


Fig. 4.2 Illustration of test-loop symmetry for data groups St1, Wa2, and An3 with a horizontal inlet and horizontal outlets

After the symmetry of the loop was proven, it was decided to check its ability to produce reliable results. This was done by generating some of the phase-redistribution results reported in earlier research. Three full runs under inlet conditions similar to those tested by El-Shaboury (2005) were conducted. The three data sets were selected such that they include one stratified inlet flow regime (St1), one wavy inlet flow regime (Wa2), and one annular inlet flow regime (An2). El-Shaboury obtained phase-redistribution data for two-phase mixtures of air and water with an equal-sided impacting tee junction (37.8 mm I.D.) at $P_s = 150$ kPa. His work was selected because of the similarity of the inlet conditions covered by his work and the present study. Figure 4.3 shows data corresponding to inlet conditions St1, Wa2, and An2 at $P_s = 150$ kPa. The figure shows

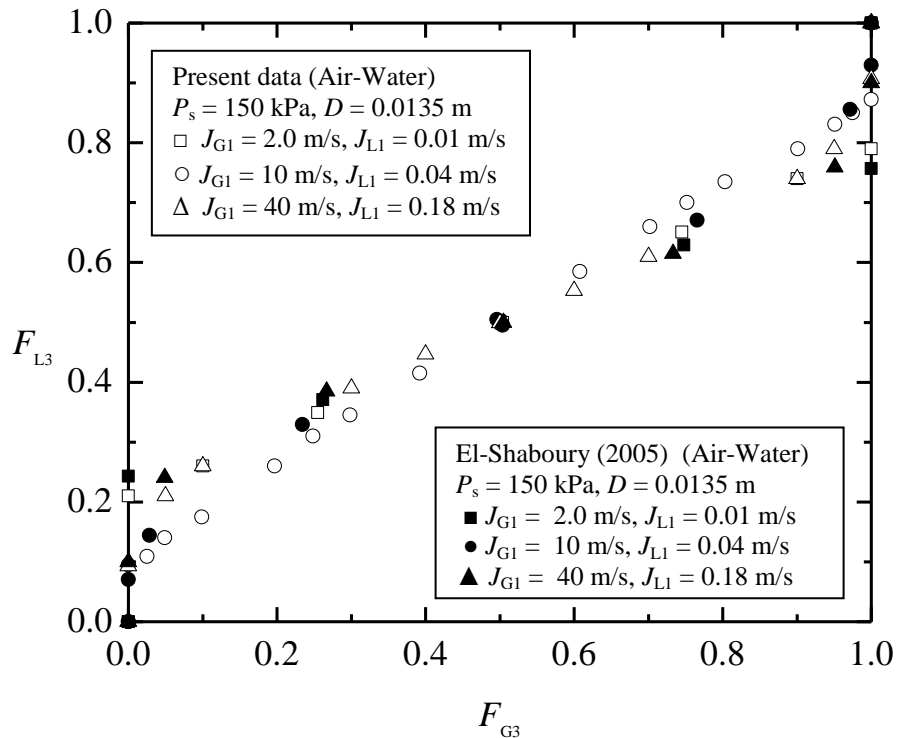


Fig. 4.3 Comparison between the present data of St1, Wa2, and An2 and similar data from El-Shaboury, (2005) at $P_s = 150$ kPa

good agreement between the present data and those of El-Shaboury for the entire range of mass extraction ratios between 0 and 1.0. All data lines seem to obey the symmetry conditions which are further proof that the test loop is symmetric around the inlet centerline. The difference in diameter and experimental error would probably account for the slight deviation between the two data sets.

4.4 Phase-Redistribution Data

4.4.1 Overview

The phase-redistribution data for an impacting tee junction with a horizontal inlet and inclined outlet obtained in this study are presented in this section. A total number of 4 to 7 angles of inclination were tested for every inlet condition. The data are plotted graphically using F_{L3} , where $F_{L3} = W_{L3}/W_{L1}$ versus F_{G3} , where $F_{G3} = W_{G3}/W_{G1}$. Geometric symmetry is expected to disappear as a result of outlet inclination. Consequently, the data lines will not pass through the ($F_{G3} = F_{L3} = 0.5$) symmetry point.

4.4.2 Data of the Stratified Flow Regime

Figures 4.4 and 4.5 show the phase-redistribution data for stratified-flow data sets St1 and St2, respectively at various angles of inclination. These data were obtained at fixed $J_{G1} = 2.0$ m/s and two values of J_{L1} ($J_{L1} = 0.01$ and 0.04 m/s), corresponding to $x_1 = 0.32$ and 0.10 for St1 and St2, respectively. For the special case of horizontal outlets ($\theta = 0^\circ$), most of the data points in set St1 lie close to the line of even phase redistribution

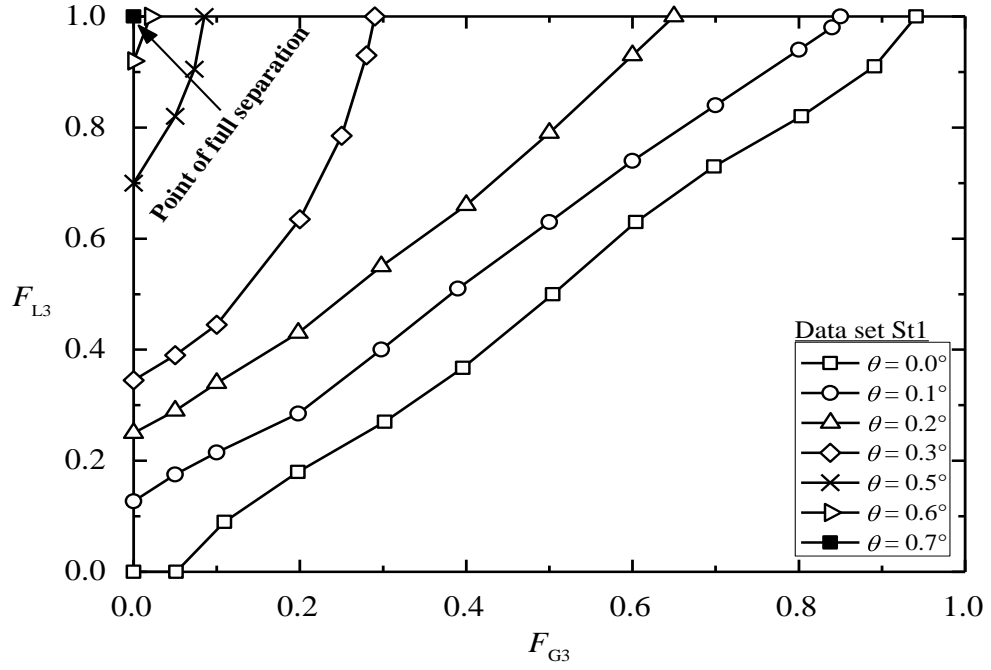


Fig. 4.4 Phase-redistribution data for stratified flow (St1)

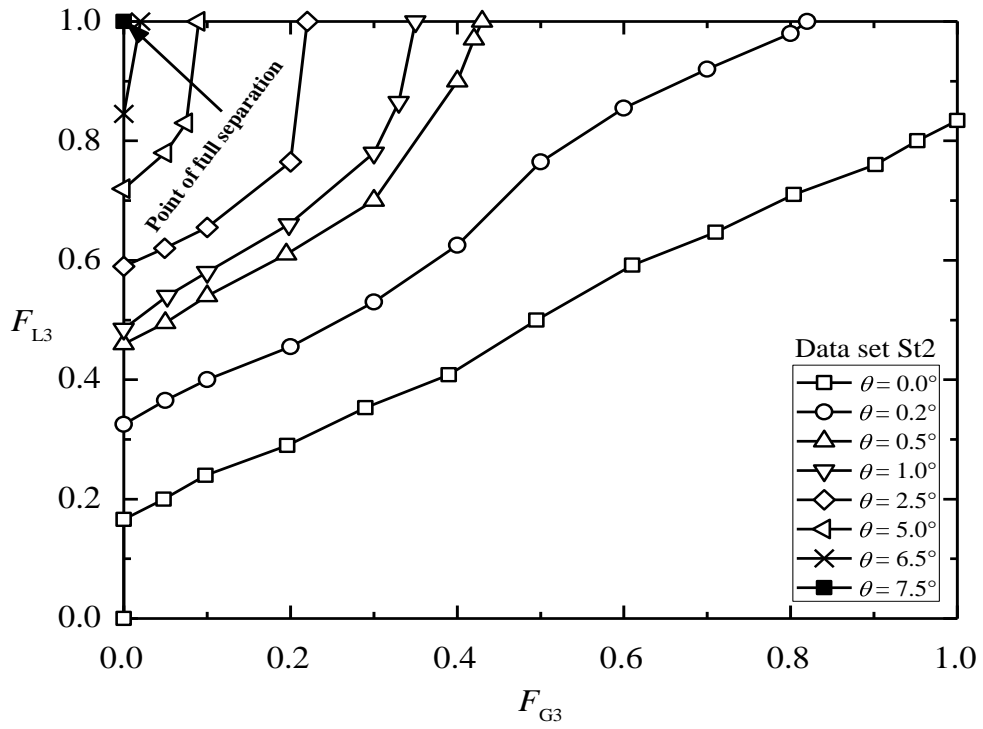


Fig. 4.5 Phase-redistribution data for stratified flow (St2)

(i.e., along the line of $F_{L3} = F_{G3}$). On the other hand, data set St2 shows significant maldistribution of phases, except around the point $F_{L3} = F_{G3} = 0.5$. The two cases of horizontal outlets illustrate that as J_{L1} increases at a fixed J_{G1} there is an increasing preference of the liquid phase to exit through Outlet 3 over the range $0.0 < F_{G3} < 0.5$. This trend is consistent with the observation made by other researchers, as reported by El-Shaboury et al. (2006). As the outlets were inclined, the water was more readily diverted to Outlet 3 as compared to the case where Outlet 3 was horizontal. For data set St1, data were acquired with Outlet 3 inclined downward by 0.1° , 0.2° , 0.3° , 0.5° , 0.6° and 0.7° . The results show a strong dependence of the splitting phenomenon on the outlet angle of inclination with the liquid preference to exit through Side 3 increasing as the angle increases. At an angle of 0.1° , the entire liquid flows in Side 3 over the range of $0.85 \leq F_{G3} \leq 1.0$ and for the angle of 0.5° , the entire liquid flows in Side 3 over the range of $0.085 \leq F_{G3} \leq 1.0$. With an angle of inclination of 0.7° , the gravity force acting on the liquid phase became so high to the point that no liquid phase was observed in Outlet 2 over the entire range of $0.0 > F_{G3} > 1.0$. An inclination angle of 0.7° was enough to achieve full separation of phases where the entire liquid phase flows downward while the entire gas phase flows upward at all mass splits. Figure 4.5 shows the experimental results of data set St2. Data were acquired for inclinations between 0° and 7.5° . The trends in these data are similar to those observed in Fig. 4.4. In comparison with the previous case (St1), an angle of 7.5° was required to achieve full separation of the phases.

4.4.3 Data of the Wavy Flow Regime

Figures 4.6 and 4.7 show the phase-redistribution data for sets Wa1 and Wa2,

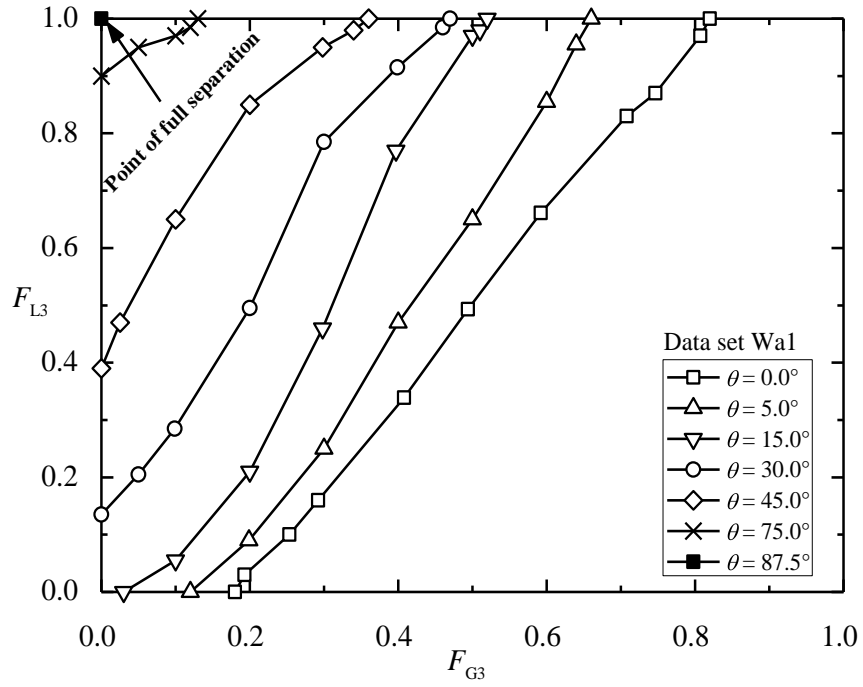


Fig. 4.6 Phase-redistribution data for wavy flow (Wa1)

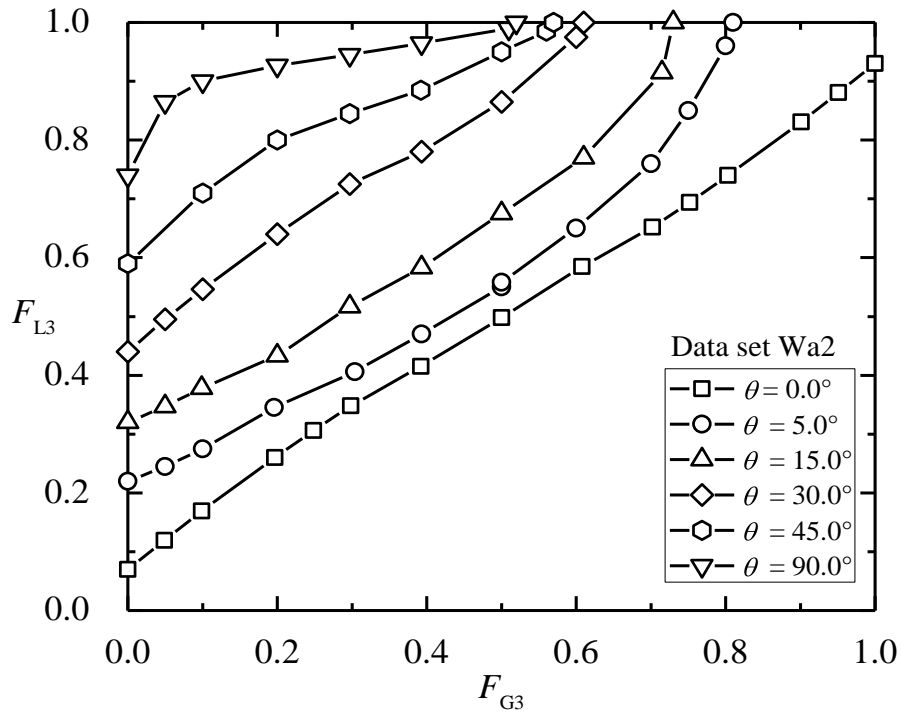


Fig. 4.7 Phase-redistribution data for wavy flow (Wa2)

respectively, of the wavy flow regime. It can be seen from the figures that the observations on the stratified flow are valid for these data. For the case of horizontal outlets ($\theta = 0^\circ$), the data line of data set Wa1 with $x_1 = 0.7$ lies below the line of even phase distribution over the range $0.0 < F_{G3} < 0.5$. For data set Wa2 with $x_1 = 0.37$, the data line lies above the line of even phase distribution over the range $0.0 < F_{G3} < 0.5$. These results show that there is a continuous trend in the data such that as x_1 increases, the data line rotates around the point (0.5, 0.5) in a counter-clockwise direction. This observed effect of x_1 is consistent with the case of stratified flow (seen in Figs. 4.4 and 4.5) and also consistent with the observation made by Ottens et al. (1995) and El-Shaboury (2006) for the same flow regimes. Data were also acquired for the inlet regime of wavy flow with inclined outlets. The results for data set Wa1 are shown in Fig. 4.6. An angle of 87.5° was required to achieve full separation of the phases. Figure 4.7 shows the experimental results for data set Wa2 with inclination angles ranging from 5.0° to 90° . The results show similar characteristics of the phase-redistribution behaviors to that of data set of Wa1. An angle of 90° was not enough to achieve full separation of phases. These results show clearly that the magnitude of the inclination effect on the phase-distribution data depends on the inlet conditions. The stratified-flow data are very sensitive to inclination, while the wavy flow data are less sensitive to inclination.

4.4.4 Data of the Annular Flow Regime

The phase-redistribution data for the annular-flow regime are shown in Figs. 4.8 to 4.10. The three data sets have a fixed J_{G1} of 40 m/s with J_{L1} of 0.01, 0.04, and 0.18 m/s

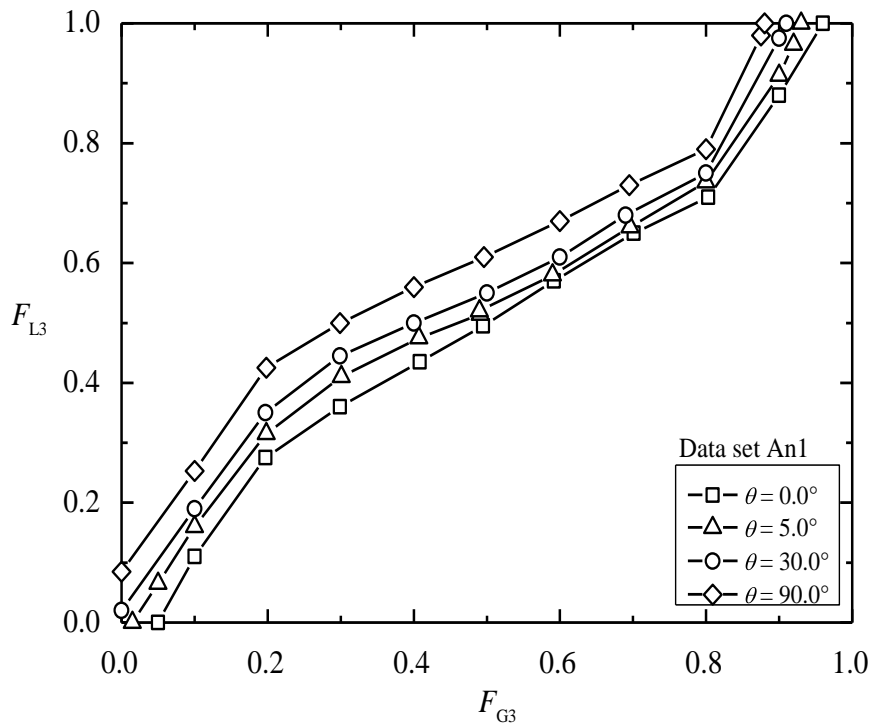


Fig. 4.8 Phase-redistribution data for annular flow (An1)

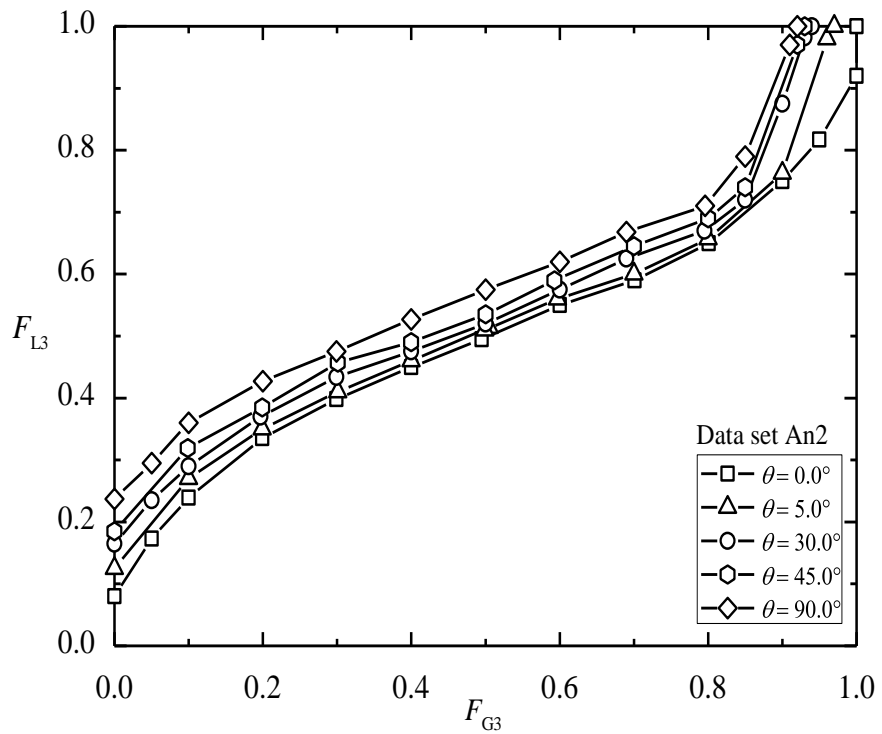


Fig. 4.9 Phase-redistribution data for annular flow (An2)

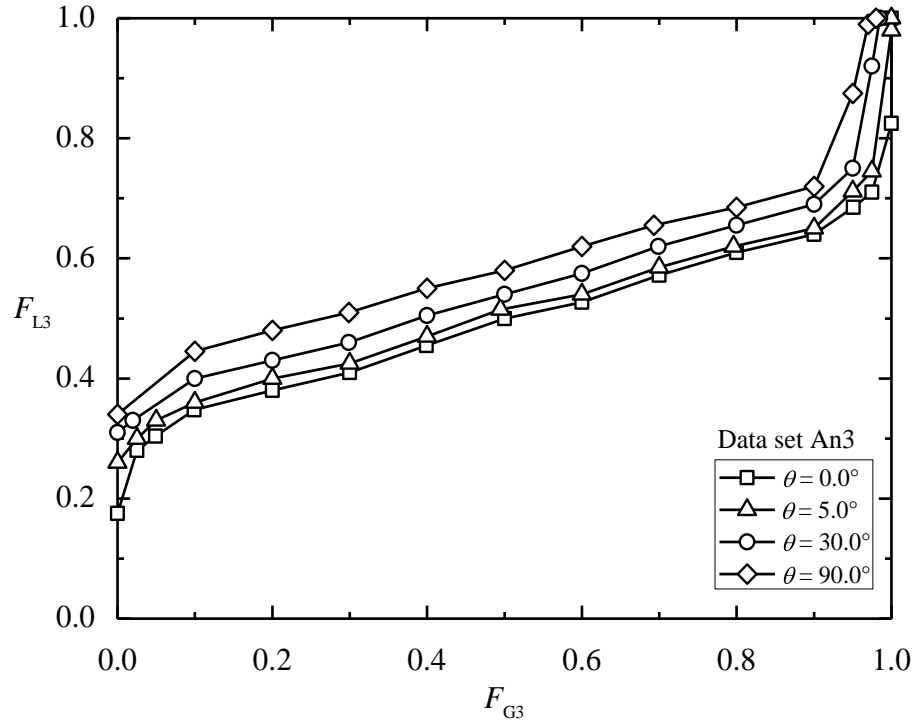


Fig. 4.10 Phase-redistribution data for annular flow (An3)

(which corresponds to $x_1 = 0.9, 0.7,$ and 0.34) for data sets An1, An2, and An3, respectively. For the case of horizontal outlets, the data for set An1 fell above the even phase-redistribution line over the range $0.1 < F_{G3} < 0.5$ and there is an increasing preference for the liquid phase to exit through Outlet 3 as J_{LI} increases in sets An2 and An3. As a result, there is a continuous trend for the x_1 effect on the phase-redistribution data within the annular flow regime, whereby the data line rotates around the $(0.5, 0.5)$ point in a counter-clockwise direction as x_1 increases. This trend in the annular-flow-regime data in terms of the effect of x_1 is consistent with the trend found earlier for the stratified and wavy flow regimes. The experimental results for the three different inlet conditions An1, An2, and An3 show that F_{L3} increases as θ increases for all values of F_{G3} . However, the effect of θ on F_{L3} for the inlet regime of annular flow is much less

pronounced than the effects seen earlier for the inlet regimes of wavy and stratified flow. An inclination angle of 90° produced a comparatively small change in the phase-redistribution data relative to data for the horizontal outlets.

4.4.5 Discussion of the Phase-Split Mechanism

The phenomenon of phase split at the junction is a complicated one due to the large number of parameters that could play a role in this split. Figures 4.11 to 4.14 demonstrate that F_{L3} is a function of F_{G3} , J_{G1} , J_{L1} , and θ . Keeping in mind that these data were generated for a specific gas-liquid combination (air-water), and a specific junction diameter and pressure, it is expected that fluid properties (e.g., viscosity, surface tension, and density of both phases), as well as the junction diameter can be additional parameters influencing the value of F_{L3} . Furthermore, the flow regimes in Sides 2 and 3 of the junction can certainly affect the amounts of gas and liquid flowing in the two outlets, and thus influence the phase split at the junction.

Two of the parameters that can be expected to play a significant role in the phase split at impacting tees with inclined outlets are the liquid gravity, represented by $\rho_{LG} \sin(\theta)$, which acts to push the liquid down to Side 3 of the junction, and the gas inertia force, represented by $\rho_G J_{G1}^2$, which acts to pull the liquid up into Side 2. Figures 4.4 to 4.10 demonstrate the effect of θ at fixed values of J_{G1} and J_{L1} . These figures show clearly that increasing the value of θ while keeping J_{G1} constant, which in turn increases the gravity force while keeping the gas inertia force constant, causes more liquid to flow into Side 3 as evidenced by increasing the value of F_{L3} at any value of F_{G3} . This observation is valid for all the inlet flow regimes considered in this investigation. Figures 4.11 and 4.12

show a representative sample of the effect of J_{G1} at fixed values of J_{L1} and θ on the degree of phase split represented by the value of F_{L3} at any given F_{G3} . These figures show clearly that increasing the value of J_{G1} while keeping θ constant, which in turn increases the gas inertia force while keeping the gravity force constant, forces more liquid into Side 2 as evidenced by the decrease in the value of F_{L3} at any value of F_{G3} . The data in Fig. 4.11 correspond to inlet flow regimes of stratified, wavy, and annular, while the data in Fig. 4.12 correspond to inlet flow regimes of wavy and annular. Therefore, this observation about the effect of increasing the gas inertia force while keeping the gravity force constant appears to be valid for all the inlet flow regimes considered in this investigation.

Figures 4.13 and 4.14 explore the effect of J_{L1} at fixed values of J_{G1} and θ on the degree of phase split, which is represented by the value of F_{L3} at any given F_{G3} . The trends seen in Figs. 4.13 and 4.14 are typical of all the data generated in this study. Fixing the values J_{G1} and θ while changing J_{L1} produces no change in the gas inertia and liquid gravity forces as formulated above. Therefore, any trends observed in Figs. 4.13 and 4.14 cannot be attributed to changes in these forces. The results in Figs. 4.13 and 4.14 show that the effect of J_{L1} on F_{L3} does not have a consistent trend. The value of F_{L3} starts out increasing with J_{L1} up to a certain value of F_{G3} after which the trend reverses. It is postulated that the gas inertia and liquid gravity forces have little or no effect on this behavior, and that the trends seen in these two figures are more influenced by changes in the flow regimes and viscous forces in the two outlets of the junction as F_{G3} changes. The development of a theoretical model or an empirical correlation for predicting the present experimental data may prove to be a challenging task and would undoubtedly be the subject of future studies.

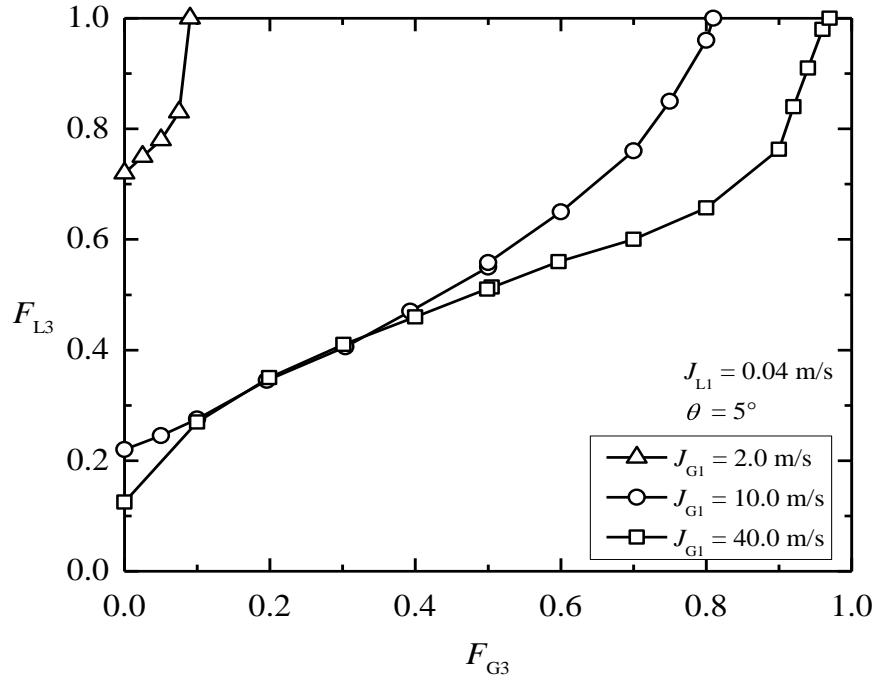


Fig. 4.11 Effect of J_{G1} on the phase split at $J_{L1} = 0.04$ m/s and $\theta = 5.0^\circ$

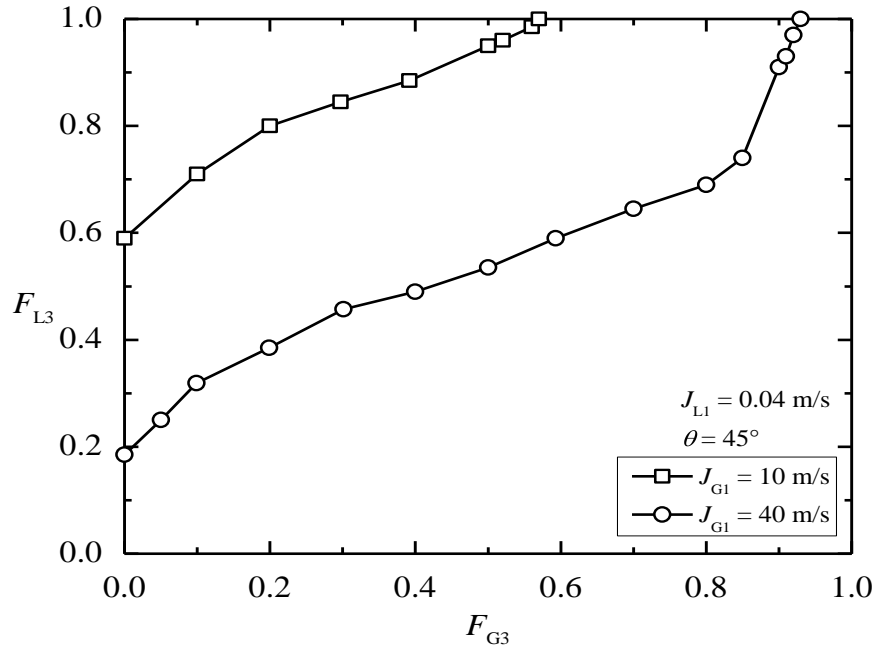


Fig. 4.12 Effect of J_{G1} on the phase split at $J_{L1} = 0.04$ m/s and $\theta = 45.0^\circ$

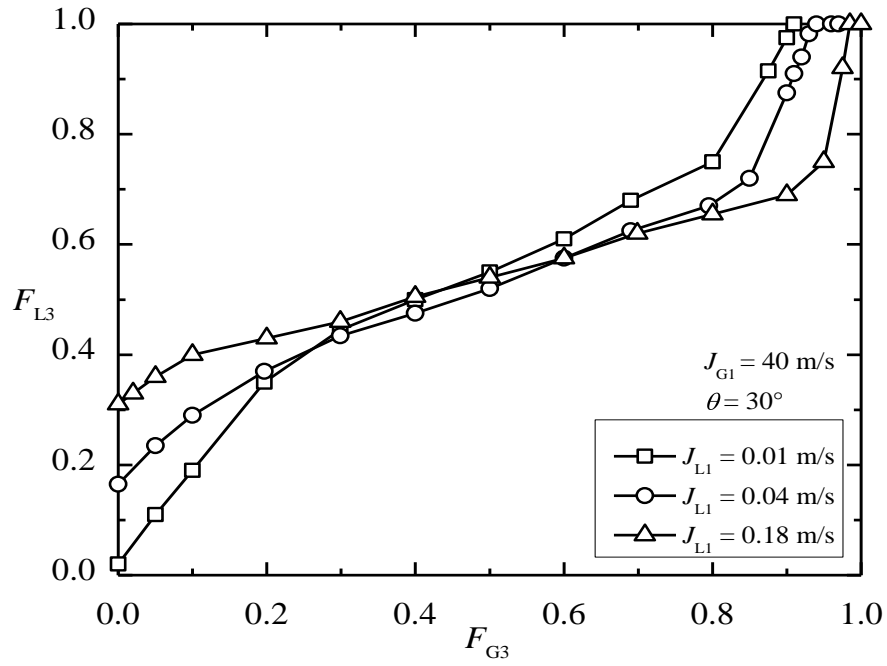


Fig. 4.13 Effect of J_{L1} on the phase split at $J_{G1} = 40 \text{ m/s}$ and $\theta = 30.0^\circ$

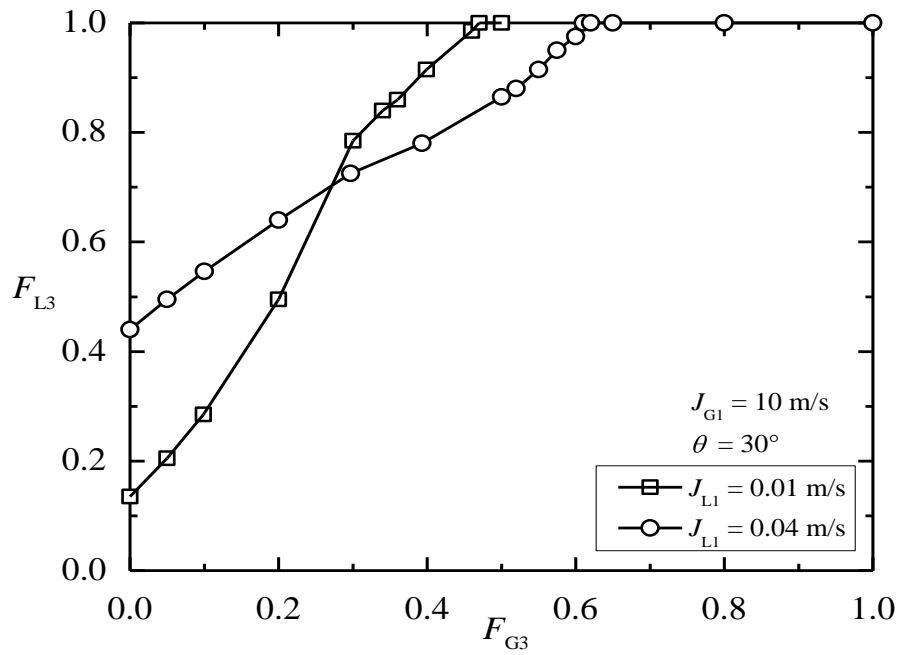


Fig. 4.14 Effect of J_{L1} on the phase split at $J_{G1} = 10 \text{ m/s}$ and $\theta = 30.0^\circ$

4.5 Observed Flow Regimes in the Outlets

The flow regimes were observed through the three visual sections in the inlet and two outlet sides throughout the experimental investigation. A sample of the results for the flow regimes in the outlets is shown in Figs. 4.15 to 4.20. Because of the location of the visual sections (56 tube diameters downstream from the junction), it is assumed that these flow regimes were fully developed. Comparisons were made between the observed flow regimes and flow-regime maps of inclined pipes published in the literature. The flow regimes observed in the horizontal inlet and in the outlets when they were oriented horizontally were compared with the Mandhane et al. (1974) map. The results show good agreement between the current observations and the transition boundaries of the maps (see for example Fig. 4.1 for the inlet side of the junction). The flow regimes observed in Outlet 3 for the downward inclinations of 5° , 30° , and 90° were compared with the experimental flow-regime map developed by Shoham (1982) for the same inclinations. Shoham's map was generated for air-water mixtures in a 2.5-cm pipe. The angles of 5° , 30° , and 90° were selected because multiple data points generated in the present study included these angles of inclination. The observed regimes in the present investigation agree well with the boundaries of Shoham's map. Several flow regimes were observed in Outlet 3 for the downward inclination. At an angle of inclination of 5.0° (Fig. 4.15), stratified flow was the dominant flow regime and the other major flow regimes that were observed were the wavy and annular flow regimes, as well as the transitional regimes between these major flow regimes. The results show that there is an apparent difference between the horizontal inlet and the downward-inclined outlet. The transition boundaries move significantly toward higher velocity when the outlet was inclined. For the vertical

case (Fig. 4.17), the region of annular flow expanded, while the region of stratified flow completely disappeared. The slug flow regime was not observed at any downward inclination in the present study.

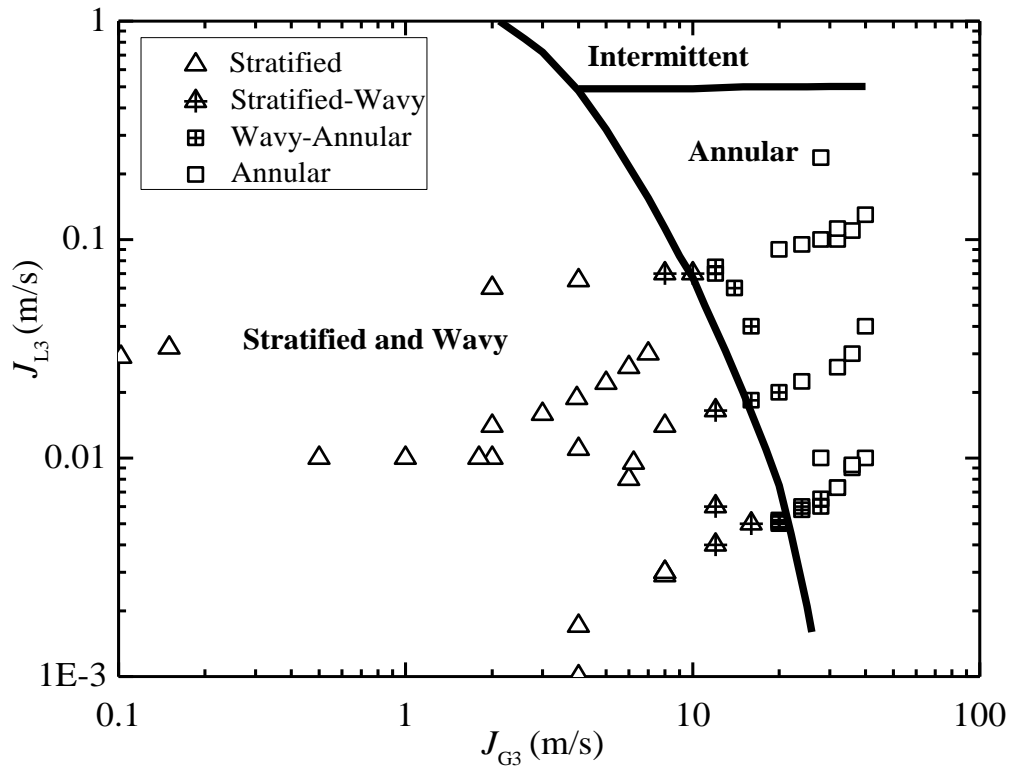


Fig. 4.15 Comparison between the observed flow regimes in Outlet 3 at 5° downward inclination and the map of Shoham (1982)

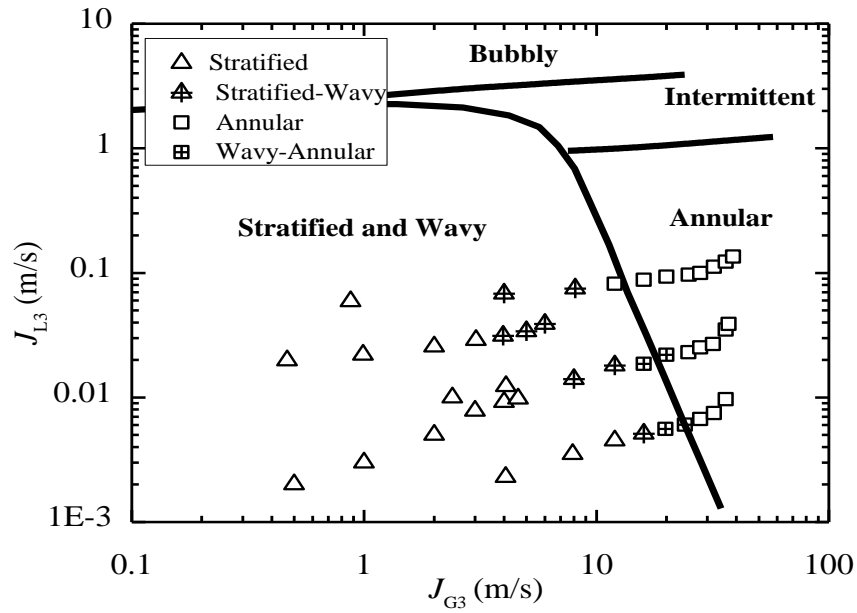


Fig. 4.16 Comparison between the observed flow regimes in Outlet 3 at 30° downward inclination and the map of Shoham (1982)

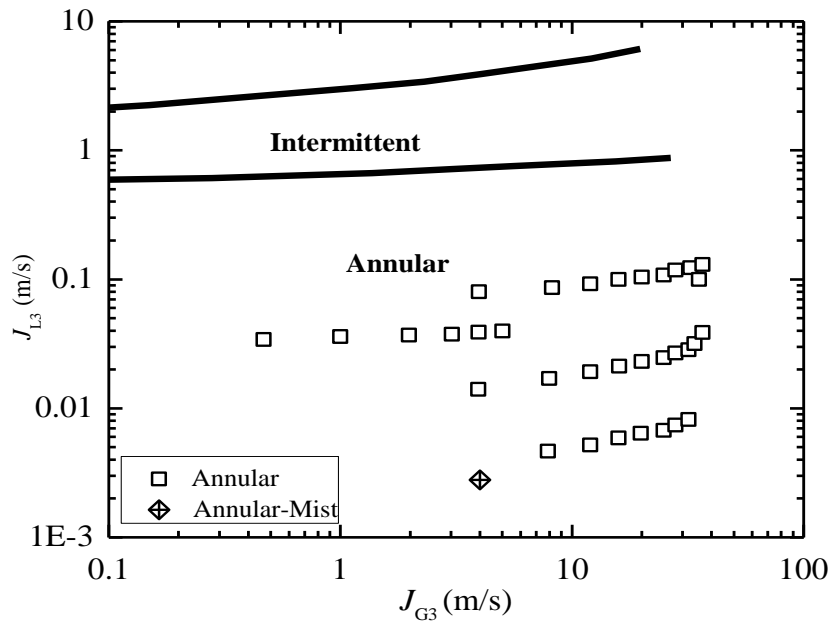


Fig. 4.17 Comparison between the observed flow regimes in Outlet 3 at 90° downward inclination and the map of Shoham (1982)

Several flow regimes were observed in Outlet 2 for the upward inclination. The major regimes included the stratified, wavy, slug, churn, and annular, as well as transitional regimes between these major flow regimes. The dominant flow regimes were the slug and annular flow. The transition from stratified to wavy flow was only observed at an angle of inclination up to 5.0° with low gas flow rates. Churn flow appeared only at angles of 75° or higher. A comparison was made between the flow regimes observed in Outlet 2 at the inclination angles of 5° , 30° , and 90° and the map of Shoham (1982) for upward inclined pipes. The comparison, shown in Figs. 4.18 to 4.20, indicates good agreement between the observed regimes in this study and Shoham's maps. The minor discrepancies may be due to flow-regime classification and occurred at the transition boundaries.

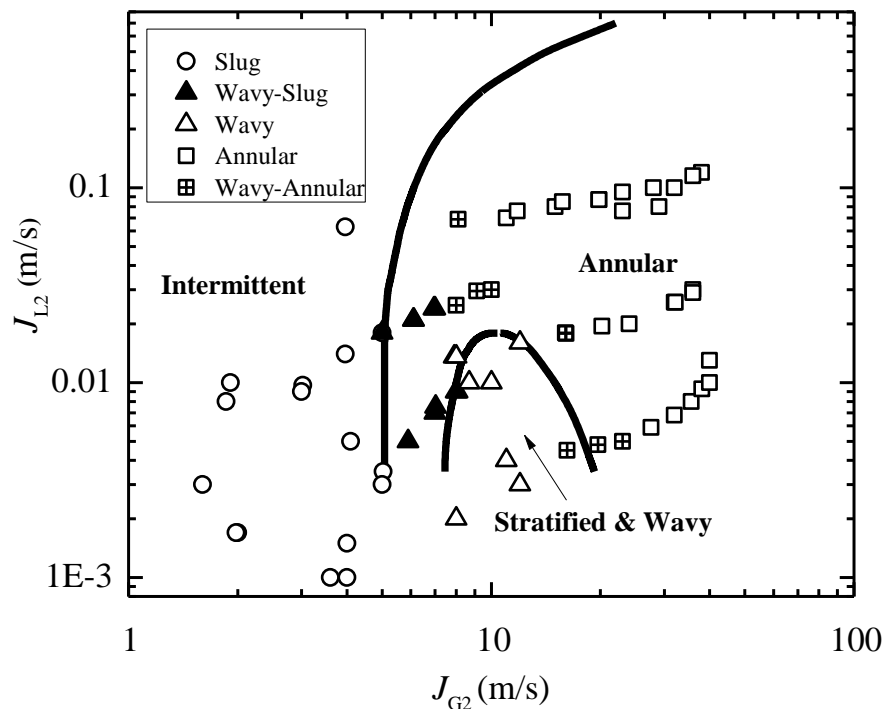


Fig. 4.18 Comparison between the observed flow regimes in Outlet 2 at 5° upward inclination and the map of Shoham (1982)

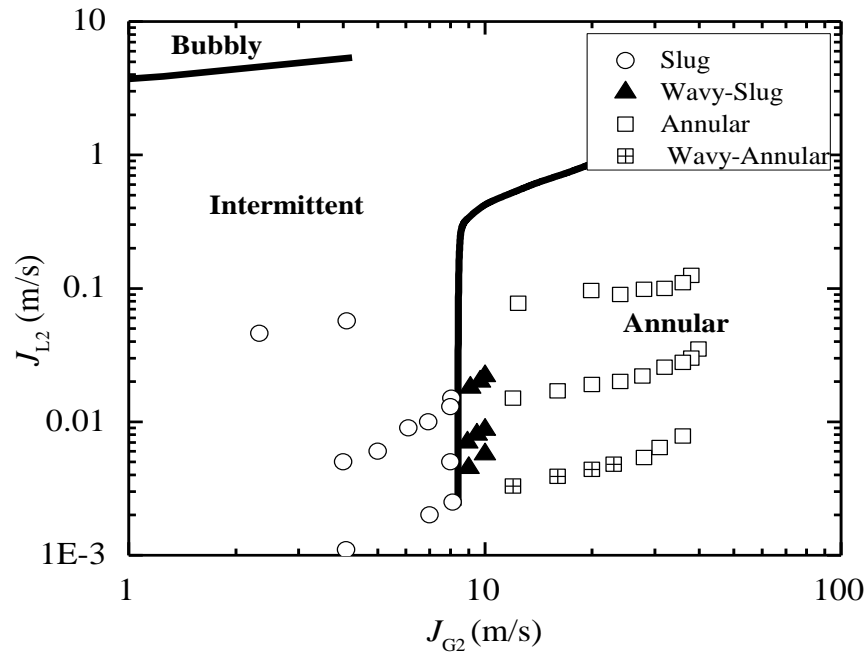


Fig. 4.19 Comparison between the observed flow regimes in Outlet 2 at 30° upward inclination and the map of Shoham (1982)

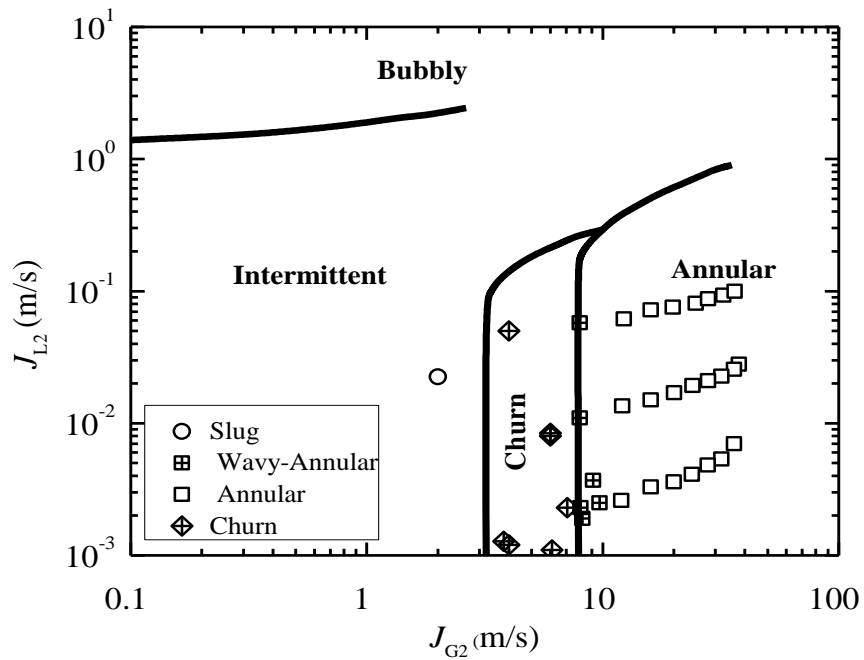


Fig. 4.20 Comparison between the observed flow regimes in Outlet 2 at 90° upward inclination and the map of Shoham (1982)

4.6 Full Phase Separation

4.6.1 Full-Separation Data

The data for the limiting values of J_{G1} and J_{L1} for full separation at various inclinations of the outlets are shown in Fig. 4.21, plotted on the flow-regime map of Mandhane et al. (1974). The observed flow regimes in the inlet side of the junction were consistent with the predictions of the Mandhane et al. map. For each inclination angle, the area under the line formed by the data corresponds to inlet conditions for which full separation is possible, while only partial separation is possible above the data line. As expected, the limiting values of J_{G1} and J_{L1} for full separation increase as θ increases. For each θ , the behavior of the data suggests that the value of J_{L1} becomes insensitive to J_{G1} as J_{G1} decreases and the value of J_{G1} becomes insensitive to J_{L1} as J_{L1} decreases. At low inclinations ($\theta \leq 30^\circ$), the inlet flow regime is mainly stratified, while for higher inclinations ($\theta \geq 60^\circ$), inlet flow regimes of wavy, slug, and plug were observed.

4.6.2 Visual Observations of Flow Phenomena

At any inclination, θ , full separation was obtained in the junction at sufficiently low values of J_{G1} and J_{L1} with all the gas flowing into Side 2 and all the liquid flowing into Side 3. Starting from this condition and gradually increasing either J_{G1} or J_{L1} , conditions were reached whereby liquid started to flow into Side 2. The objective of this section is to discuss the flow phenomena observed at the junction near the limiting conditions.

Basically, three types of flow phenomena were observed, depending on the inclination angle and the inlet velocities. These three types are as follows:

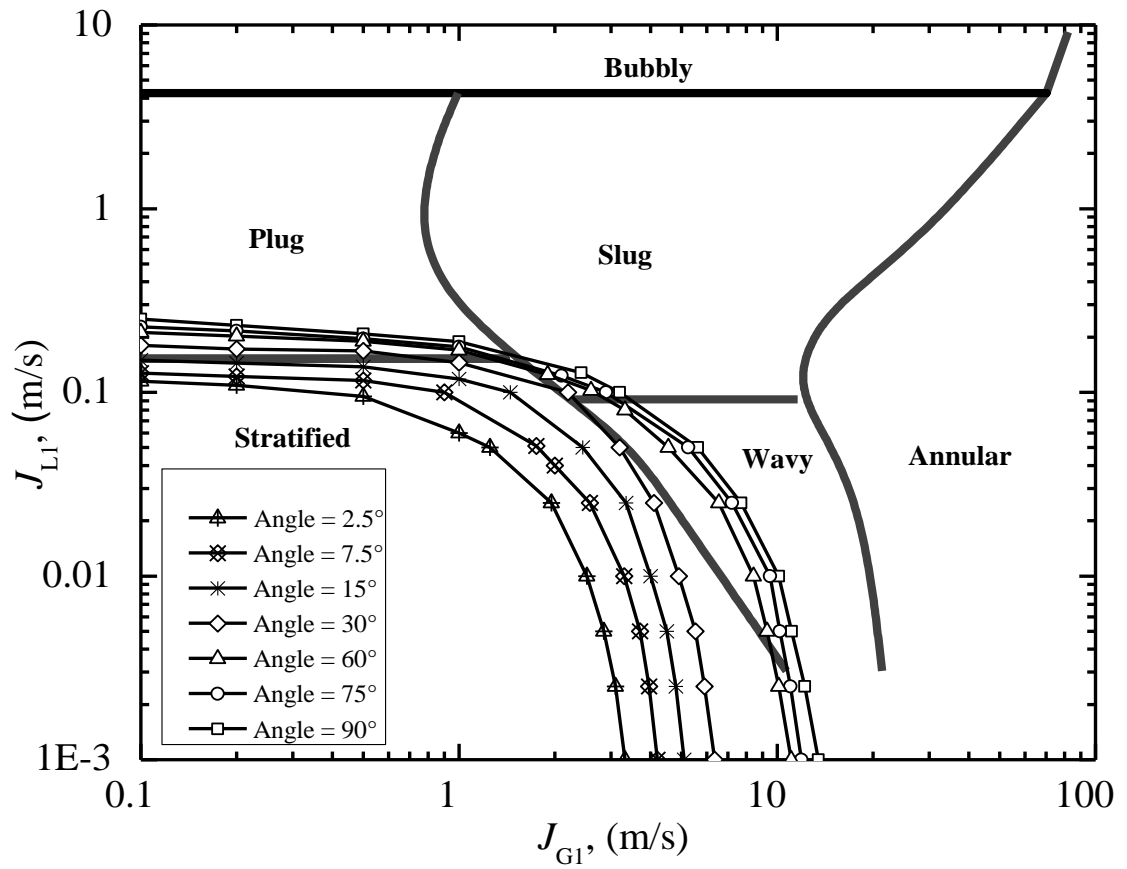


Fig. 4.21 Limiting conditions for full separation at various outlet inclinations plotted on the flow-regime map of Mandhane et al. (1974)

- (a) Type A ($\theta \leq 30^\circ$): The inlet flow regime approaching the junction was essentially stratified in these cases (see Fig. 3). The flow phenomenon observed in these experiments was typically characterized by the appearance of a liquid body shaped like a hump or a standing wave in Side 2, as shown in Fig. 4.22(a). The size and location of this liquid hump within Side 2 were dependent on θ , J_{G1} , and J_{L1} ; however, no liquid flow was detected in Side 2 at that stage. The photograph in Fig. 4.22(a) was taken looking into the axis of the inlet side of the junction.

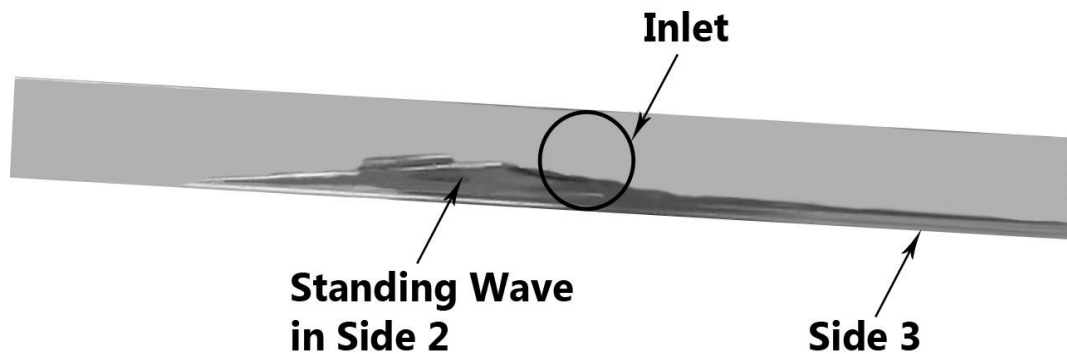


Fig. 4.22(a) Observed flow phenomena at $\theta = 7.5^\circ$, $J_{L1} = 0.05$ m/s, and $J_{G1} = 1.6$ m/s
(Type A before entrainment)

Increasing the value of J_{G1} or J_{L1} , a limiting condition was reached where liquid became entrained into the gas flow in Side 2 (see Fig. 4.22(b)), and a liquid stream was visible through the transparent part of the test section, the visual section on Side 2, and the tygon tubing connecting Side 2 to its separation tank.

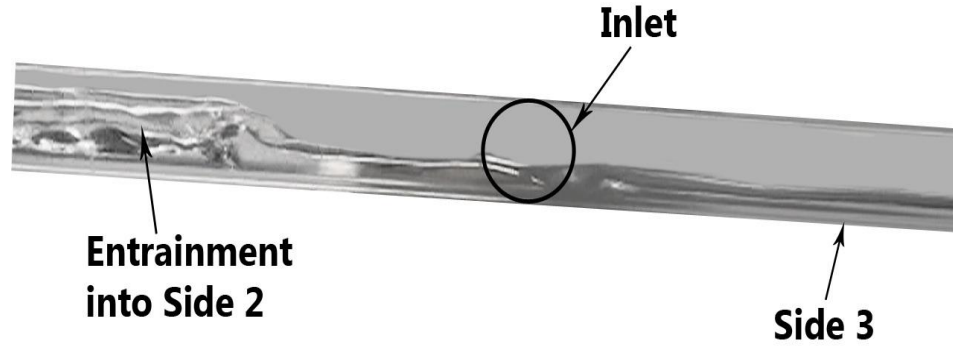


Fig. 4.22(b) Observed flow phenomena at $\theta = 7.5^\circ$, $J_{L1} = 0.05$ m/s, and $J_{G1} = 1.75$ m/s
(Type A after entrainment)

- (b) Type B ($60^\circ \leq \theta < 90^\circ$ and $J_{L1} < 0.08$ m/s): In this region, with $J_{G1} > 3$ m/s the inlet flow regime approaching the junction was stratified or stratified-wavy and the condition of full separation was achieved, as shown in Fig. 4.23(a).

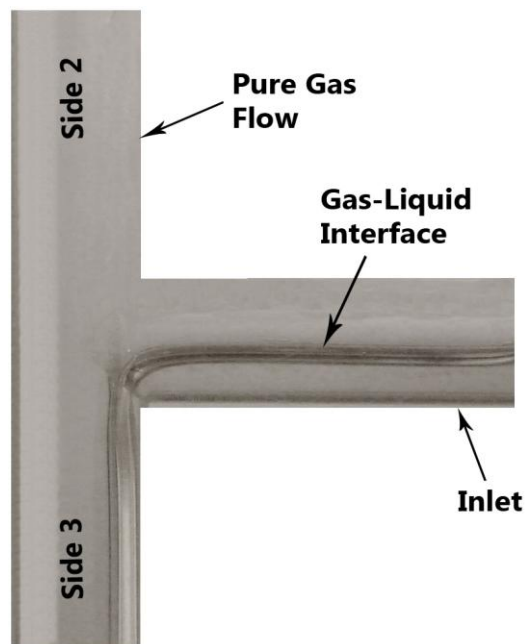


Fig. 4.23(a) Observed flow phenomena at $\theta = 90^\circ$, $J_{L1} = 0.025$ m/s, and $J_{G1} = 5.1$ m/s
(Type B before entrainment)

As J_{G1} was increased, a limiting condition was reached whereby liquid was suddenly entrained in the upward gas flow in Side 2, as shown in Fig. 4.23(b), while the flow approaching the junction remained mainly wavy.

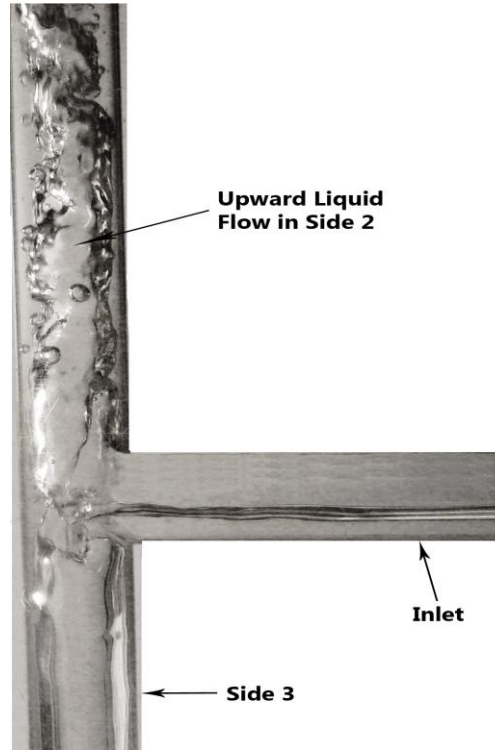


Fig. 4.23(b) Observed flow phenomena at $\theta = 90^\circ$, $J_{L1} = 0.025$ m/s, and $J_{G1} = 5.6$ m/s
(Type B after entrainment)

- (c) Type C ($60^\circ \leq \theta \leq 90^\circ$ and $J_{G1} < 3$ m/s): In this region, with $J_{L1} < 0.08$ m/s the inlet flow regime approaching the junction was stratified and full separation existed at the junction. Increasing the value of J_{L1} , the inlet flow regime changed from stratified to either slug or plug with full separation still occurring at the junction, as shown in Fig. 4.24(a).

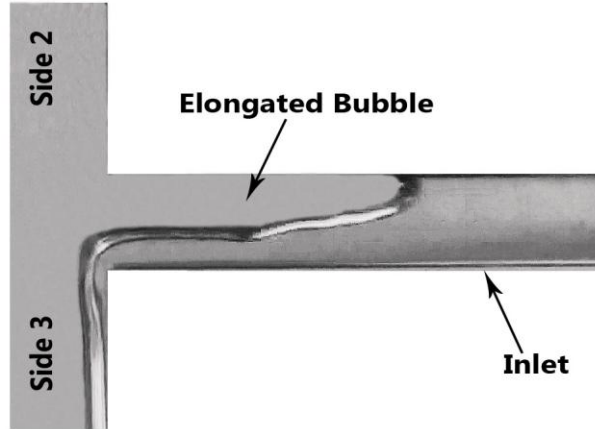


Fig. 4.24(a) Observed flow phenomena at $\theta = 90^\circ$, $J_{L1} = 0.13$ m/s, and $J_{G1} = 0.5$ m/s
(Type C full separation before entrainment)

A further increase in J_{L1} resulted in the appearance of a churning zone of gas and liquid in the lower part of Side 2 near the junction center, as shown in Fig. 4.24(b); however, all the inlet liquid still flowed into Side 3. Continuing the increase in J_{L1} beyond this point, a limiting condition was reached whereby liquid was pulled up by the gas flow all the way through Side 2.

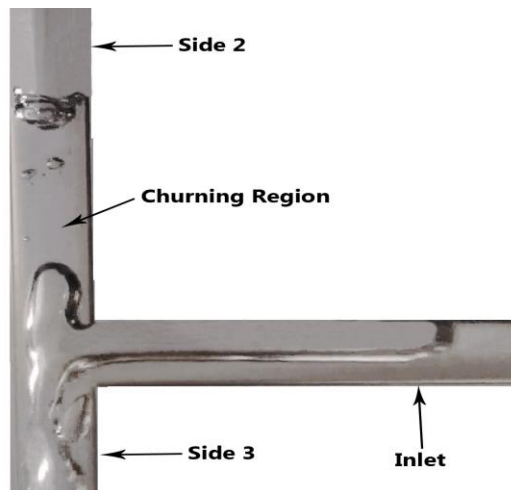


Fig. 4.24(b) Observed flow phenomena at $\theta = 90^\circ$, $J_{L1} = 0.17$ m/s, and $J_{G1} = 0.5$ m/s
(Type C churning region in Side 2 before entrainment)

4.6.3 Correlation of the Full-Separation Data

The visual observations discussed above suggest that there is similarity between the mechanism by which liquid is entrained by the gas into the upward branch of the junction and the mechanism of liquid entrainment in small upward branches. There has been significant research into the conditions for the onsets of gas and liquid entrainment in small branches (e.g., Rouse et al., 1956; Smoglie and Reimann, 1986; Schrock et al, 1986; Micaelli and Mempoiteil, 1989; Yonomoto and Tasaka, 1991; Hassan et al., 1998; Welter et al., 2004). This research was motivated by the need for data and models for predicting the two-phase flow through small pipe breaks during loss-of-coolant accidents in nuclear reactors. These investigations considered horizontal branches, vertically upward branches, and vertically downward branches. More recently, Bartley et al. (2008) considered the onsets of gas and liquid entrainment in branches with various angles of inclinations from vertically upward to vertically downward.

The parameters relevant to the phenomenon of liquid entrainment, according to the above studies, are illustrated in Fig. 4.25. Gas is withdrawn from a stratified two-phase region with a velocity J_G through an upward branch of diameter d . At a certain vertical distance between the gas-liquid interface and the branch entrance, h_G , a critical condition is reached where liquid begins being entrained in the exiting gas stream. In all the above investigations, the onset of this phenomenon has been correlated in the following form:

$$\frac{h_G}{d} = C_1 Fr_G^{C_2}, \quad (4.1)$$

where, C_1 and C_2 are constants, and Fr_G is the gas Froude number given by

$$\text{Fr}_G = \frac{J_G}{\sqrt{g d \rho_L - \rho_G / \rho_G}}, \quad (4.2)$$

where, g is the gravitational acceleration, and ρ_G and ρ_L are the gas and liquid densities, respectively. Values of C_1 and C_2 were obtained empirically in most investigations and the value $C_2 = 0.4$ was frequently reported for vertically upward branches (e.g., Rouse et al., 1956; Smoglie and Reimann, 1986; Schrock et al., 1986; Bartley et al., 2008).

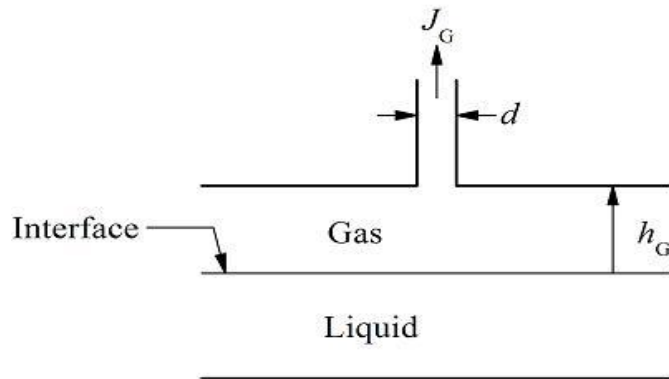


Fig. 4.25 Relevant parameters for liquid entrainment in upward branches.

An attempt was made to correlate the present data using the form of Eqs. 4.1 and 4.2. In order to determine the height of the liquid in the inlet side of the branch, the void fraction (α) was required. Since α was not measured in the present experiment, it was necessary to use one of the existing models/correlations for determining this parameter. Woldesemayat and Ghajar (2007) performed a systematic comparison between 68 void-fraction correlations and a data base containing 2845 data points out of which 900 were for horizontal tubes. Of the empirical correlations that correctly predicted a high

percentage of the data of horizontal flow within $\pm 15\%$ were those of Rouhani and Axelsson (1970), and Chisholm (1973). The mechanistic model of Taitel and Dukler (1976) was not considered in Woldesemayat and Ghajar's study. However, this model is of a special interest in the present study because it was mechanistic and based on stratified flow, which is the flow regime where most of the present results occur.

In order to confirm further the validity of the void-fraction model/correlation to be used in the present study, the predictions from Rouhani and Axelsson (1970), Chisholm (1973), and Taitel and Dukler (1976) were compared against experimental data reported by Franca and Lahey (1992) for conditions close to the present ones (horizontal air-water flow in a horizontal pipe with $d = 15$ mm, $1.5 < J_G < 23$ m/s, and $0.0056 < J_L < 0.277$ m/s). It was found that the model of Taitel and Dukler gave the best predictions with an arithmetic-mean deviation of -1.86% , root-mean-square deviation of 14.7% , and 92% of the data predicted within $\pm 20\%$, and therefore, this model was used in predicting α in this study. This comparison is shown in Fig. 4.26.

Values of h_G/d in the inlet side and Fr_G in Outlet2 of the junction were calculated for all the experimental data points shown in Fig. 4.21. The results for each θ were fitted to Eq. (4.1) and best-fit values for C_1 and C_2 were obtained for each θ using the least-squares method. It was found that the value of C_2 ranged between 0.389 and 0.416, which is a very narrow range, and the average value ($C_2 = 0.4$) is identical to the value obtained by Rouse et al. (1956), Smoglie and Reimann (1986), Schrock et al. (1986), Bartley et al. (2008) for the onset of liquid entrainment in vertically upward branches. Therefore, the least-square fits were repeated with C_2 fixed at 0.4 and new values for C_1 were obtained; these are shown in Fig. 4.27.

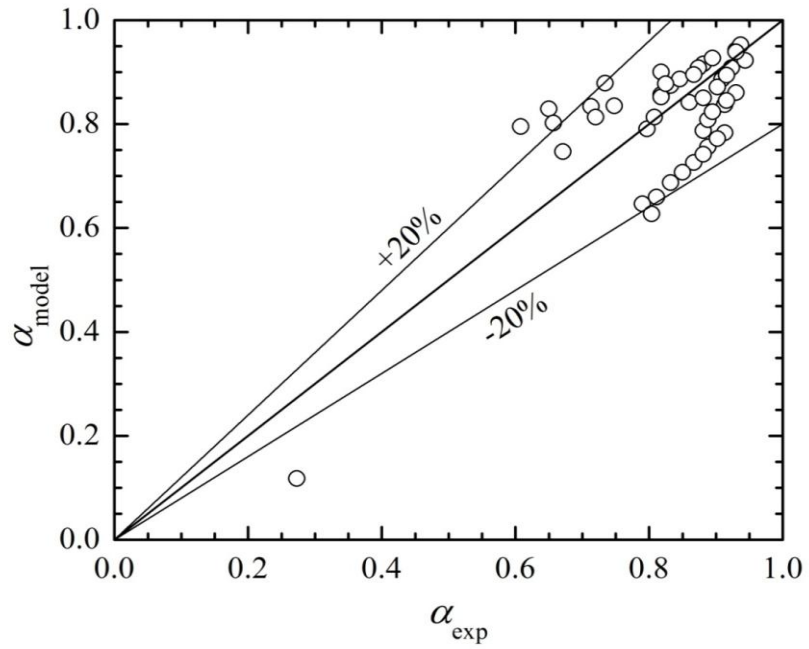


Fig. 4.26 Comparison between the data of Franca and Lahey (1992) and the model of Taitel and Dukler (1976)

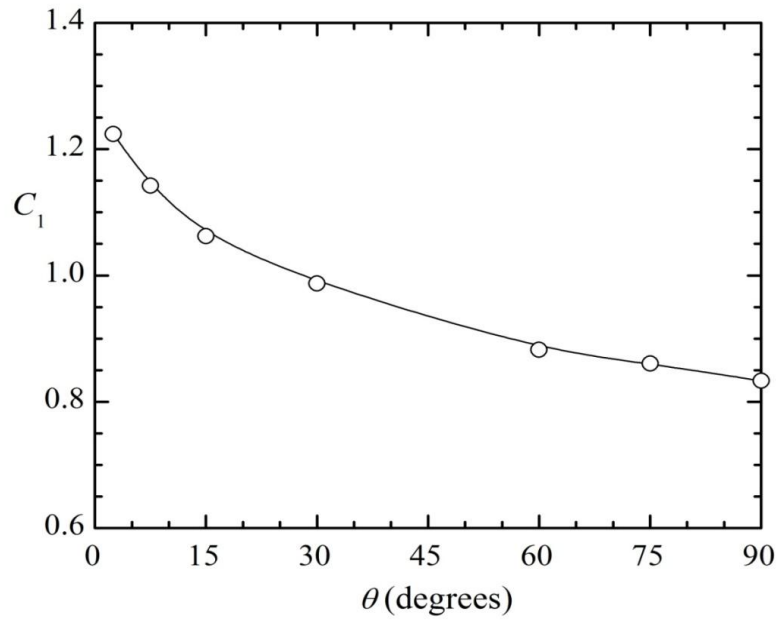


Fig.4.27 Values of C_1 in Eq. (4.1) with $C_2 = 0.4$

A comparison between the data for the limiting inlet conditions for full phase separation and Eq. (4.1) with C_1 from Fig. 4.27 and $C_2 = 0.4$ is shown in Fig. 4.28. It is fair to conclude from this comparison that the simple correlation given by Eq. (4.1) can be used in predicting the form of the J_{L1} versus J_{G1} relationship, as well as the effect of θ on this relationship. In order to quantify the accuracy of prediction by Eq. (4.1), the predicted values of J_{G1} were compared against the experimental J_{G1} at the same J_{L1} and the results are shown in Fig. 4.29. The arithmetic-mean deviation between the two sets of data in Fig. 4.29 is 5.3%, the root-mean-square deviation is 35.2%, and 90% of the experimental values are predicted within $\pm 20\%$ (most of the larger deviations correspond to $J_{G1} < 1.8$ m/s).

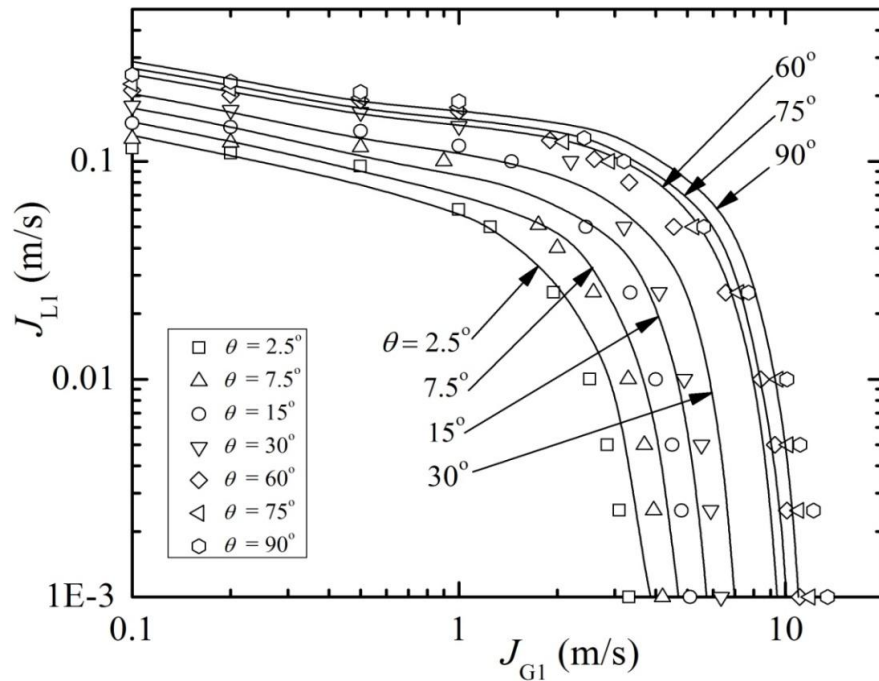


Fig. 4.28 Comparison between the experimental data and the predictions from Eq. (4.1) with $C_2 = 0.4$ and C_1 from Fig. 4.27

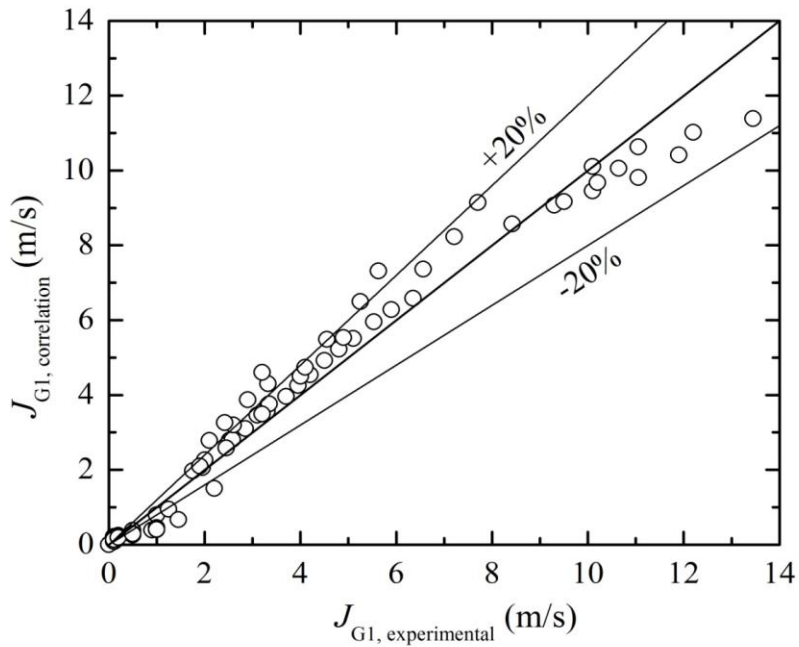


Fig 4.29 Quantitative comparison between experimental and predicted values of J_{G1} at the same J_{L1}

The larger deviations in prediction for $J_{G1} < 1.8$ m/s relate to the shape of the curves in Figs. 4.21 and 4.28. An experimental data point (J_{G1} , J_{L1}) in the region $J_{G1} < 1.8$ m/s can be located close to the correlation curve with a small percentage deviation in the value of J_{L1} at the given J_{G1} . However, due to the flatness of the correlation curve, the percentage deviation between the experimental and the predicted J_{G1} at the given J_{L1} can be significantly high. Since the present data are the only information currently available on the limiting conditions for full separation in impacting tees, the author feels that a further effort to develop a mechanistic model accounting for possible effects of tube diameter and other fluid properties (viscosity, surface tension) is not warranted at this time since the model cannot be tested. As more data become available, there will be an opportunity to test Eq. (4.1), and if necessary, develop other predictive methods.

4.7 Tee Junction with Short Outlets

4.7.1 Phase-Redistribution Data

Phase-redistribution experiments with short outlets were performed for some of the same inlet conditions tested earlier with long outlets. The three data sets selected included: one data set of stratified flow, one data set of wavy flow, and one data set of annular flow. Figures 4.30 to 4.32 give a comparison between the phase-redistribution data of long outlets and those of short outlets for data sets St1, Wa2, and An2, respectively. The differences between the two sets of data can be seen to be small in all three diagrams. Figure 4.30 gives a comparison between phase-redistribution data from data set St1 obtained with long outlets and the data obtained with short outlets. The difference between the two sets of data is very small at $\theta = 0^\circ$ and $\theta = 5.0^\circ$ as well. Very small differences can be seen in Figs. 4.31 and 4.32 for data sets Wa2 and An2.

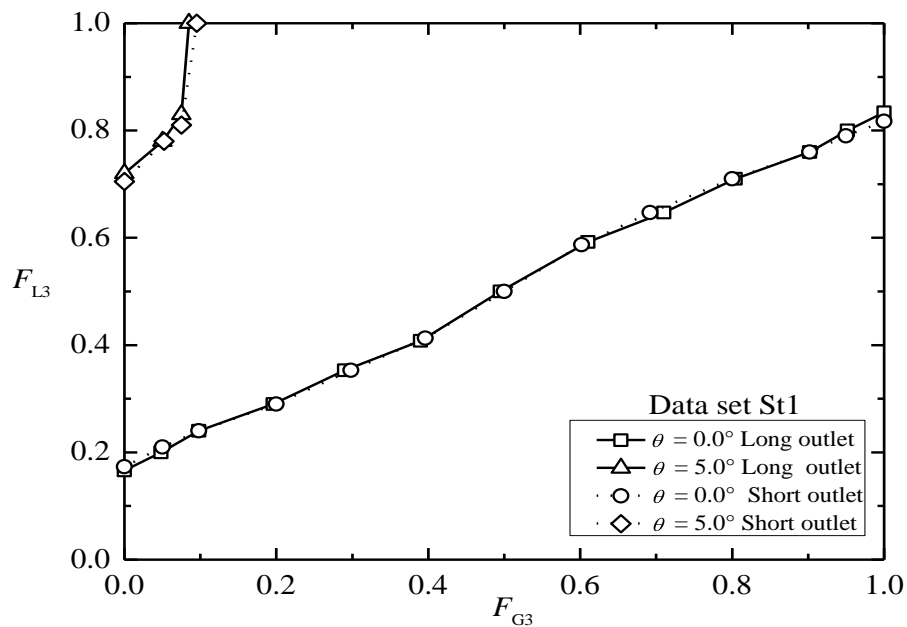


Fig. 4.30 Comparison between phase-redistribution data from data set (St1) obtained with long outlets and data obtained with short outlets

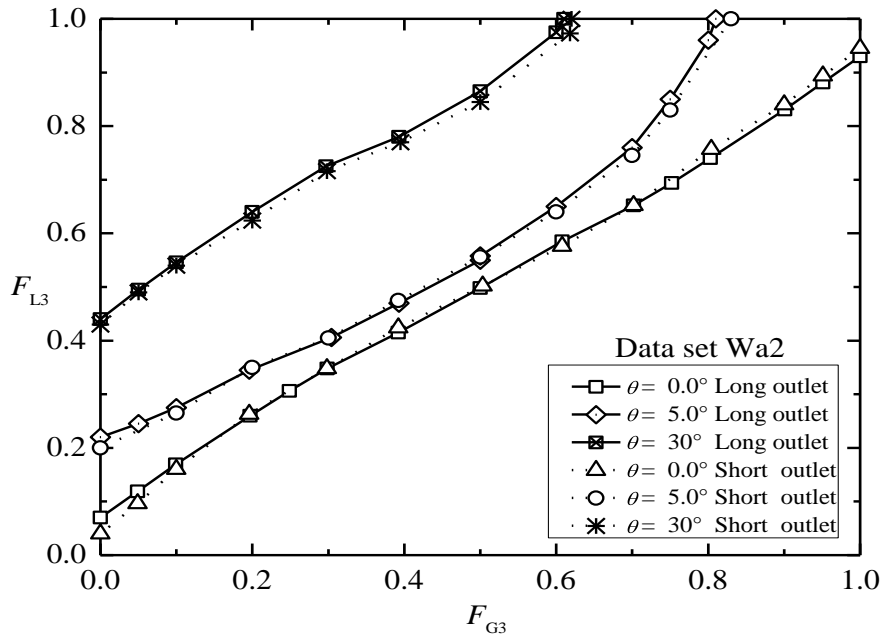


Fig. 4.31 Comparison between phase-redistribution data from data set (Wa2) obtained with long outlets and data obtained with short outlets

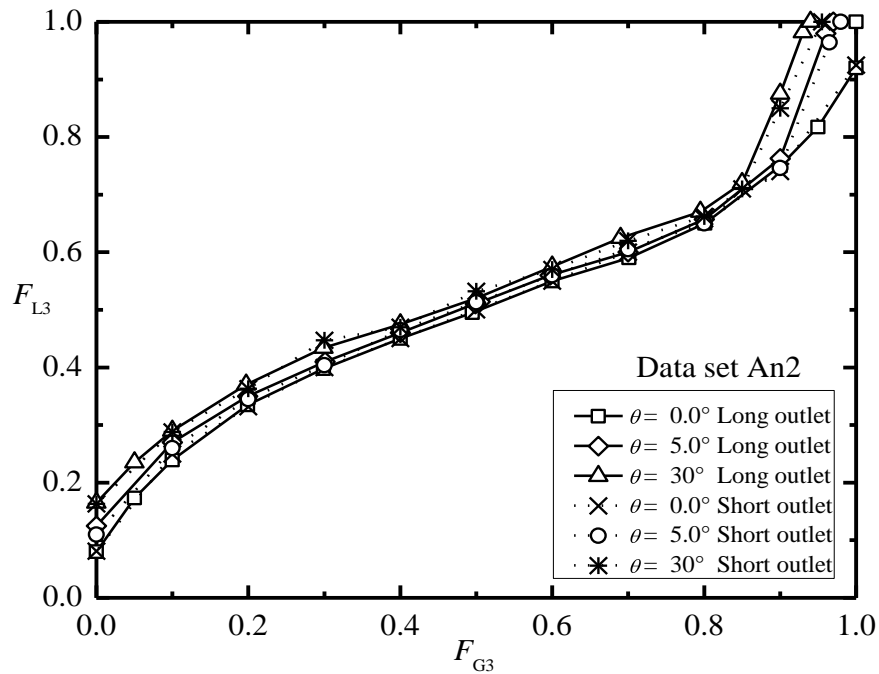


Fig. 4.32 Comparison between phase-redistribution data from data set (An2) obtained with long outlets and data obtained with short outlets

4.7.2 Full-Separation Data

Figure 4.33 shows the full-separation results of all data points obtained with short outlets. The full-separation data reported here correspond to conditions immediately after the liquid just passed the outside edge of the transparent tee junction on Side 2. Comparing the results in Fig. 4.33 for short outlets with the results in Fig. 4.21 for long outlets reveals that there are some differences in certain areas on the map, while the results are identical in most areas. At $\theta = 2.5^\circ$, $J_{LI} = 0.06$ m/s, and $J_{GI} < 1.0$ m/s, the liquid hump that appeared near the junction extended into Outlet 2 passing the transparent part of the tee junction. Based on the criterion suggested for full separation with short outlet, full separation was assumed at $J_{LI} = 0.06$ m/s for $J_{GI} < 1.0$ m/s. For long outlets in this region with $\theta = 2.5^\circ$, full separation did not occur until $J_{LI} = 0.115$ m/s.

At an inlet condition of ($60^\circ \leq \theta \leq 90^\circ$ and $1 \text{ m/s} < J_{GI} < 3 \text{ m/s}$) the flow in Outlet 2 is characterized by the appearance of a churning zone of gas and liquid near the junction center. For short outlets, the liquid may pass the transparent part of the test section while the flow into the separation of Side 2 is still single-phase gas. On the other hand, for long outlets, higher liquid velocities were required in this region to cause liquid entrainment in Side 2. Therefore, values of J_{LI} in this region for short outlets (Fig. 4.33) are lower than those for long outlets (Fig. 4.21). Outside the two regions of Fig. 4.33 mentioned above, the limiting conditions in Fig. 4.21 and Fig. 4.33 are essentially the same.

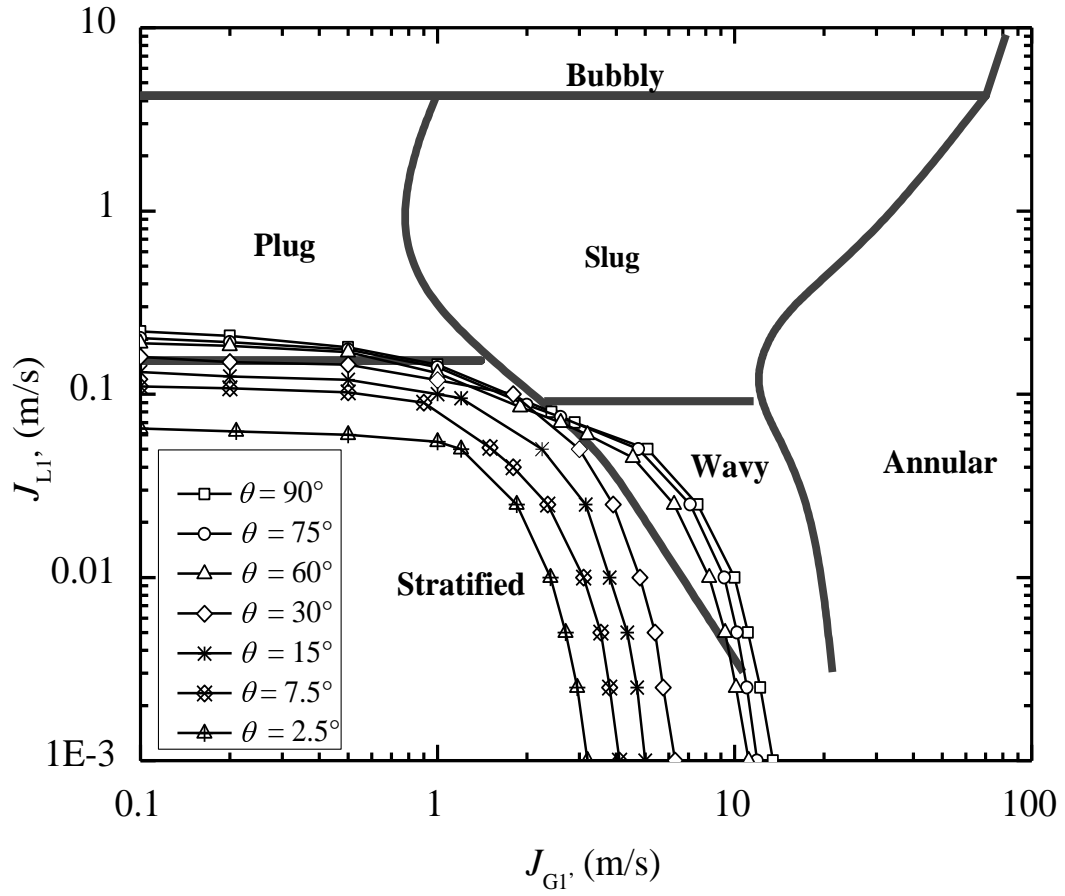


Fig. 4.33 Full-separation data with short outlets plotted on the Mandhane et al. (1974) Flow-regime map.

Chapter 5

CONCLUSIONS AND RECOMMENDATIONS

5.1 Conclusions

In the current study, experimental data were generated for phase-redistribution and full-phase separation of air-water two-phase flow in an equal-sided impacting tee junction with a horizontal inlet and inclined outlets. The test matrix for the phase-redistribution experiments is given in Table 4.1, and the test matrix for the full separation is given in Table 4.2. The following are the general conclusions that can be drawn from the results of the present study:

1. In general, uneven phase split occurs at impacting tees with horizontal or inclined outlets.
2. In impacting tees with a horizontal inlet and horizontal outlets, the degree of maldistribution of the phases is function of the inlet conditions and the mass-split ratio at the junction.
3. In impacting tees with a horizontal inlet and inclined outlets, the degree of maldistribution of the phases is function of the inlet conditions, the mass-split ratio at the junction, and the inclination angle of the outlets.
4. For all inlet conditions and all mass splits, the tendency of the liquid to exit preferentially through Outlet 3 increases as the angle of inclination increases.
5. The magnitude of the inclination effect on the phase distribution is dependent on the inlet conditions. The phase redistribution in stratified flow is very sensitive to the

outlet angle and full separation can be achieved at angles as low as 0.7° . Wavy flow is less sensitive to the outlet angle and annular flow is even less sensitive to the outlet angle.

6. A single impacting tee junction with an outlet inclined $2.5^\circ \leq \theta \leq 90^\circ$ can perform as a full phase separator. The separation capabilities of the junction are dependent on the inclination angle. For vertical outlets, the limiting separation capabilities are up to $J_{G1} = 13.5$ m/s at low liquid loading and up to $J_{L1} \approx 0.25$ m/s at low gas loading. Beyond these conditions, only partial separation is possible, and multiple junctions would be necessary to achieve a desirable degree of separation.
7. A correlation is proposed for predicting the form of the J_{L1} versus J_{G1} relationship that sets the limiting condition at which the junction can perform as a full phase separator, as well as the effect of θ on this relationship. The proposed correlation for full separation predicted 90% of the data within $\pm 20\%$.

5.2 Recommendations for Future Work

This investigation expands the two-phase-flow knowledge base by considering parameters that have never been investigated before. Progress has been made in highlighting the potential application of such systems as full phase separators. Nevertheless, several recommendations for future work can be made.

1. More experimental investigation for the effects of outlet inclination on phase redistribution are required at untested inlet conditions of slug, plug, and bubbly flow regimes.

2. Modeling the effect of outlet inclination on phase redistribution and full phase separation is still an area that has not been investigated. If the flow split is going to be modeled successfully, then much-improved modeling for more established fully horizontal systems needs to be developed for the full range of geometries and inlet conditions. Experimental evaluation of pressure drop should be generated under current operating conditions. This should aid in the development of an empirical correlation/model to predict phase redistribution with inclined outlets.
3. In case there is the a desire to implement such tee-junction separators within industrial settings, then it would be advantageous to generate experimental data on more industrially relevant junction diameters, two or more junctions coupled together, and more industrially relevant fluids (with different density, viscosity and surface tension).

REFERENCES

- Arirachakaran, S., "Two-Phase Flow Splitting Phenomenon at a Regular Horizontal Side-Arm Tee", Ph.D. Thesis, University of Tulsa, 1990.
- Asano, H., Fujii, T., Takenaka, N., and Sakoda, K., "A Study of the Phase Separation Characteristics in Gas-Liquid Two-Phase Flows by an Impacting Y-Junction" (1st Report, Experimental Results for Air-Water Two-Phase Flow under Normal Gravity Condition). Transactions of the Japan Society of Mechanical Engineers, Series B, Vol. 67-654, pp. 350-355, 2001.
- Asano, H., Fujii, T., Takenaka, N., Sakoda, K. and Arakawa, T., "Phase Separation Characteristics of Gas-Liquid Two-Phase Flow in a T-Junction (Experiments for a One-Component Two-Phase Flow)", Proceeding of the 16th Multiphase Flow Symposium, Lake Toya, Japan, pp. 103-104, 1997.
- Azzopardi, B.J., "T-Junctions as Phase Separators for Gas/Liquid Flows: Possibilities and Problems", Chemical Engineering Research & Design, Vol. 71, pp. 273-281, 1993.
- Azzopardi, B.J., "Phase Separation at T Junctions", Multiphase Science and Technology, Vol. 11, pp. 223-329, 1999.
- Azzopardi, B.J. and Hervieu, E., "Phase Separation at Junctions", Multiphase Science and Technology, Vol. 8, pp. 645-714, 1994.
- Azzopardi, B.J., and Smith, P.A., "Two-Phase Flow Split at T Junctions: Effect of Side Arm Orientation and Downstream Geometry." International Journal of Multiphase Flow, Vol. 18(6), pp. 861-875, 1992.

- Azzopardi, B.J., and Memory, S.B., “The Split of Two-Phase Flow at a Horizontal T-Annular and Stratified Flow”, 4th International Conference on Multiphase Flow, Nice, France, 1989.
- Azzopardi, B.J., Colman, D.A., and Nicholson, D., “Plant Application of a T-Junction as a Partial Phase Separator” Chemical Engineering Research & Design, Vol. 80, pp. 87-96, 2002.
- Azzopardi, B.J., Patrick, L., and Memory, S.B., “The Split of Two-Phase Flow at a Horizontal T-Junction with a Reduced Diameter Side Arm”, UKAEA Report AERE-R 13614, 1990.
- Azzopardi, B.J., Purvis, A., and Govan, A.H., “Two-Phase Flow Split at an Impacting T”, UKAEA Report, AERE-R-12179, 1986a.
- Azzopardi, B.J., Purvis, A., and Govan, A.H., “Flow Split of Churn Flow at a Vertical Impacting T”, UKAEA Report, AERE-R-12440, 1986b.
- Azzopardi, B.J., Wagstaff, D., Patrick, L., Memory, S.B., and Dowling, J., “The Split of Two-Phase at a Horizontal T-Annular and Stratified Flow” UKAEA Report AERE-R 13059, 1988.
- Baker, G., “Separation and Control of Gas-Liquid Flows at Horizontal T-Junctions”, School of Chemical, Environmental and Mining Engineering. Nottingham, Ph.D. Thesis, University of Nottingham, 2003.
- Baker, G., Azzopardi, B.J., Clark, W.W., and Wilson, J.A., “Controlling the Phase Separation of Gas-Liquid Flows at Horizontal T-Junctions”, AIChE Journal, Vol. 53, pp. 1908-1915, 2007.

- Ballyk, J.D., Shoukri, M., and Chan, A.M.C., "Steam-Water Annular Flow in a Horizontal Dividing T-Junction", *International Journal of Multiphase Flow*, Vol. 14, pp. 265-285, 1988.
- Ballyk, J. D., Shoukri, M., and Peng, F., "The Effect of Branch Size and Orientation on Two-Phase Annular Flow in T-Junctions with Horizontal Inlet", *International Conference on Multiphase Flows*, Tsukuba, Japan, 1991.
- Bartley, J.T., Soliman, H.M., Sims, G.E., "Experimental Investigation of the Onset of Gas and Liquid Entrainment from a Small Branch Mounted on an Inclined Wall", *International Journal of Multiphase Flow*, Vol. 34, pp. 905-915, 2008.
- Bos, A., and du Chatinier, J.G., "Simulation of Gas/Liquid Flow in Slug Catchers", *SPE Production Engineering*. Vol. 2, pp. 178-182, 1987.
- Buell, J.R., Soliman, H.M., and Sims, G.E., "Two-Phase Pressure Drop and Phase Distribution at a Horizontal Tee Junction", *International Journal of Multiphase Flow*, Vol. 20, pp. 819-836, 1994.
- Chien, S.F., and Rubel, M.T., "Phase Splitting of Wet Steam in Annular Flow Through a Horizontal Impacting Tee", *SPE Production Engineering*, Vol. 7, pp. 368-374, 1992.
- Chisholm, D., "Pressure Gradients Due to Friction During the Flow of Evaporating Two-Phase Mixtures in Smooth Tubes and Channels", *International Journal of Heat and Mass Transfer*, Vol. 16, pp. 347-358, 1973.
- Das, G., Das, K.P., and Azzopardi, B.J., "The Split of Stratified Gas-Liquid Flow at a Small Diameter T-Junction", *International Journal of Multiphase Flow*, Vol. 31, pp. 514-528, 2005.

- El-Shaboury, A.M.F., Soliman, H.M., and Sims, G.E., “Current State of Knowledge on Two-Phase Flow in Horizontal Impacting Tee Junctions”, *Multiphase Science and Technology*, Vol. 13, pp. 139-178, 2001.
- El-Shaboury, A.M.F., “Phase Distribution and Pressure Drop of Two-Phase Flows in a Horizontal Impacting Tee Junction”, Ph.D. Thesis, University of Manitoba, 2005.
- El-Shaboury, A.M.F., Soliman, H.M., and Sims, G.E., “Two-Phase Flow in a Horizontal Equal-sided Impacting Tee Junction”, *International journal of Multiphase Flow*, Vol. 33, pp. 411-431, 2006.
- Franca, F., and Lahey, R.T., “The Use of Drift-Flux Techniques for the Analysis of Horizontal Two-Phase Flows” *International Journal of Multiphase Flow*”, Vol. 18, pp. 787-801, 1992.
- Fujii, T., Asano, H., Takenaka, N., and Sakoda, K., “Phase Separation Characteristics of Gas-Liquid Two-Phase Flow in T-Junction (Effects of the Geometry of Junctions)”, *Proceeding of the 15th Multiphase Flow Symposium*, Fukui, Japan, pp. 61-64, 1996.
- Fujii, T., Takenaka, N., Nakazawa, T., and Asano, H., “The Phase Separation Characteristics of a Gas-Liquid Two-Phase Flow in the Impacting T-Junction”, *Proceeding of the 2nd International Conference on Multiphase Flow*, Kyoto, Japan, pp. 627-632, 1995.
- Guangbin, D., Zongming, I., Guangli, C., Shougen, H., and Jun, Z., “Experimental Investigation of Gas–Solid Two-Phase Flow in Y-Shaped Pipeline”, *Advanced Powder Technology*, Vol. 21, pp. 468-476, 2010.

- Hassan, I.G., Soliman, H.M., Sims, G.E., and Kowalski, J.E., “Two-Phase Flow from a Stratified Region Through a Small Side Branch”, *ASME Journal of Fluids Engineering*, Vol. 120, pp. 605-612, 1998.
- Hong, K.C., “Two-Phase Flow Splitting at a Pipe Tee”, *Journal of Petroleum Technology*, Vol. 2, pp. 290-296, 1978.
- Hong, K.C., and Griston, S., “Two-Phase Flow Splitting at an Impacting Tee”, *SPE Production and Facilities*, Vol. 10, pp. 184-190, 1995.
- Hwang, S.T., “A Study on Phase Separation Phenomena in Branching Conduits”, Ph.D. Thesis, Rensselaer Polytechnic Institute, 1986.
- Hwang, S.T., Soliman, H.M., and Lahey, R.T., “Phase Separation in Impacting Wyes and Tees”, *International Journal of Multiphase Flow*, Vol. 15, pp. 965-975, 1989.
- Lahey, R.T., “Current Understanding of Phase Separation Mechanisms in Branching Conduits”, *Nuclear Engineering and Design*, Vol. 55, pp. 145-161, 1986.
- Mandhane, J.M., Gregory, G.A., and Aziz, K., “A Flow Pattern Map for Gas-Liquid Flow in Horizontal Pipes”, *International Journal of Multiphase Flow*, Vol. 1, pp. 537-553, 1974.
- Marti, S., and Shoham, O., “A Unified Model for Stratified-Wavy Two-Phase Flow Splitting at a Reduced T-Junction with an Inclined Branch Arm”, *International Journal of Multiphase Flow*, Vol. 23, No. 4, pp. 725-748, 1997.
- Micaelli, J.C., and Mempondeil, A., “Two-Phase Flow Behaviour in a Tee Junction, the CATHARE Model”, In *Proceedings of the 4th Int. Topical Meeting on Nuclear Reactor Thermal-Hydraulics, Karlsruhe, Germany*, Vol. 2, pp. 1024-1030, 1989.

- Moffat, R.J., "Describing the Uncertainties in Experimental Results", *Experimental Thermal and Fluid Science*, Vol. 1, pp. 3-17, 1988.
- Muller, U., and Reimann, J., "Redistribution of Two-Phase Flow in Branching Conduits, A Survey", In 1st International Conference on Multiphase Flow, Tuskuba, Japan, Vol 3. pp. 85-107, 1991.
- Oranje, L., "Condensate Behavior in Gas Pipelines is Predictable", *Oil Gas Journal*, Vol. 71, pp. 39-44, 1973.
- Ottens, M., De Swart, A., Hoefsloot, H.C.J., and Hamersma, P.J., "Gas-Liquid Flow Splitting in Regular, Reduced and Impacting Tee Junctions", *Impiantistica Italiana*, Vol. 8, pp. 23-33, 1995.
- Ottens, M., Hoefsloot, H.C.J., and Hamersma, P.J., "Effect of Small Branch Inclination on Gas-Liquid Flow Separation in T-Junctions", *AIChE Journal*, Vol. 45, No. 3, pp. 465-474, 1999.
- Pandey, S., Gupta, A., Chakrabarti, D.P., Das, G., and Ray, S., "Liquid-Liquid Two Phase Flow Through a Horizontal T-Junction", *Trans IChemE, Part A, Chemical Engineering Research and Design*, Vol. 84(A10), pp. 895-904, 2006.
- Peng, F., Shoukri, M., and Ballyk, J.D., "An Experimental Investigation of Stratified Steam-Water Flow in Junctions", 3rd International Conference on Multiphase Flow, Lyon, France, June 8-12, 1998.
- Peng, F., Shoukri, M., and Chan, A. M., "Annular Flow in T-Junctions with Horizontal Inlet and Downwardly Inclined Branches", *ASME, Gas Liquid Flows*, Vol. 165, pp. 13-24, 1993.

- Penmatcha, V.R., Ashton, P.J., and Shoham, O., “Two-Phase Stratified Flow Splitting at a T-Junction with an Inclined Branch Arm”, *International Journal of Multiphase Flow*, Vol. 22, pp. 1105–1122, 1996.
- Rea, S., and Azzopardi, B.J., “The Split of Horizontal Stratified Flow at a Large Diameter T-Junction”, *Chemical Engineering Research*, Vol. 79 (Part A), pp. 470–476, 2001.
- Reimann, J., Brinkmann, H.J., and Domanski, R., “Gas-Liquid Flow in Dividing T-Junctions with a Horizontal Inlet and Different Branch Orientations and Diameters”, *Kernforschungszentrum Karlsruhe, Institut für Reaktorbauelemente*, Report KfK 4399, 1988.
- Roberts, P.A., Azzopardi, B.J., and Hibberd, S., “The Split of Horizontal Semi-Annular Flow at a Large Diameter T-Junction”, *International Journal of Multiphase Flow*, Vol. 21, pp. 455-466, 1995.
- Rouhani, S.Z., and Axelsson, E., “Calculation of Void Volume Fraction in the Subcooled and Quality Boiling Regions”, *International Journal of Heat and Mass Transfer*, Vol. 13, pp. 383-393, 1970.
- Rouse, H., Davidian, J., Glover, J.E., and Appel, D.W., “Development of the Non-Circulatory Waterspout”, *ASCE Journal Hydraul. Div.*, Vol. 82, pp. 1038(3)-1038(7), 1956.
- Rubel, M.T., Timmerman, B.D., Soliman, H.M., Sims, G.E., and Ebidian, M.A., “Phase Distribution of High-Pressure Steam-Water Flow at Large-Diameter Tee Junctions”, *Trans. ASME, Journal of Fluids Engineering*, Vol. 170, pp. 1-10, 1994.

- Saba, N., and Lahey, R.T., "The Analysis of Phase Separation Phenomena in Branched Conduits", *International Journal of Multiphase Flow*, Vol. 10, pp. 1-20, 1984.
- Seeger, W., Reimann, J., and Muller, U., "Two-phase Flow in a T-Junction with a Horizontal Inlet Part I: Phase Separation", *International Journal of Multiphase Flow*, Vol. 12, pp. 575-585, 1986.
- Shoham, D., "Flow Pattern Transition and Characterization in Gas-Liquid Two Phase Flow in Inclined Pipes", Ph.D. Thesis, Tel-Aviv University, 1982.
- Shoham, O., Arirachakaran, S., and Brill, J.P., "Two-Phase Flow Splitting in a Horizontal Reduced Pipe Tee", *Chemical Engineering Science*, Vol. 44, pp. 2388-2391, 1989.
- Schrock, V.E., Revankar, S.T., Mannheimer, R., Wang, C.H., and Jia, D., "Steam-Water Critical Flow Through Small Pipes from Stratified Upstream Regions", In: *Proceedings of the Eighth International Heat Transfer Conference*, San Francisco, CA, Vol. 5, pp. 2307-2311, 1986.
- Smoglie, C., and Reimann, J., "Two-Phase Flow Through Small Branches in a Horizontal Pipe with Stratified Flow", *International Journal of Multiphase Flow*, Vol. 12, pp. 609-625, 1986.
- Stacey, T., Azzopardi, B.J., and Conte, G., "The Split of Annular Two-Phase Flow at a Small Diameter T-Junction," *Int. Journal of Multiphase Flow*, Vol. 26, pp. 845-856, 2000.
- Taitel, Y., and Dukler, A., "A Model for Predicting Flow Regime Transitions in a Horizontal and Near-Horizontal Gas-Liquid Flow", *AIChE Journal*, Vol. 22, pp. 47-55, 1976.

- Van Gorp, C.A., Soliman, H.M., and Sims, G.E., “Two-Phase Pressure Drop and Phase Distribution at a Reduced Horizontal Tee Junction: The Effect of System Pressure”, *International Journal of Multiphase Flow*, Vol. 27, pp. 571-576, 2001.
- Walters, L.C., Soliman, H.M., and Sims, G.E., “Two-Phase Pressure Drop and Phase Distribution at Reduced T-Junction”, *International Journal of Multiphase Flow*, Vol. 24, pp. 775-792, 1998.
- Wang, S.F., and Shoji, M., “Fluctuation Characteristics of Two-Phase Flow Splitting at a Vertical Impacting T-Junctions”, *International Journal of Multiphase Flow*, Vol. 28, pp. 2007-2016, 2002.
- Wang, S.F., Mosdorf, R., and Shoji, M., “Nonlinear Analysis on Fluctuation Feature of Two-Phase Flow through a T-Junction”, *International Journal of Heat and Mass Transfer*, Vol. 46, pp. 1519-1528, 2003.
- Welter, K.B., Wu, Q., You, Y., Abel, K., McCreary, D., Bajorek, S.M., and Reyes Jr, J.N., “Experimental Investigation and Theoretical Modeling of Liquid Entrainment in a Horizontal Tee with a Vertical-up Branch”, *International Journal of Multiphase Flow*, Vol. 30, pp. 1451-1484, 2004.
- Woldesemayat, M.A., and Ghajar, A.J., “Comparison of Void Fraction Correlations for Different Flow Patterns in Horizontal and Upward Inclined Pipes” *International Journal of Multiphase Flow*, Vol. 33, pp. 347-370, 2007.
- Wren, E., “Geometric Effect on Phase Split at a Large Diameter T-Junction”, Ph.D. Thesis, University of Nottingham, UK, 2001.

- Wren, E., and Azzopardi, B.J., “The Phase Separation Capabilities of Two T-Junctions Placed in Series”, *Trans. Institution of Chemical Engineering*, Vol. 82 (A3), pp. 364-371, 2004.
- Wren, E., Baker, G., Azzopardi, B.J., and Jones, R., “Slug Flow in Small Diameter Pipes and T-Junctions”, *Experimental Thermal and Fluid Science*, Vol. 29, pp. 893-899, 2005.
- Yang, L., and Azzopardi, B.J., “Phase Split of Liquid–Liquid Two-Phase Flow at a Horizontal T-Junction”, *International Journal of Multiphase flow*, Vol. 33, pp. 207-216, 2007.
- Yonomoto, T., and Tasaka, K., “Liquid and Gas Entrainment to a Small Break Hole from a Stratified Two-Phase Region”, *International Journal of Multiphase Flow*, Vol. 17, pp. 745-765, 1991.

Appendix A

CALIBRATION OF THE MEASURING DEVICES

All measurement devices used in the experiments are listed in Tables 3.1 to 3.4. The instruments were calibrated in-house and the calibration results were compared with manufacturers' recommendations. The purpose of that was to eliminate any source of error related to the measuring device itself. Calibration results of flow meters, pressure gauges, and thermocouples are listed in this appendix. The in-house calibration values were used in the data analysis. In the cases where the device reading was located between two calibration points, linear interpolation between these two points was used to obtain the corresponding measurement.

A.1 Pressure Gauges

The pressure gauges used in this investigation consist of eight Bourdon pressure gauges and one Ashcroft gauge pressure. The location and range of each pressure gauge is given in Table 3.1. Only the range from 0 to 60 psi was calibrated using a dead-weight tester. It should be mentioned that the gauge installed before the pressure controller was not calibrated. It was used to monitor the pressure at the main supply line and this reading was not used in the data analysis. The results of the calibration are presented in tabular format in Tables A1.1 to A1.8. The manufacturer's reading indicated by the pressure gauge is compared to the actual pressure measured by the dead-weight tester. The correction, which is defined as (Actual pressure – manufacturer's reading) is shown in the tables.

Table A1.1 Calibration data of pressure gauge No. 1

After pressure controller		
Indicated pressure (kPa)	Actual pressure (kPa)	Correction (kPa)
0	0	0
34.5	34.5	0
68.9	68.9	0
103.4	103.4	0
137.9	137.9	0
172.4	172.4	0
206.8	205.1	-1.7
241.3	237.9	-3.4
275.8	272.4	-3.4
310.3	306.9	-3.4
344.7	339.5	-5.2
379.2	374	-5.2
413.7	408.5	-5.2

Table A1.2 Calibration data of pressure gauge No. 2

Water inlet		
Indicated pressure (kPa)	Actual pressure (kPa)	Correction (kPa)
0	0	0
34.5	32.8	-1.7
68.9	67.2	-1.7
103.4	101.7	-1.7
137.9	136.2	-1.7
172.4	170.7	-1.7
206.8	203.4	-3.4
241.3	237.9	-3.4
275.8	272.4	-3.4
310.3	305.1	-5.2
344.7	339.5	-5.2
379.2	374	-5.2
413.7	408.5	-5.2

Table A1.3 Calibration data of pressure gauge No. 3

Air inlet		
Indicated pressure (kPa)	Actual pressure (kPa)	Correction (kPa)
0	0	0
34.5	34.5	0
68.9	68.9	0
103.4	103.4	0
137.9	137.9	0
172.4	172.4	0
206.8	206.8	0
241.3	241.3	0
275.8	274.1	-1.7
310.3	308.6	-1.7
344.7	343	-1.7
379.2	377.5	-1.7
413.7	412	-1.7

Table A1.4 Calibration data of pressure gauge No. 4

Tee junction		
Indicated pressure (kPa)	Actual pressure (kPa)	Correction (kPa)
0	0	0
34.5	34.5	0
68.9	68.9	0
103.4	103.15	-1.7
137.9	137.65	-1.7
172.4	172.4	-1.7
206.8	205.1	-1.7
241.3	239.6	-1.7
275.8	272.4	-3.4
310.3	306.9	-3.4
344.7	341.3	-3.4
379.2	375.8	-3.4
413.7	410.3	-3.4

Table A1.5 Calibration data of pressure gauge No. 5

Separation Tank 2		
Indicated pressure (kPa)	Actual pressure (kPa)	Correction (kPa)
0	0	0
34.5	34.5	0
68.9	68.9	0
103.4	103.4	0
137.9	139.6	+1.7
172.4	174.1	+1.7
206.8	207.5	+1.7
241.3	246.5	+5.2
275.8	281	+5.2
310.3	313.7	+3.4
344.7	348.1	+3.4
379.2	380.9	+1.7
413.7	415.4	+1.7

Table A1.6 Calibration data of pressure gauge No. 6

Air Outlet 2		
Indicated pressure (kPa)	Actual pressure (kPa)	Correction (kPa)
0	0	0
34.5	34.5	0
68.9	67.1	-1.8
103.4	100	-3.4
137.9	133.5	-3.4
172.4	169	-3.4
206.8	203.4	-3.4
241.2	237.8	-3.4
275.7	272.3	-3.4
310.3	308.6	-1.7
344.7	344.7	0
379.2	379.2	0
413.7	413.7	0

Table A1.7 Calibration data of pressure gauge No. 7

Separation Tank 3		
Indicated pressure (kPa)	Actual pressure (kPa)	Correction (kPa)
0	0	0
34.5	34.5	0
68.9	68.9	0
103.4	103.4	0
137.9	137.9	0
172.4	172.4	0
206.8	205.1	-1.7
241.3	237.9	-3.4
275.8	272.4	-3.4
310.3	306.9	-3.4
344.7	339.5	-5.2
379.2	374	-5.2
413.7	408.5	-5.2

Table A1.8 Calibration data of pressure gauge No. 8

Air Outlet 3		
Indicated pressure (kPa)	Actual pressure (kPa)	Correction (kPa)
0	0	0
34.5	34.5	0
68.9	70.6	+1.7
103.4	105.1	+1.7
137.9	137.9	0
172.4	172.4	0
206.8	206.8	0
241.3	241.3	0
275.8	275.8	0
310.3	310.3	0
344.7	344.7	0
379.2	379.2	0
413.7	415.4	+1.7

A.2 Calibration of Flow Meters

The calibration results of the air and water rotameters are presented in this section. The actual flow rates were measured using wet test meters and venturi meters for the air rotameters and a weight-and-time method for the water rotameters. The glass tube of each rotameter is divided into a linear percentage scale provided by the manufacturer. The manufacturer's calibration of some rotameters was provided in tabular format, while for the rest the calibration was indicated on a scale mounted inside the rotameter beside the glass tube.

A.2.1 Air Flow Meters

The 11 rotameters used in this investigation were calibrated using wet test meters and venturi meters (the calibrations of which are traceable to NIST standards). Two wet test meters, Elster-Handel GmbH, with calibration ranges of (0.06-0.6 m³/hr) and (0.15-15 m³/hr) were used. The in-house calibration values were used in the data analysis. The following procedure was followed to calibrate any rotameter using a wet test meter:

1. The rotameter was connected to the selected wet test meter. Care was taken to ensure that the device is well levelled and all connection were leak-free.
2. Room pressure (P_o) and temperature (T_o) readings were used to calculate the air density as :
$$\rho_{\text{dry}} = P_o/RT_o$$
3. The air was passed through the rotameter for a time (t) and the total volume of the air was measured by the wet tester (V_a)
4. The mass flow rate of dry air is calculated as $m_{\text{dry}} = (V_a/t) \times \rho_{\text{dry}}$
5. The saturated pressure from thermodynamic tables at room temperature was used

to calculate the vapor (P_V) and air (P_a) partial pressures.

6. The specific humidity (ϕ) was calculated as:

$$\phi = 0.622 \times P_V / P_a$$

7. The actual density of air passing through the wet tester is calculated using the ideal gas law as: $\rho_{\text{wet}} = P_a / RT_o$

8. Mass flow rate of wet air is calculated as : $m_{\text{wet}} = (V_a / t) * \rho_{\text{wet}}$

9. The mass flow rate of wet air was plotted against the standard mass flow rate provided by the manufacturer.

10. For the rotameter with flow rate capacity higher than $15 \text{ m}^3/\text{hr}$, a venturi meter was used for the calibration of those rotameters.

The calibration results for the air rotametes are presented in tabular format in Tables A2.1 to A2.11.

A.2.2 Water Flow Meters

The 11 water rotameters used in this experiment were calibrated using a weigh-and-time method. The scale used in the calibration, Signum series, model number “SIWADCP-1-35-S”, have a maximum capacity of 35 kg with an accuracy of 0.5 g. A stop watch, Lab-Chron (model number 1401), was used for time measurement. The calibration results for the water rotametes are presented in tabular format in tables A2.12 to A2.22.

Table A2.1 Calibration data of
air rotameter AI-1

Air inlet-1		
Scale reading (%)	Indicated flow rate (SLPM)	Actual flow rate (SLPM)
10	5	6
20	10.5	10.25
30	16.2	16.3
40	22.2	22.6
50	28.5	28.3
60	36	36.4
70	42.2	42.9
80	49.2	49.3
90	56.5	56
100	64	65.2

Table A2.2 Calibration data of
air rotameter AI-2

Air inlet-2		
Scale reading (%)	Indicated flow rate (SLPM)	Actual flow rate (SLPM)
10	44	44
20	82	83
30	120	120
40	155	156
50	192	192
60	225	226
70	262	260
80	297	293
90	336	336
100	375	374

Table A2.3 Calibration data of
air rotameter AI-3

Air inlet-3		
Scale reading (%)	Indicated flow rate (SLPM)	Actual flow rate (SLPM)
10	200	187
20	375	375
30	560	560
40	740	745
50	930	935
60	1125	1130
70	1325	1360
80	1545	-
90	1760	-
100	1990	-

Table A2.4 Calibration data of
air rotameter AO2-1

Air Outlet 2 -1		
Scale reading (%)	Indicated flow rate (SLPM)	Actual flow rate (SLPM)
10	0.86	0.86
20	1.7	1.66
30	2.58	2.5
40	3.44	3.32
50	4.3	4.18
60	5.16	5.07
70	6.02	6.05
80	6.88	6.82
90	7.74	7.72
100	8.6	8.5

Table A2.5 Calibration data of
air rotameter AO2-2

Air Outlet 2-2		
Scale reading (%)	Indicated flow rate (SLPM)	Actual flow rate (SLPM)
10	7.3	5.5
20	12.4	12.9
30	17	16.5
40	22	21.5
50	26.5	25.5
60	30.75	30
70	35.5	34.7
80	39.5	39.5
90	43.5	42.9
100	-	-

Table A2.6 Calibration data of
air rotameter AO2-3

Air Outlet 2-3		
Scale reading (%)	Indicated flow rate (SLPM)	Actual flow rate (SLPM)
10	47	49
20	87	88
30	123	125
40	158	158
50	195	195
60	230	233
70	266	267
80	305	306
90	342	342
100	379	378

Table A2.7 Calibration data of
air rotameter AO2-4

Air Outlet 2-4		
Scale reading (%)	Indicated flow rate (SLPM)	Actual flow rate (SLPM)
10	73	83
20	146	143
30	219	206
40	292	272
50	365	346
60	432	420
70	505	495
80	584	580
90	660	662
100	729.5	738

Table A2.8 Calibration data of
air rotameter AO3-1

Air Outlet 3-1		
Scale reading (%)	Indicated flow rate (SLPM)	Actual flow rate (SLPM)
10	0.68	0.58
20	1.55	1.52
30	2.45	2.45
40	3.35	3.35
50	4.2	4.2
60	5.175	5.35
70	6	6.2
80	6.9	7.1
90	7.8	7.94
100	8.68	8.8

Table A2.9 Calibration data of
air rotameter AO3-2

Air Outlet 3-2		
Scale reading (%)	Indicated flow rate (SLPM)	Actual flow rate (SLPM)
10	6	5.8
20	10.5	10.75
30	16.2	16.1
40	22.5	22.6
50	29	30.4
60	36	37
70	42.5	43.2
80	49.5	51
90	56.8	56.5
100	65	64.9

Table A2.10 Calibration data of
air rotameter AO3-3

Air Outlet 3-3		
Scale reading (%)	Indicated flow rate (SLPM)	Actual flow rate (SLPM)
10	47	48
20	87	89
30	124	125
40	158	158
50	195	195
60	230	233
70	265	267
80	305	306
90	342	340
100	378	377

Table A2.11 Calibration data of
air rotameter AO3-4

Air Outlet 3-4		
Scale reading (%)	Indicated flow rate (SLPM)	Actual flow rate (SLPM)
10	210	210
20	375	378
30	560	565
40	740	755
50	930	945
60	1120	-
70	1320	-
80	1540	-
90	1755	-
100	-	-

Table A2.12 Calibration data of
water rotameter WI-1

Water inlet-1		
Scale reading (%)	Indicated flow rate (cm ³ /min)	Actual flow rate (cm ³ /min)
10	-	3.8
20	10.5	11.0
30	19.2	20.5
40	28.5	29.5
50	38.75	39.6
60	47	48.5
70	57	58.5
80	66	65.5
90	75	76.2
100	85.4	85

Table A2.13 Calibration data of
water rotameter WI-2

Water inlet-1		
Scale reading (%)	Indicated flow rate (cm ³ /min)	Actual flow rate (cm ³ /min)
10	35	34
20	87	89
30	133	144
40	189	192
50	240	246
60	290	298
70	341	342
80	393	388
90	447	435
100	495	490

Table A2.14 Calibration data of
water rotameter WI-3

Water inlet-3		
Scale reading (%)	Indicated flow rate (cm ³ /min)	Actual flow rate (cm ³ /min)
10	385	405
20	660	675
30	925	925
40	1175	1190
50	1455	1470
60	1730	1740
70	2030	2035
80	2320	2340
90	2630	2635
100	2960	2955

Table A2.15 Calibration data of
water rotameter WO2-1

Water Outlet 2-1		
Scale reading (%)	Indicated flow rate (cm ³ /min)	Actual flow rate (cm ³ /min)
10	1	0.75
20	2	1.5
30	3	2.8
40	4	3.8
50	5	4.5
60	6	5.6
70	7	6.3
80	8	7.2
90	9	8
100	10	8.8

Table A2.16 Calibration data of
water rotameter WO2-2

Water Outlet 2-2		
Scale reading (%)	Indicated flow rate (cm ³ /min)	Actual flow rate (cm ³ /min)
10	7.5	7.0
20	15	14.5
30	22.5	21.5
40	30	28.5
50	37.5	36.75
60	45	44.5
70	52.5	51.5
80	60	60
90	67.5	68
100	75	75

Table A2.17 Calibration data of water rotameter WO2-3

Water Outlet 2-3		
Scale reading (%)	Indicated flow rate (cm ³ /min)	Actual flow rate (cm ³ /min)
10	48	46
20	96	95
30	144	143
40	192	192
50	240	240
60	288	294
70	336	340
80	384	392
90	432	441
100	480	487

Table A2.18 Calibration data of water rotameter WO2-4

Water Outlet 2-4		
Scale reading (%)	Indicated flow rate (cm ³ /min)	Actual flow rate (cm ³ /min)
10	291	281
20	583	573
30	875	849
40	1166	1122
50	1457	1433
60	1749	1722
70	2040	2010
80	2332	2312
90	2613	2620
100	2915	2908

Table A2.19 Calibration data of water rotameter WO3-1

Water Outlet 3-1		
Scale reading (%)	Indicated flow rate (cm ³ /min)	Actual flow rate (cm ³ /min)
10	1	1
20	2	1.5
30	3	2.2
40	4	3.25
50	5	4.1
60	6	5.25
70	7	5.95
80	8	7.2
90	9	8.1
100	10	9.1

Table A2.20 Calibration data of water rotameter WO3-2

Water Outlet 3-2		
Scale reading (%)	Indicated flow rate (cm ³ /min)	Actual flow rate (cm ³ /min)
10	7.5	5.5
20	15	14.5
30	22.5	21.5
40	30	28.8
50	37.5	37.2
60	45	44.3
70	52.5	52
80	60	59.5
90	67.5	68
100	75	75

Table A2.21 Calibration data of water rotameter WO3-3

Water Outlet 3-3		
Scale reading (%)	Indicated flow rate (cm ³ /min)	Actual flow rate (cm ³ /min)
10	48	44
20	96	92.5
30	144	142
40	192	192.5
50	240	240
60	288	285
70	336	330
80	384	377
90	432	428
100	480	477

Table A2.22 Calibration data of water rotameter WO3-4

Water Outlet 3-4		
Scale reading (%)	Indicated flow rate (cm ³ /min)	Actual flow rate (cm ³ /min)
10	291	237
20	583	548
30	875	852
40	1166	1120
50	1457	1456
60	1749	1748
70	2040	2020
80	232	2312
90	2614	2620
100	2955	2908

A.3 Thermocouples

All six thermocouples, TRP-K-type used in these experiments were calibrated using ice point cell (Omega TRCIII) at ice point and at room temperature against standard mercury-in-glass thermometer with an accuracy of 0.05°C. the calibration results for the thermocouples used in this investigation are presented in Tables A3.1 and A3.2.

Table A3.1 Calibration data of the air thermocouples (All data in °C)

Air inlet			
Ice point	Thermocouple	Thermometer	Thermocouple
0.0	0.0	21.8	21.7
Air Outlet 2			
Ice point	Thermocouple	Thermometer	Thermocouple
0.1	0.0	21.3	21.1
Air Outlet 3			
Ice point	Thermocouple	Thermometer	Thermocouple
0.0	0.0	22.2	22.2

Table A3.2 Calibration data of the water thermocouples (All data in °C)

Water inlet			
Ice point	Thermocouple	Thermometer	Thermocouple
0.0	0.1	22	21.8
Water Outlet 2			
Ice point	Thermocouple	Thermometer	Thermocouple
0.1	0.1	21.8	21.8
Water Outlet 3			
Ice point	Thermocouple	Thermometer	Thermocouple
0.0	0.0	22	21.9

Appendix B

PHASE-REDISTRIBUTION AND FULL-SEPARATION DATA

This appendix contains tabulated values for all the experimental data obtained in this investigation. Tables B.1 provides a listing of the operating conditions and corresponding phase-redistribution data for all data points. Table B.2 provides a listing of the mass flow rates of air and water in the three sides of the junction for all data points. For the case of the junction with horizontal inlet and horizontal outlets, only data points for the range of $0 < W_3/W_1 < 0.5$ were included. The values of F_{L3} and F_{G3} for the data points of $0.5 < W_3/W_1 < 1.0$ can be estimated based on symmetry. Table B provides a listing of the operating conditions and corresponding full-separation data for all data points covered in this investigation. The air mass-balance error for data points with $J_{G1} < 0.5$ m/s and water mass balance error for data points with $J_{L1} > 0.0025$ m/s were not recorded. The gas mass flow rate of the inlet was too small to be measured within the acceptable range of the smallest rotamater.

Legend

F_{G3}	Fraction of inlet gas entering Outlet 3
F_{L3}	Fraction of inlet liquid entering Outlet 3
J_{G1}	Inlet superficial gas velocity, m/s
J_{L1}	Inlet superficial liquid velocity, m/s
P_s	Test-section pressure, kPa
T_s	Temperature at the tee junction inlet, °C
W_3/W_1	Mass split ratio
x_1	Inlet quality, percentage
	Mass-balance error, (%)

ble B.1 Phase-redistribution data

(a) Long outlets

Test Number	θ	J_{G1} (m/s)	J_{L1} (m/s)	P_s kPa	T_s K	x_1 (%)	W_3/W_1	F_{G3}	F_{L3}	Mass balance error (%)	
										Air	Water
St1-1-1	0.0°	2.014	0.010	199.95	294.75	32.2	0.000	0.000	0.000	1.52	1.16
St1-1-2		2.006	0.010	199.95	295.35	31.9	0.016	0.051	0.000	0.17	-0.58
St1-1-3		2.014	0.010	199.90	294.75	32.2	0.098	0.109	0.093	-0.65	1.16
St1-1-4		2.014	0.010	199.90	294.75	32.1	0.188	0.196	0.185	-2.30	0.58
St1-1-5		2.014	0.010	199.90	294.75	32.1	0.280	0.304	0.269	-1.38	-0.87
St1-1-6		2.014	0.010	200.35	294.75	32.1	0.379	0.397	0.370	-0.31	-0.58
St1-1-7		2.004	0.010	201.90	294.65	32.2	0.496	0.493	0.497	1.43	0.58
St1-2-1	0.1°	2.020	0.010	199.65	295.35	32.2	0.087	0.000	0.128	-1.13	0.00
St1-2-2		2.019	0.010	199.85	295.35	32.2	0.135	0.051	0.174	-0.62	0.58
St1-2-3		2.006	0.010	200.10	295.35	31.8	0.181	0.106	0.216	-0.80	0.86
St1-2-4		2.004	0.010	201.33	295.35	32.0	0.250	0.196	0.289	-1.18	-1.73
St1-2-5		1.999	0.010	200.85	294.15	32.0	0.371	0.298	0.405	-1.05	0.58
St1-2-6		1.990	0.010	201.38	295.15	32.1	0.481	0.410	0.517	-0.69	1.16
St1-2-7		1.990	0.010	201.45	295.15	32.0	0.580	0.490	0.620	0.71	-2.32
St1-2-8		1.990	0.010	201.42	295.15	32.0	0.690	0.590	0.730	-0.56	-1.43
St1-2-9		1.990	0.010	201.45	295.15	32.0	0.790	0.690	0.840	0.92	0.58
St1-2-10		2.000	0.010	201.35	295.35	32.0	0.890	0.800	0.930	-0.45	-1.15
St1-2-11		2.000	0.010	201.31	295.35	32.0	0.930	0.840	0.970	0.99	-1.44
St1-2-12		2.004	0.010	201.32	295.35	32.1	0.949	0.852	0.994	0.27	0.58
St1-3-1	0.2°	2.012	0.010	198.72	294.25	32.1	0.174	0.000	0.256	-1.31	-1.16
St1-3-2		2.014	0.010	199.88	295.35	32.1	0.218	0.051	0.297	-0.86	1.74
St1-3-3		2.000	0.010	200.12	295.35	32.0	0.270	0.110	0.340	-1.02	2.32
St1-3-4		2.000	0.010	201.35	295.35	32.0	0.350	0.200	0.430	-0.44	0.00

Table B.1(a) (continued)

Test Number	θ	J_{G1} (m/s)	J_{L1} (m/s)	P_s kPa	T_s K	x_1 (%)	W_3/W_1	F_{G3}	F_{L3}	Mass balance error (%)	
										Air	Water
St1-3-5	0.2°	2.000	0.010	200.2	294.15	31.0	0.460	0.29	0.55	1.26	0.00
St1-3-6		2.010	0.010	199.0	295.15	32.0	0.570	0.39	0.66	0.68	-1.16
St1-3-7		2.010	0.010	199.0	295.15	32.0	0.690	0.490	0.790	1.32	-1.16
St1-3-8		2.011	0.010	199.08	295.15	32.0	0.823	0.595	0.930	1.31	-1.16
St1-3-9		1.995	0.010	200.63	294.65	31.9	0.879	0.657	0.983	-0.64	1.73
St1-4-1	0.3°	2.009	0.010	200.15	295.15	31.9	0.235	0.000	0.345	-1.43	1.15
St1-4-2		2.000	0.010	201.13	294.35	32.0	0.280	0.058	0.380	-1.94	0.58
St1-4-3		2.000	0.010	201.00	294.35	32.0	0.330	0.110	0.440	-1.91	1.15
St1-4-4		2.000	0.010	201.00	295.35	32.0	0.490	0.200	0.630	1.01	-0.57
St1-4-5		2.010	0.010	200.81	295.15	32.0	0.720	0.280	0.930	-0.79	-1.16
St1-4-6		2.011	0.010	200.81	295.15	32.2	0.776	0.305	1.000	-0.07	0.00
St1-5-1	0.5°	1.998	0.010	201.55	295.35	32.0	0.470	0.000	0.700	-2.05	-0.87
St1-5-2		2.004	0.010	201.13	295.35	32.0	0.570	0.050	0.820	-1.39	-2.32
St1-5-3		2.000	0.010	201.47	295.35	32.1	0.640	0.072	0.912	-0.64	0.58
St1-5-4		2.001	0.010	201.48	295.35	32.2	0.706	0.088	1.000	-0.65	0.00
St1-6-1	0.6°	1.990	0.010	201.82	294.35	32.2	0.631	0.000	0.930	-2.12	-1.16
St1-6-2		2.014	0.010	199.14	295.35	32.1	0.694	0.022	1.012	-0.87	-1.16
St1-7-1	0.7°	2.010	0.010	199.82	295.35	31.0	0.670	0.000	0.990	-1.42	0.57
St2-1-1	0.1°	2.020	0.040	199.74	295.15	10.0	0.140	0.000	0.160	2.07	0.29
St2-1-2		2.025	0.040	199.75	295.25	10.6	0.194	0.050	0.212	-0.10	0.58

Table B.1(a) (continued)

Test Number	θ	J_{G1} (m/s)	J_{L1} (m/s)	P_s kPa	T_s K	x_1 (%)	W_3/W_1	F_{G3}	F_{L3}	Mass balance error (%)	
										Air	Water
St2-1-3	0.1°	2.025	0.040	199.75	295.25	10.6	0.226	0.101	0.241	-2.42	0.58
St2-1-4		2.025	0.040	199.75	295.25	10.6	0.268	0.202	0.275	1.90	0.00
St2-1-5		2.021	0.039	200.23	295.25	10.7	0.343	0.289	0.350	1.87	0.87
St2-1-6		2.018	0.040	200.23	295.25	10.7	0.408	0.405	0.408	-2.08	-0.58
St2-1-7		2.028	0.040	200.23	295.25	10.7	0.502	0.503	0.501	-0.68	-0.29
St2-2-1	0.2°	2.001	0.040	199.75	294.25	10.5	0.290	0.000	0.325	1.07	0.87
St2-2-2		1.996	0.040	201.34	295.25	10.4	0.333	0.051	0.365	-1.53	0.57
St2-2-3		2.001	0.040	199.75	294.25	10.5	0.369	0.102	0.400	-0.38	0.58
St2-2-4		2.001	0.040	199.75	294.25	10.5	0.429	0.204	0.455	-1.84	0.87
St2-2-5		2.005	0.040	199.40	294.25	10.5	0.510	0.291	0.536	1.07	2.00
St2-2-6		2.005	0.040	201.35	295.25	10.6	0.600	0.408	0.623	0.91	0.00
St2-2-7		2.008	0.040	200.81	295.25	10.6	0.735	0.495	0.764	1.05	-1.16
St2-2-8		2.010	0.040	200.28	295.15	10.6	0.827	0.596	0.854	-0.25	0.58
St2-2-9		2.016	0.040	199.78	294.65	10.6	0.895	0.698	0.918	1.15	0.58
St2-2-10		2.011	0.040	199.78	293.25	10.7	0.960	0.798	0.980	-0.07	0.58
St2-2-11		2.011	0.040	199.78	293.25	10.7	0.986	0.819	1.006	0.66	-0.58
St2-3-1	0.5°	1.996	0.040	200.81	294.25	10.6	0.415	0.000	0.464	0.80	1.45
St2-3-2		2.008	0.040	200.81	295.15	10.6	0.449	0.058	0.496	-1.85	-0.58
St2-3-3		1.996	0.040	200.81	294.25	10.6	0.490	0.102	0.536	-2.28	1.45
St2-3-4		2.000	0.040	200.01	294.25	10.5	0.566	0.204	0.609	-1.91	0.00
St2-3-5		2.005	0.040	199.40	294.25	10.5	0.653	0.291	0.696	1.07	1.45
St2-3-6		2.008	0.040	200.81	295.25	10.6	0.852	0.407	0.904	1.05	0.87
St2-3-7		2.050	0.040	200.81	295.25	10.8	0.917	0.428	0.977	0.22	0.15

Table B.1(a) (continued)

Test Number	θ	J_{G1} (m/s)	J_{L1} (m/s)	P_s kPa	T_s K	x_1 (%)	W_3/W_1	F_{G3}	F_{L3}	Mass balance error (%)	
										Air	Water
St2-3-8	0.5°	2.008	0.040	200.81	295.25	10.6	0.940	0.437	1.000	-1.86	0.00
St2-4-1	1.0°	2.010	0.040	199.78	295.25	10.5	0.433	0.000	0.484	0.63	2.32
St2-4-2		1.999	0.040	200.81	295.15	10.6	0.491	0.058	0.542	-2.28	-0.29
St2-4-3		1.996	0.040	200.81	294.25	10.6	0.537	0.102	0.588	-0.66	-0.87
St2-4-4		1.990	0.040	202.01	294.25	10.6	0.612	0.198	0.661	-0.24	-0.87
St2-4-5		1.999	0.041	200.47	294.25	10.4	0.727	0.299	0.777	0.07	0.86
St2-4-6		1.990	0.040	202.01	294.25	10.6	0.807	0.329	0.864	-0.24	-0.87
St2-4-7		1.999	0.041	200.47	294.25	10.4	0.919	0.350	0.986	0.80	1.43
St2-3-8		2.008	0.040	200.81	295.25	10.6	0.940	0.437	1.000	-1.86	0.00
St2-5-1	2.5°	1.997	0.040	201.21	295.15	10.6	0.544	0.000	0.609	0.54	-2.90
St2-5-2		1.997	0.04	201.21	295.15	10.5	0.563	0.058	0.623	-2.38	1.44
St2-5-3		1.993	0.040	201.35	294.25	10.6	0.704	0.205	0.764	-2.26	2.33
St2-5-4		1.993	0.040	201.35	294.25	10.6	0.909	0.219	0.991	-0.80	0.87
St2-6-1	5.0°	1.995	0.040	201.27	294.15	10.6	0.643	0.000	0.719	0.61	-0.87
St2-6-2		1.989	0.040	201.48	293.25	10.6	0.715	0.058	0.793	-2.12	0.29
St2-6-3		1.995	0.040	201.27	294.15	10.6	0.747	0.080	0.826	-1.58	0.00
St2-6-4		1.989	0.040	201.48	293.25	10.6	0.890	0.088	0.985	0.80	1.46
St2-7-1	6.5°	1.994	0.040	201.88	295.15	10.6	0.756	0.000	0.845	0.37	-0.58
St2-7-2		1.994	0.040	201.88	295.15	10.6	0.880	0.022	0.983	-1.82	1.75
St2-8-1	7.5°	2.002	0.040	200.95	295.15	10.6	0.889	0.000	0.994	0.78	0.58

Table B.1(a) (continued)

Test Number	θ	J_{G1} (m/s)	J_{L1} (m/s)	P_s kPa	T_s K	x_1 (%)	W_3/W_1	F_{G3}	F_{L3}	Mass balance error (%)	
										Air	Water
W1-1-1	0.0°	10.01	0.010	200.55	294.15	70.2	0.000	0.000	0.000	-0.25	0.58
W1-1-2		10.01	0.010	200.55	294.15	70.2	0.126	0.180	0.000	-0.56	1.73
W1-1-3		10.08	0.010	200.55	294.15	70.4	0.147	0.195	0.035	-0.83	0.58
W1-1-4		10.08	0.010	200.55	294.15	70.4	0.209	0.254	0.104	-2.24	2.89
W1-1-5		9.969	0.010	201.61	294.15	70.2	0.261	0.303	0.162	-0.36	-1.73
W1-1-6		9.959	0.010	201.27	294.15	70.2	0.378	0.392	0.347	1.14	-2.89
W1-1-7		10.02	0.010	198.60	295.15	70.0	0.500	0.502	0.497	-0.31	0.00
W1-2-1	5.0°	10.05	0.010	201.61	294.15	70.4	0.000	0.000	0.000	0.03	1.73
W1-2-2		10.05	0.010	201.61	294.15	70.4	0.081	0.115	0.000	1.27	1.73
W1-2-3		10.05	0.010	201.61	294.15	70.4	0.168	0.199	0.092	0.46	0.58
W1-2-4		10.04	0.010	200.81	296.15	70.2	0.287	0.303	0.249	-0.13	0.00
W1-2-5		9.982	0.010	201.08	294.15	70.2	0.414	0.399	0.451	1.11	2.89
W1-2-6		9.999	0.010	201.08	294.15	70.3	0.545	0.501	0.647	-0.32	0.58
W1-2-7		9.982	0.010	201.08	294.15	70.2	0.671	0.593	0.855	0.69	-1.16
W1-2-8		9.996	0.010	200.81	294.15	70.2	0.735	0.642	0.954	0.83	0.00
W1-2-9		9.996	0.010	200.81	294.15	70.2	0.760	0.665	0.983	-0.34	1.73
W1-3-1	15°	10.00	0.010	201.08	295.15	70.3	0.000	0.000	0.000	0.22	1.16
W1-3-2		10.00	0.010	201.08	295.15	70.3	0.020	0.029	0.000	3.17	0.00
W1-3-3		10.00	0.010	201.08	295.15	70.3	0.086	0.100	0.055	0.82	-0.29
W1-3-4		9.999	0.010	201.08	295.15	70.3	0.203	0.198	0.215	0.88	-1.16
W1-3-5		9.975	0.010	201.75	295.15	70.1	0.349	0.299	0.466	0.60	1.15
W1-3-6		9.999	0.010	201.75	295.15	70.4	0.506	0.396	0.767	0.80	-0.58
W1-3-7		10.02	0.010	201.08	295.75	70.1	0.640	0.501	0.966	-0.28	1.15

Table B.1(a) (continued)

Test Number	θ	J_{G1} (m/s)	J_{L1} (m/s)	P_s kPa	T_s K	x_1 (%)	W_3/W_1	F_{G3}	F_{L3}	Mass balance error (%)	
										Air	Water
W1-3-8		10.02	0.010	201.08	295.75	70.1	0.660	0.524	0.977	-2.61	2.30
W1-4-1	30°	10.01	0.010	200.81	295.15	70.3	0.040	0.000	0.134	-0.31	-0.58
W1-4-2		10.01	0.010	200.81	295.15	70.3	0.094	0.050	0.198	0.63	0.00
W1-4-3		10.00	0.010	201.21	295.15	70.3	0.156	0.099	0.291	0.75	-0.58
W1-4-4		10.01	0.010	201.21	295.15	70.3	0.292	0.204	0.500	-0.84	-1.16
W1-4-5		9.973	0.010	199.49	294.15	70.2	0.443	0.300	0.779	0.07	1.16
W1-4-6		9.976	0.010	201.21	294.55	70.3	0.552	0.397	0.919	0.33	0.00
W1-4-7		9.999	0.010	201.21	294.75	70.5	0.614	0.460	0.982	1.07	-1.75
W1-4-8		9.999	0.010	201.21	294.75	70.5	0.629	0.472	1.006	-0.09	-0.58
W1-5-1	45°	9.979	0.010	200.81	294.15	70.3	0.116	0.000	0.390	0.03	2.91
W1-5-2		9.979	0.010	200.81	294.15	70.3	0.155	0.024	0.465	1.11	-1.16
W1-5-3		9.993	0.010	200.81	294.55	70.3	0.251	0.082	0.651	1.43	0.00
W1-5-4		10.00	0.010	200.81	294.55	70.3	0.391	0.198	0.849	-0.09	1.16
W1-5-5		10.00	0.010	200.81	294.55	70.3	0.492	0.297	0.953	1.15	-1.16
W1-5-6		9.979	0.010	200.81	294.15	70.3	0.511	0.338	0.919	1.49	2.33
W1-3-7		10.02	0.010	201.08	295.75	70.1	0.660	0.524	0.977	-2.61	2.30
W1-5-8		9.929	0.010	200.55	295.15	70.1	0.555	0.365	1.000	-1.14	0.00
W1-6-1	75°	10.01	0.010	200.41	294.15	70.3	0.269	0.000	0.907	0.55	0.00
W1-6-2		10.01	0.010	200.41	294.15	70.3	0.311	0.049	0.930	-0.30	2.33
W1-6-3		10.01	0.010	200.95	295.15	70.3	0.358	0.099	0.971	0.82	0.58
W1-6-4		9.99	0.010	201.08	294.75	70.3	0.380	0.123	0.988	0.21	0.00
W1-6-5		9.99	0.010	201.08	294.75	70.3	0.384	0.128	0.988	-0.96	1.16

Table B.1(a) (continued)

Test Number	θ	J_{G1} (m/s)	J_{L1} (m/s)	P_s kPa	T_s K	x_1 (%)	W_3/W_1	F_{G3}	F_{L3}	Mass balance error (%)	
										Air	Water
W1-7-1	87.5°	10.01	0.010	200.41	294.15	70.3	0.293	0.000	0.988	0.55	1.16
W2-1-1	0.0°	10.09	0.040	200.23	294.55	37.3	0.045	0.000	0.072	1.20	-1.45
W2-1-2		10.09	0.040	200.23	294.55	37.3	0.096	0.052	0.122	0.08	0.87
W2-1-3		10.11	0.040	199.75	294.15	37.3	0.142	0.098	0.168	0.22	-0.87
W2-1-4		10.06	0.040	201.56	294.85	37.4	0.239	0.202	0.261	0.54	1.45
W2-1-5		10.09	0.040	201.56	294.85	37.4	0.285	0.249	0.307	-0.04	-0.29
W2-1-6		10.09	0.040	200.23	294.55	37.3	0.326	0.300	0.342	0.89	0.58
W2-1-7		10.09	0.040	200.23	294.55	37.3	0.404	0.392	0.412	0.31	0.87
W2-1-8		10.09	0.040	200.23	294.55	37.3	0.495	0.490	0.499	2.04	0.29
W2-2-1	5.0°	10.00	0.040	200.95	295.15	37.5	0.140	0.000	0.224	-0.01	-0.29
W2-2-2		10.00	0.040	200.95	295.15	37.5	0.172	0.053	0.244	0.62	-0.88
W2-2-3		10.00	0.040	200.95	295.15	37.5	0.210	0.099	0.276	-1.10	-2.65
W2-2-4		10.10	0.040	200.01	294.55	37.3	0.291	0.196	0.348	1.43	1.45
W2-2-5		9.92	0.040	200.36	294.55	37.2	0.363	0.305	0.397	-1.44	0.00
W2-2-6		9.92	0.040	200.23	294.55	36.9	0.440	0.399	0.464	-1.92	0.87
W2-2-7		9.95	0.040	200.01	295.55	37.2	0.537	0.499	0.559	0.17	-1.47
W2-2-8		10.09	0.040	200.55	294.55	37.3	0.637	0.612	0.652	-0.40	-1.45
W2-2-9		10.08	0.040	201.08	294.55	37.5	0.736	0.700	0.758	-0.04	-0.58
W2-2-10		10.07	0.040	200.95	294.55	37.7	0.904	0.804	0.965	-0.09	-0.88
W2-2-11		10.07	0.040	200.95	294.55	37.7	0.940	0.816	1.015	1.06	-1.47
W2-3-1	15°	10.09	0.040	200.15	295.15	37.2	0.200	0.000	0.319	0.79	1.45
W2-3-2		10.07	0.040	201.56	295.15	37.7	0.235	0.049	0.347	-1.24	-0.88

Table B.1(a) (continued)

Test Number	θ	J_{G1} (m/s)	J_{L1} (m/s)	P_s kPa	T_s K	x_1 (%)	W_3/W_1	F_{G3}	F_{L3}	Mass balance error (%)		
										Air	Water	
W2-3-3	15°	10.10	0.040	200.15	295.15	37.4	0.274	0.098	0.379	-0.22	-0.58	
W2-3-4		9.94	0.040	199.80	294.55	36.9	0.350	0.206	0.435	-1.03	1.45	
W2-3-5		9.94	0.040	200.15	294.55	37.2	0.438	0.293	0.524	-0.30	-0.88	
W2-3-6		9.90	0.040	201.16	295.15	36.9	0.514	0.401	0.580	-1.90	1.45	
W2-3-7		10.09	0.040	200.81	295.55	37.3	0.605	0.499	0.669	0.30	1.16	
W2-3-8		10.09	0.040	200.55	294.55	37.3	0.708	0.612	0.765	-0.40	-0.29	
W2-3-9		10.11	0.040	199.75	295.15	37.3	0.841	0.711	0.918	0.03	-0.58	
W2-3-10		9.95	0.040	199.75	295.75	37.1	0.901	0.735	1.000	-0.51	0.00	
W2-4-1		30°	9.91	0.040	201.56	295.15	37.3	0.277	0.000	0.441	-0.82	1.47
W2-4-2			9.91	0.040	201.56	295.15	37.3	0.331	0.047	0.500	-2.36	-1.47
W2-4-3	10.08		0.040	201.21	295.15	37.5	0.383	0.098	0.554	-0.52	-0.58	
W2-4-4	10.09		0.040	200.87	294.55	37.5	0.475	0.197	0.641	0.44	-2.04	
W2-4-5	10.07		0.040	200.95	294.55	37.6	0.568	0.301	0.729	1.01	-0.59	
W2-4-6	9.90		0.040	201.16	295.15	36.9	0.638	0.401	0.777	-1.90	-0.87	
W2-4-7	10.06		0.040	201.35	294.55	37.4	0.723	0.498	0.858	0.33	-0.87	
W2-4-8	10.07		0.040	200.95	294.55	37.7	0.904	0.804	0.965	-0.09	-0.88	
W2-4-9	10.09		0.039	200.54	295.55	37.8	0.859	0.613	1.005	0.99	-0.58	
W2-5-1	45°	10.11	0.040	199.48	295.15	37.3	0.373	0.000	0.595	0.89	-0.29	
W2-5-2		10.11	0.040	199.48	295.15	37.3	0.484	0.098	0.714	-0.17	-0.58	
W2-5-3		9.93	0.041	200.87	294.55	36.6	0.580	0.200	0.800	-1.24	1.43	
W2-5-4		10.07	0.040	200.95	294.55	37.6	0.642	0.301	0.847	-0.15	-2.35	
W2-5-5		9.90	0.040	201.16	295.15	36.9	0.706	0.401	0.884	-1.90	-2.03	
W2-5-6		10.12	0.041	199.48	295.75	36.8	0.782	0.497	0.949	0.62	0.86	

Table B.1(a) (continued)

Test Number	θ	J_{G1} (m/s)	J_{L1} (m/s)	P_s kPa	T_s K	x_1 (%)	W_3/W_1	F_{G3}	F_{L3}	Mass balance error (%)	
										Air	Water
W2-5-7	45°	10.06	0.040	201.21	294.75	37.3	0.827	0.561	0.986	0.43	-1.74
W2-5-8		10.06	0.040	201.21	294.75	37.3	0.835	0.573	0.991	1.00	0.87
W2-6-1	90°	10.08	0.040	201.48	295.15	37.7	0.462	0.000	0.741	0.69	-2.06
W2-6-2		10.08	0.040	201.48	295.15	37.7	0.556	0.046	0.865	-1.02	0.29
W2-6-3		10.14	0.040	199.48	294.55	37.4	0.602	0.098	0.904	0.24	0.29
W2-6-4		9.91	0.041	201.21	294.75	36.6	0.653	0.200	0.914	-1.82	2.86
W2-6-5		10.13	0.040	199.48	295.15	37.6	0.704	0.300	0.947	0.88	-0.59
W2-6-6		9.91	0.040	199.83	294.15	36.8	0.760	0.399	0.971	-1.37	0.00
W2-6-7		10.14	0.040	199.75	294.75	37.3	0.802	0.494	0.986	1.13	0.00
W2-6-8		10.14	0.041	199.75	294.75	37.0	0.812	0.517	0.986	1.13	1.43
An1-1-1	0.0°	40.03	0.010	199.94	293.55	90.5	0.000	0.000	0.000	0.79	3.10
An1-1-2		40.03	0.010	199.94	293.55	90.5	0.045	0.049	0.000	-1.75	2.33
An1-1-3		40.03	0.010	199.94	293.55	90.5	0.104	0.099	0.151	2.04	2.33
An1-1-4		40.12	0.010	200.95	295.15	90.5	0.206	0.197	0.291	0.79	1.16
An1-1-5		37.31	0.010	201.21	274.75	90.6	0.300	0.290	0.400	1.37	3.24
An1-1-6		40.18	0.010	200.41	294.55	90.6	0.396	0.390	0.447	1.72	1.18
An1-1-7		40.03	0.010	201.35	294.55	90.6	0.496	0.495	0.506	0.17	-1.18
An1-2-1	5.0°	39.87	0.010	202.55	294.65	90.6	0.000	0.000	0.000	0.70	1.18
An1-2-2		39.87	0.010	202.55	294.65	90.6	0.013	0.015	0.000	0.87	2.35
An1-2-3		39.87	0.010	202.55	294.65	90.6	0.052	0.050	0.071	-0.17	1.18
An1-2-4		39.99	0.010	200.73	294.55	90.5	0.109	0.102	0.174	0.76	1.16
An1-2-5		40.04	0.010	200.95	294.55	90.4	0.210	0.199	0.314	0.62	1.16

Table B.1(a) (continued)

Test Number	θ	J_{G1} (m/s)	J_{L1} (m/s)	P_s kPa	T_s K	x_1 (%)	W_3/W_1	F_{G3}	F_{L3}	Mass balance error (%)		
										Air	Water	
An1-2-6	5.0°	40.02	0.010	201.21	294.75	90.5	0.313	0.302	0.412	1.20	2.35	
An1-2-7		40.11	0.010	200.05	295.65	90.5	0.412	0.405	0.482	1.20	1.18	
An1-2-8		41.06	0.010	200.73	295.55	90.7	0.490	0.485	0.541	2.20	-2.35	
An1-2-9		41.06	0.010	200.73	295.55	90.5	0.584	0.584	0.586	2.27	1.15	
An1-2-10		39.78	0.010	201.21	294.65	90.5	0.688	0.698	0.600	-0.04	1.18	
An1-2-11		40.93	0.010	200.73	295.65	90.5	0.907	0.905	0.920	0.91	2.30	
An1-2-12		40.93	0.010	200.73	295.65	90.5	0.895	0.893	0.920	2.18	2.30	
An1-2-13		40.93	0.010	200.73	295.65	90.5	0.929	0.925	0.966	-1.05	1.15	
An1-2-14		40.03	0.010	201.08	295.65	90.3	0.991	0.991	0.989	0.87	1.15	
An1-3-1		30°	39.92	0.010	199.61	294.15	90.4	0.002	0.000	0.023	0.19	2.33
An1-3-2			39.92	0.010	199.61	294.15	90.4	0.110	0.102	0.186	-1.00	2.33
An1-3-3			39.99	0.010	199.27	294.15	90.3	0.212	0.197	0.345	0.57	2.30
An1-3-4			39.92	0.010	199.61	294.15	90.3	0.315	0.301	0.448	-0.02	1.15
An1-3-5			40.07	0.010	198.58	294.65	90.3	0.414	0.404	0.506	1.40	1.15
An1-3-6	40.00		0.010	199.61	294.55	90.4	0.502	0.496	0.558	0.05	0.00	
An1-3-7	39.78		0.010	200.05	294.25	90.4	0.602	0.602	0.605	-0.48	1.16	
An1-3-8	39.96		0.010	200.34	294.25	90.4	0.698	0.700	0.686	-0.34	1.16	
An1-3-9	40.12		0.010	199.61	294.25	90.3	0.788	0.792	0.747	0.50	2.30	
An1-3-10	40.05		0.010	198.58	294.15	90.4	0.910	0.904	0.971	-0.31	-0.58	
An1-3-11	40.05		0.010	198.58	294.15	90.4	0.919	0.912	0.988	-0.69	1.16	
An1-4-1	90°	40.05	0.010	200.68	295.15	90.5	0.008	0.000	0.088	1.21	0.59	
An1-4-2		40.18	0.010	199.80	294.55	90.5	0.116	0.102	0.256	-0.61	1.74	
An1-4-3		40.08	0.010	200.15	294.55	90.3	0.219	0.197	0.425	0.84	2.30	

Table B.1(a) (continued)

Test Number	θ	J_{G1} (m/s)	J_{L1} (m/s)	P_s kPa	T_s K	x_1 (%)	W_3/W_1	F_{G3}	F_{L3}	Mass balance error (%)		
										Air	Water	
An1-4-4	90°	40.08	0.010	200.15	294.55	90.4	0.322	0.303	0.500	-0.01	1.74	
An1-4-5		40.07	0.010	200.47	294.65	90.4	0.415	0.399	0.563	0.57	2.30	
An1-4-6		40.06	0.010	200.47	294.55	90.6	0.506	0.495	0.612	0.13	1.18	
An1-4-7		40.12	0.010	199.80	294.25	90.4	0.613	0.606	0.674	-0.46	1.16	
An1-4-8		40.12	0.010	199.80	294.25	90.4	0.701	0.697	0.738	0.03	0.00	
An1-4-9		40.07	0.010	200.15	294.55	90.5	0.793	0.794	0.788	0.12	1.18	
An1-4-10		40.28	0.010	200.15	295.65	90.4	0.886	0.876	0.977	-0.64	0.00	
An1-4-11		40.28	0.010	200.15	295.65	90.4	0.897	0.887	0.989	-0.32	1.15	
An2-1-1		0.0°	39.45	0.040	201.48	293.55	70.4	0.024	0.000	0.082	0.93	2.06
An2-1-2			40.27	0.041	201.21	294.15	70.2	0.086	0.049	0.171	0.25	1.43
An2-1-3			40.10	0.040	201.75	294.65	70.4	0.142	0.102	0.238	-0.41	0.87
An2-1-4	40.14		0.040	200.95	295.25	70.6	0.238	0.197	0.338	0.03	1.47	
An2-1-5	37.35		0.040	201.75	274.25	70.4	0.328	0.299	0.397	1.17	0.87	
An2-1-6	40.11		0.040	200.95	295.65	70.3	0.424	0.413	0.449	-0.90	0.00	
An2-1-7	39.90		0.040	200.81	294.65	70.2	0.500	0.500	0.500	0.67	0.14	
An2-2-1	5.0°	40.02	0.040	200.87	294.55	70.3	0.036	0.000	0.122	1.98	0.87	
An2-2-2		40.08	0.040	201.00	295.65	70.2	0.154	0.102	0.275	-1.00	1.45	
An2-2-3		39.59	0.040	201.00	295.25	70.3	0.247	0.200	0.359	-1.52	-1.18	
An2-2-4		39.98	0.040	201.35	295.25	70.3	0.334	0.301	0.412	-1.20	0.29	
An2-2-5		39.96	0.040	201.00	295.25	70.2	0.420	0.404	0.458	-0.69	0.58	
An2-2-6		39.22	0.040	201.35	295.65	69.8	0.506	0.504	0.510	-1.15	0.29	
An2-2-7		39.96	0.040	201.00	295.25	70.2	0.593	0.607	0.559	-1.17	0.58	
An2-2-8		39.97	0.040	201.13	295.65	70.2	0.678	0.711	0.600	-1.17	-0.58	

Table B.1(a) (Continued)

Test Number	θ	J_{G1} (m/s)	J_{L1} (m/s)	P_s kPa	T_s K	x_1 (%)	W_3/W_1	F_{G3}	F_{L3}	Mass balance error (%)	
										Air	Water
An2-2-9	5.0°	40.25	0.040	201.35	295.25	70.4	0.758	0.801	0.655	0.22	0.58
An2-2-10		40.30	0.040	199.61	296.65	70.1	0.863	0.905	0.765	-0.68	0.29
An2-2-11		40.08	0.040	201.48	295.55	70.3	0.964	0.955	0.986	0.41	0.58
An2-2-12		40.08	0.040	201.48	295.55	70.3	0.977	0.972	0.991	-0.07	0.87
An2-3-1	30°	40.16	0.040	201.56	295.55	70.4	0.049	0.000	0.165	1.64	0.87
An2-3-2		40.24	0.040	201.21	295.65	70.4	0.106	0.051	0.238	0.39	1.74
An2-3-3		40.15	0.040	201.21	295.65	70.3	0.160	0.102	0.299	-0.65	0.58
An2-3-4		40.24	0.040	199.67	295.25	70.5	0.248	0.197	0.371	0.85	-0.29
An2-3-5		39.98	0.040	201.21	295.65	70.2	0.343	0.304	0.435	0.19	-0.29
An2-3-6		39.93	0.040	200.87	294.65	70.2	0.425	0.404	0.475	-0.55	0.29
An2-3-7		40.01	0.040	201.21	294.15	70.3	0.509	0.504	0.522	-0.60	1.45
An2-3-8		40.17	0.040	199.94	295.25	70.2	0.608	0.622	0.577	-2.30	0.00
An2-3-9		40.17	0.040	199.94	295.25	70.21	0.675	0.696	0.626	0.06	-0.29
An2-3-10		40.00	0.041	200.01	293.25	69.96	0.756	0.793	0.669	0.22	0.29
An2-3-11		40.00	0.041	200.01	293.25	69.96	0.816	0.856	0.723	-6.07	0.57
An2-3-12		40.17	0.040	200.01	295.65	70.18	0.897	0.906	0.875	-0.81	0.87
An2-3-13		40.26	0.040	200.01	295.55	70.24	0.947	0.931	0.986	-0.37	0.00
An2-3-14		40.26	0.040	200.01	295.55	70.24	0.955	0.942	0.986	-0.05	1.45
An2-4-1	45°	40.32	0.040	200.47	295.55	70.32	0.055	0.000	0.186	1.26	0.29
An2-4-2		40.30	0.040	200.81	295.65	70.33	0.166	0.102	0.319	-0.34	0.29
An2-4-3		39.98	0.040	200.73	294.25	70.56	0.254	0.198	0.388	0.55	-0.88
An2-4-4		40.14	0.040	200.47	296.25	70.17	0.349	0.304	0.455	0.03	-0.58
An2-4-5		39.98	0.040	200.47	294.65	70.20	0.432	0.403	0.499	-0.14	0.29

Table B.1(a) (continued)

Test Number	θ	J_{G1} (m/s)	J_{L1} (m/s)	P_s kPa	T_s K	x_1 (%)	W_3/W_1	F_{G3}	F_{L3}	Mass balance error (%)	
										Air	Water
An2-4-6	45°	40.32	0.040	200.81	295.15	70.38	0.509	0.499	0.533	0.09	-0.29
An2-4-7		39.91	0.040	200.87	294.25	70.24	0.605	0.609	0.594	-1.28	0.00
An2-4-8		40.10	0.040	200.87	295.65	70.23	0.689	0.708	0.643	-1.26	0.29
An2-4-9		39.75	0.041	201.08	293.25	69.94	0.776	0.813	0.691	-1.25	0.86
An2-4-10		40.22	0.040	201.08	294.65	70.39	0.820	0.854	0.739	-0.40	0.00
An2-4-11		40.09	0.040	201.16	295.55	70.27	0.938	0.924	0.971	-0.37	0.87
An2-4-12		40.09	0.040	201.16	295.55	70.27	0.948	0.932	0.986	0.27	1.45
An2-4-13		40.17	0.040	199.94	295.25	70.21	0.675	0.696	0.626	0.06	-0.29
An2-5-1	90°	40.18	0.040	200.63	294.55	70.3	0.071	0.000	0.238	0.31	0.29
An2-5-2		40.09	0.040	201.21	294.65	70.3	0.122	0.049	0.296	0.73	0.87
An2-5-3		40.14	0.040	200.28	295.65	70.2	0.177	0.099	0.359	-0.48	0.29
An2-5-4		39.83	0.040	200.73	294.25	70.2	0.268	0.200	0.426	0.00	0.87
An2-5-5		40.24	0.040	200.34	296.25	70.2	0.355	0.303	0.475	0.28	-0.29
An2-5-6		39.98	0.040	200.47	294.65	70.2	0.440	0.403	0.528	-0.14	-0.87
An2-5-7		40.03	0.040	200.68	295.15	70.2	0.524	0.502	0.574	-0.64	0.29
An2-5-8		39.96	0.040	200.41	294.65	70.2	0.623	0.624	0.620	-1.51	0.29
An2-5-9		40.26	0.040	200.07	295.25	70.3	0.688	0.697	0.667	0.02	1.45
An2-5-10		39.80	0.041	200.15	293.25	69.9	0.774	0.800	0.714	-0.34	0.57
An2-5-11		39.99	0.040	200.15	294.65	70.2	0.829	0.846	0.788	0.26	0.58
An2-5-12		39.99	0.040	200.49	295.55	70.1	0.933	0.917	0.971	-1.18	0.58
An2-5-13		39.99	0.040	200.49	295.55	70.1	0.944	0.927	0.986	1.49	1.45
An3-1-1	0.0°	39.89	0.180	200.81	295.15	34.4	0.115	0.000	0.176	1.91	1.49
An3-1-2		39.89	0.180	200.81	295.15	34.4	0.199	0.025	0.290	0.24	-0.19

Table B.1(a) (continued)

Test Number	θ	J_{G1} (m/s)	J_{L1} (m/s)	P_s kPa	T_s K	x_1 (%)	W_3/W_1	F_{G3}	F_{L3}	Mass balance error (%)		
										Air	Water	
An3-1-3	0.0°	39.89	0.180	200.81	295.15	34.4	0.208	0.025	0.304	0.24	0.32	
An3-1-4		40.13	0.180	200.81	295.55	34.5	0.260	0.100	0.345	-0.30	0.26	
An3-1-5		40.12	0.180	200.81	295.55	34.5	0.320	0.202	0.382	-0.29	0.32	
An3-1-6		39.91	0.180	200.95	294.55	34.6	0.374	0.303	0.412	-0.34	0.32	
An3-1-7		40.20	0.180	199.78	296.00	34.5	0.445	0.399	0.469	1.31	0.52	
An3-1-8		40.08	0.180	200.68	296.00	34.5	0.501	0.501	0.502	0.21	0.00	
An3-2-1		5.0°	40.05	0.180	200.81	295.55	34.5	0.157	0.000	0.239	1.93	0.32
An3-2-2			40.05	0.180	200.81	295.55	34.5	0.206	0.025	0.301	0.02	0.65
An3-2-3	40.05		0.180	200.81	295.55	34.5	0.235	0.050	0.333	-0.03	0.00	
An3-2-4	40.05		0.180	200.81	295.55	34.5	0.271	0.100	0.361	-0.51	0.00	
An3-2-5	39.98		0.180	200.81	294.55	34.5	0.332	0.200	0.401	-0.15	-0.65	
An3-2-6	40.04		0.180	200.95	295.55	34.5	0.383	0.302	0.426	-0.27	0.13	
An3-2-7	40.04		0.180	200.95	295.65	34.5	0.445	0.400	0.469	1.59	0.00	
An3-2-8	39.97		0.180	200.41	296.65	34.3	0.510	0.494	0.518	1.24	-0.32	
An3-2-9	39.91		0.180	200.68	294.55	34.5	0.565	0.607	0.544	0.19	0.32	
An3-2-10	39.91		0.180	200.68	294.55	34.5	0.636	0.733	0.586	-2.18	-0.84	
An3-2-11	39.91		0.180	200.68	294.55	34.5	0.684	0.796	0.625	0.37	0.00	
An3-2-12	40.03		0.180	201.13	294.25	34.6	0.739	0.907	0.650	-0.59	-0.52	
An3-2-13	39.88		0.180	201.13	294.55	34.5	0.797	0.959	0.712	-1.06	0.32	
An3-2-14	39.88		0.180	201.13	294.55	34.5	0.826	0.976	0.748	-2.38	0.32	
An3-2-15	39.88		0.180	201.13	294.55	34.5	0.987	0.992	0.984	0.81	0.00	
An3-3-1	30°	40.13	0.180	200.81	295.55	34.5	0.203	0.000	0.311	1.88	0.32	
An3-3-2		40.13	0.180	200.81	295.55	34.5	0.224	0.022	0.330	1.32	0.65	

Table B.1(a) (continued)

Test Number	θ	J_{G1} (m/s)	J_{L1} (m/s)	P_s kPa	T_s K	x_1 (%)	W_3/W_1	F_{G3}	F_{L3}	Mass balance error (%)		
										Air	Water	
An3-3-3	30°	40.16	0.180	200.55	295.55	34.5	0.297	0.100	0.401	-0.22	0.97	
An3-3-4		40.32	0.180	200.55	295.15	34.6	0.351	0.201	0.430	-0.32	0.32	
An3-3-5		39.98	0.180	200.55	295.55	34.4	0.406	0.303	0.460	-0.54	-0.32	
An3-3-6		39.94	0.180	200.20	295.65	34.4	0.460	0.398	0.492	-0.21	0.45	
An3-3-7		40.19	0.180	200.68	294.55	34.6	0.529	0.502	0.544	0.31	0.00	
An3-3-8		40.11	0.180	200.15	295.25	34.5	0.585	0.601	0.576	0.83	-0.32	
An3-3-9		40.11	0.180	200.15	295.25	34.5	0.648	0.697	0.621	-0.69	0.00	
An3-3-10		40.18	0.180	200.15	295.25	34.5	0.707	0.801	0.657	-0.52	0.65	
An3-3-11		40.35	0.180	200.55	295.55	34.7	0.760	0.895	0.688	0.30	-0.97	
An3-3-12		40.40	0.180	199.25	294.15	34.7	0.824	0.958	0.753	0.58	0.32	
An3-3-13		40.40	0.180	199.25	294.15	34.7	0.940	0.974	0.922	1.11	0.32	
An3-3-14		40.40	0.180	199.25	294.15	34.7	0.969	0.983	0.961	0.29	-0.65	
An3-4-1		90°	40.04	0.180	201.56	294.55	34.6	0.259	0.099	0.343	-0.46	0.971
An3-4-2			40.04	0.180	201.56	294.55	34.6	0.326	0.099	0.447	-0.46	0.000
An3-4-3	40.42		0.180	200.87	295.15	34.7	0.383	0.204	0.479	-0.82	0.324	
An3-4-4	40.20		0.180	200.55	294.55	34.6	0.439	0.302	0.511	0.22	0.324	
An3-4-5	40.09		0.180	200.20	294.65	34.5	0.498	0.398	0.550	-1.78	0.000	
An3-4-6	40.12		0.180	201.21	294.55	34.7	0.551	0.503	0.576	0.16	0.324	
An3-4-7	39.96		0.180	201.08	294.65	34.5	0.620	0.625	0.618	-2.13	-0.647	
An3-4-8	39.98		0.180	200.15	294.25	34.5	0.674	0.705	0.657	-1.46	0.000	
An3-4-9	40.04		0.180	200.15	294.25	34.4	0.723	0.802	0.681	-0.66	0.00	
An3-4-10	40.42		0.180	201.35	295.55	34.8	0.786	0.907	0.721	-0.57	0.00	
An3-4-11	40.42		0.180	201.35	295.55	34.8	0.904	0.956	0.877	0.83	0.65	
An3-4-12	39.72		0.180	201.69	294.15	34.6	0.988	0.977	0.994	0.28	-0.13	

Table B.1 Phase-redistribution data

(b) Short outlets

Test Number	θ	J_{G1} (m/s)	J_{L1} (m/s)	P_s kPa	T_s K	x_1 (%)	W_3/W_1	F_{G3}	F_{L3}	Mass balance error (%)	
										Air	Water
St1-1-1	0.0°	2.02	0.04	199.74	295.1	0.10	0.165	0.00	0.180	-0.80	0.58
St1-1-2		2.00	0.039	199.74	295.25	0.10	0.193	0.05	0.215	-2.26	0.58
St1-1-3		2.00	0.039	199.74	295.25	0.10	0.222	0.10	0.246	-2.23	0
St1-1-4		1.99	0.040	199.74	295.25	0.11	0.286	0.21	0.288	-1.51	0.57
St1-1-5		2.02	0.039	200.22	295.2	0.11	0.352	0.30	0.354	-1.01	-0.58
St1-1-6		2.01	0.040	200.22	295.25	0.11	0.422	0.40	0.428	-1.18	-0.29
St1-1-7		2.00	0.040	201.42	295.25	0.11	0.506	0.51	0.502	-1.40	-0.29
St1-2-1	0.5°	1.99	0.040	200.86	294.15	0.10	0.64	0.000	0.723	0.67	-0.29
St1-2-2		1.98	0.040	201.47	293.25	0.10	0.712	0.058	0.785	-2.12	-0.87
St1-2-3		1.99	0.040	201.26	294.15	0.10	0.755	0.085	0.824	-1.58	0.00
St1-2-4		1.98	0.040	201.47	293.25	0.11	0.894	0.088	0.991	0.79	0.87
W2-1-1	0.0°	9.93	0.040	200.23	294.55	0.37	0.028	0.0009	0.034	-0.30	0.29
W2-1-2		10.09	0.040	200.23	294.55	0.37	0.082	0.056	0.105	0.08	0.58
W2-1-3		10.11	0.040	199.75	294.15	0.37	0.145	0.103	0.168	0.95	-0.87
W2-1-4		10.07	0.040	201.56	294.85	0.37	0.246	0.202	0.265	1.12	0.29
W2-1-5		9.93	0.040	200.23	294.55	0.37	0.333	0.302	0.355	0.97	0.29
W2-1-6		9.93	0.040	200.23	294.55	0.37	0.415	0.406	0.423	-0.79	0.58
W2-1-7		10.09	0.040	200.23	294.55	0.37	0.503	0.550	0.503	0.88	-0.29
W2-2-1	5.0°	10.01	0.040	200.28	295.15	0.37	0.147	0.000	0.225	-0.01	0.00
W2-2-2		10.01	0.040	200.95	295.15	0.37	0.204	0.102	0.264	-1.10	-1.47
W2-2-3		10.11	0.040	200.01	294.55	0.37	0.294	0.208	0.354	1.43	0.87
W2-2-4		9.92	0.040	200.36	294.55	0.37	0.372	0.305	0.415	-1.44	-0.88

Table B.1(b) (continued)

Test Number	θ	J_{G1} (m/s)	J_{L1} (m/s)	P_s kPa	T_s K	x_1 (%)	W_3/W	F_{G3}	F_{L3}	Mass balance error (%)	
										Air	Water
W2-2-5	5.0°	9.93	0.040	200.23	294.55	0.37	0.4854	0.409	0.475	-2.31	0.00
W2-2-6		9.96	0.040	200.01	295.55	0.37	0.5395	0.506	0.562	0.17	-1.18
W2-2-7		10.09	0.040	200.55	294.55	0.37	0.6355	0.611	0.645	-0.40	-0.58
W2-2-8		10.08	0.040	201.08	294.55	0.37	0.7330	0.705	0.760	-0.04	-0.29
W2-2-9		10.07	0.040	200.95	294.55	0.38	0.9122	0.822	0.965	-1.25	-0.88
W2-2-10		10.07	0.040	200.95	294.55	0.38	0.9455	0.82	1.016	-1.25	-0.88
W2-3-1	30°	10.08	0.041	201.56	295.15	0.38	0.308	0.055	0.454	-0.85	-0.59
W2-3-2		10.00	0.041	201.56	295.15	0.38	0.335	0.053	0.493	-1.70	-0.88
W2-3-3		10.08	0.041	201.21	295.15	0.37	0.381	0.106	0.545	-0.52	0.58
W2-3-4		10.09	0.041	200.87	294.55	0.37	0.463	0.208	0.627	0.44	-0.29
W2-3-5		10.07	0.041	200.95	294.55	0.38	0.566	0.304	0.728	1.01	0.59
W2-3-6		9.90	0.041	201.16	295.15	0.37	0.636	0.402	0.775	-1.90	-0.29
W2-3-7		10.06	0.041	201.35	294.55	0.37	0.720	0.509	0.852	0.33	0.29
W2-3-8		10.08	0.041	201.21	294.75	0.37	0.841	0.625	0.970	-1.19	0.43
W2-3-9		10.09	0.041	200.55	295.55	0.37	0.860	0.630	1.000	-0.75	0.29
An2-1-1	0.0°	39.45	0.039	201.48	293.55	0.70	0.02	0.000	0.065	0.93	-1.47
An2-1-2		40.10	0.039	201.75	294.65	0.70	0.152	0.104	0.265	-0.41	1.45
An2-1-3		40.15	0.039	200.95	295.25	0.71	0.244	0.205	0.346	0.03	-0.59
An2-1-4		40.07	0.039	201.75	294.25	0.70	0.333	0.309	0.403	1.17	0.58
An2-1-5		40.12	0.039	200.95	295.65	0.70	0.428	0.417	0.450	-0.90	0.00
An2-1-6		39.90	0.039	200.81	294.65	0.70	0.504	0.580	0.505	0.67	0.14
An2-2-1	5.0°	39.45	0.041	201.48	293.55	0.70	0.044	0.000	0.135	0.93	-1.47
An2-2-2		40.10	0.041	201.75	294.65	0.70	0.150	0.102	0.272	-0.41	0.58

Table B.1(b) (continued)

Test Number	θ	J_{G1} (m/s)	J_{L1} (m/s)	P_s kPa	T_s K	x_1 (%)	W_3/W_1	F_{G3}	F_{L3}	Mass balance error (%)	
										Air	Water
An2-2-3	5.0°	40.15	0.041	200.95	295.25	0.71	0.24	0.205	0.352	0.03	-1.47
An2-2-4		40.06	0.040	201.75	294.15	0.70	0.337	0.305	0.4141	1.17	-0.87
An2-2-5		40.12	0.040	200.95	295.65	0.70	0.435	0.412	0.478	-0.90	1.16
An2-2-6		39.90	0.040	200.81	294.65	0.70	0.503	0.500	0.505	0.67	-0.29
An2-2-7		40.12	0.040	200.95	295.65	0.70	0.585	0.601	0.560	-0.89	-0.87
An2-2-8		39.98	0.041	201.75	294.25	0.70	0.681	0.718	0.606	-0.42	0.58
An2-2-9		40.15	0.040	200.95	295.25	0.71	0.769	0.809	0.664	0.22	-0.59
An2-3-10		40.10	0.040	201.75	294.65	0.70	0.850	0.893	0.768	0.44	0.58
An2-3-11		40.10	0.040	201.75	294.65	0.70	0.972	0.970	0.995	-0.93	1.45
An2-3-1	30°	40.16	0.040	201.56	295.55	0.70	0.055	0.000	0.189	1.64	0.58
An2-3-2		40.16	0.040	201.21	295.65	0.70	0.168	0.102	0.298	-0.65	1.45
An2-3-3		40.25	0.040	199.67	295.25	0.71	0.257	0.204	0.368	0.85	-1.18
An2-3-4		39.98	0.041	201.21	295.65	0.70	0.358	0.308	0.454	0.19	-1.45
An2-3-5		39.94	0.040	200.87	294.65	0.70	0.429	0.406	0.472	-0.55	-0.29
An2-3-6		40.02	0.040	201.21	294.15	0.70	0.514	0.518	0.509	-0.90	1.45
An2-3-7		40.17	0.040	199.94	295.25	0.70	0.600	0.612	0.575	-0.99	0.00
An2-3-8		40.17	0.040	199.94	295.25	0.70	0.682	0.705	0.638	0.06	-1.45
An2-3-9		40.00	0.040	200.01	293.25	0.70	0.756	0.792	0.665	0.22	1.43
An2-3-10		40.17	0.040	200.01	295.65	0.70	0.907	0.912	0.872	-1.30	0.58
An2-3-11		40.26	0.040	200.01	295.55	0.70	0.950	0.930	0.99	-0.04	0.87

Table B.2 Phase-redistribution mass-flow-rates data
(a) Long outlets

Test Number	θ	W_{G1} (kg/h)	W_{L1} (kg/h)	W_{G2} (kg/h)	W_{L2} (kg/h)	W_{G3} (kg/h)	W_{L3} (kg/h)
St1-1-1	0.0°	2.45	5.16	2.41	5.10	0.00	0.00
St1-1-2		2.43	5.19	2.31	5.22	0.12	0.00
St1-1-3		2.45	5.16	2.20	4.62	0.27	0.48
St1-1-4		2.45	5.19	2.04	4.20	0.48	0.96
St1-1-5		2.45	5.19	1.73	3.84	0.74	1.39
St1-1-6		2.46	5.19	1.49	3.30	0.97	1.92
St1-1-7		2.46	5.19	1.21	2.58	1.21	2.58
St1-2-1	0.1°	2.45	5.16	2.48	4.50	0.00	0.69
St1-2-2		2.45	5.16	2.34	4.23	0.12	0.90
St1-2-3		2.44	5.20	2.20	4.05	0.26	1.13
St1-2-4		2.45	5.19	2.00	3.78	0.48	1.50
St1-2-5		2.45	5.19	1.74	3.06	0.73	2.10
St1-2-6		2.45	5.19	1.46	2.43	1.00	2.64
St1-2-7		2.45	5.19	1.21	2.04	1.22	3.18
St1-2-8		2.45	5.20	1.00	1.44	1.46	3.86
St1-2-9		2.45	5.16	0.71	0.78	1.71	4.35
St1-2-10		2.45	5.19	0.50	0.39	1.96	4.86
St1-2-11		2.45	5.19	0.36	0.18	2.07	5.09
St1-2-12		2.45	5.19	0.36	0.00	2.09	5.16
St1-3-1	0.2°	2.44	5.16	2.47	3.90	0.00	1.32
St1-3-2		2.44	5.16	2.34	3.54	0.12	1.53
St1-3-3		2.44	5.16	2.20	3.24	0.27	1.80
St1-3-4		2.45	5.16	1.96	2.94	0.50	2.22
St1-3-5		2.44	5.20	1.70	2.34	0.71	2.88
St1-3-6		2.43	5.16	1.45	1.80	0.97	3.42
St1-3-7		2.43	5.16	1.20	1.14	1.20	4.08
St1-3-8		2.43	5.16	0.95	0.42	1.45	4.80
St1-3-9		2.44	5.19	0.85	0.00	1.60	5.10
St1-4-1	0.3°	2.44	5.22	2.48	3.36	0.00	1.80

Tale B.2(a) (continued)

Test Number	θ	W_{G1} (kg/h)	W_{L1} (kg/h)	W_{G2} (kg/h)	W_{L2} (kg/h)	W_{G3} (kg/h)	W_{L3} (kg/h)
St1-4-2	0.3°	2.45	5.16	2.36	3.12	0.14	2.01
St1-4-3		2.45	5.19	2.21	2.88	0.29	2.31
St1-4-4		2.45	5.19	1.93	1.92	0.50	3.30
St1-4-5		2.45	5.16	1.78	0.42	0.69	4.80
St1-4-6		2.45	5.16	1.71	0.00	0.75	5.16
St1-5-1		0.5°	2.45	5.16	2.50	1.59	0.00
St1-5-2	2.45		5.16	2.36	1.02	0.12	4.26
St1-5-3	2.45		5.16	2.28	0.42	0.18	4.71
St1-5-4	2.45		5.16	2.25	0.00	0.21	5.16
St1-6-1	0.6°	2.45	5.16	2.50	0.42	0.00	4.80
St1-6-2		2.43	5.16	2.40	0.00	0.05	5.22
St1-7-1	0.7°	2.44	5.19	2.47	0.00	0.00	5.16
St2-1-1	0.1°	2.46	20.58	2.41	17.10	0.00	3.42
St2-1-2		2.46	20.70	2.34	16.20	0.12	4.38
St2-1-3		2.46	20.70	2.27	15.60	0.25	4.98
St2-1-4		2.46	20.70	1.91	15.00	0.50	5.70
St2-1-5		2.46	20.58	1.70	13.20	0.71	7.20
St2-1-6		2.45	20.58	1.56	12.30	0.99	8.40
St2-1-7		2.47	20.58	1.24	10.32	1.24	10.32
St2-2-1	0.2°	2.44	20.70	2.41	13.80	0.00	6.72
St2-2-2		2.44	21.00	2.35	13.20	0.13	7.68
St2-2-3		2.44	20.70	2.20	12.30	0.25	8.28
St2-2-4		2.44	20.70	1.99	11.10	0.50	9.42
St2-2-5		2.44	20.70	1.70	9.60	0.71	11.10
St2-2-6		2.45	20.70	1.43	7.80	1.00	12.90
St2-2-7		2.45	20.58	1.21	5.10	1.21	15.72
St2-2-8		2.45	20.58	1.00	2.88	1.46	17.58

Table B.2(a) (continued)

Test Number	θ	W_{G1} (kg/h)	W_{L1} (kg/h)	W_{G2} (kg/h)	W_{L2} (kg/h)	W_{G3} (kg/h)	W_{L3} (kg/h)
St2-2-9	0.2°	2.45	20.58	0.71	1.56	1.71	18.9
St2-2-10		2.45	20.58	0.49	0.30	1.96	20.16
St2-2-11		2.45	20.58	0.427	0.00	2.01	20.7
St2-3-1	0.5°	2.44	20.7	2.42	10.80	0.00	9.6
St2-3-2		2.45	20.58	2.35	10.50	0.14	10.2
St2-3-3		2.44	20.70	2.28	9.30	0.25	11.1
St2-3-4		2.438	20.70	1.98	8.10	0.49	12.6
St2-3-5		2.43	20.70	1.70	6.00	0.71	14.4
St2-3-6		2.45	20.70	1.42	1.80	0.99	18.72
St2-3-7		2.50	20.58	1.42	0.45	1.07	20.1
St2-3-8		2.44	20.70	1.42	0.00	1.07	20.7
St2-4-1	1.0°	2.43	20.70	2.42	10.2	0.00	10.02
St2-4-2		2.44	20.58	2.35	9.48	0.14	11.16
St2-4-3		2.44	20.70	2.20	8.70	0.25	12.18
St2-4-4		2.45	20.70	1.97	7.20	0.48	13.68
St2-4-5		2.44	20.70	1.71	4.50	0.73	16.32
St2-4-6		2.45	20.70	1.65	3.00	0.80	17.88
St2-4-7		2.44	21.0	1.56	0.00	0.85	20.70
St2-5-1	2.5°	2.44	20.70	2.43	8.70	0.00	12.6
St2-5-2		2.44	20.70	2.35	7.50	0.14	12.9
St2-5-3		2.44	20.70	2.21	7.20	0.25	13.56
St2-5-4		2.44	20.58	2.00	4.38	0.50	15.72
St2-5-5		2.44	20.58	1.93	0.00	0.53	20.4
St2-6-1	5.0°	2.44	20.70	2.43	6.00	0.00	14.88
St2-6-2		2.45	20.58	2.36	4.20	0.143	16.32
St2-6-3		2.45	20.70	2.29	3.60	0.19	17.10
St2-6-4		2.45	20.58	2.21	0.00	0.21	20.40

Table B.2(a) (continued)

Test Number	θ	W_{G1} (kg/h)	W_{L1} (kg/h)	W_{G2} (kg/h)	W_{L2} (kg/h)	W_{G3} (kg/h)	W_{L3} (kg/h)
St2-7-1	6.5°	2.44	20.58	2.43	3.30	0.00	17.4
St2-7-2		2.44	20.58	2.43	0.00	0.05	20.22
St2-8-1	7.5°	2.44	20.70	2.42	0.00	0.00	20.58
W1-1-1	0.0°	12.23	5.19	12.27	5.16	0.00	0.00
W1-1-2		12.23	5.19	10.10	5.10	2.20	0.00
W1-1-3		12.32	5.19	10.02	4.98	2.39	0.18
W1-1-4		12.32	5.19	10.02	4.5	3.12	0.54
W1-1-5		12.25	5.19	8.58	4.44	3.71	0.84
W1-1-6		12.22	5.19	7.29	3.54	4.78	1.8
W1-1-7		12.10	5.19	6.06	2.61	6.06	2.58
W1-2-1	5.0°	12.35	5.19	12.35	5.10	0.00	0.00
W1-2-2		12.35	5.19	10.77	5.12	1.42	0.00
W1-2-3		12.35	5.19	9.83	4.68	2.46	0.48
W1-2-4		12.20	5.19	8.52	3.9	3.70	1.29
W1-2-5		12.23	5.19	7.22	2.70	4.87	2.34
W1-2-6		12.25	5.19	6.14	1.80	6.14	3.36
W1-2-7		12.23	5.19	4.89	0.81	7.25	4.44
W1-2-8		12.23	5.19	4.28	0.24	7.85	4.95
W1-2-9		12.24	5.19	4.14	0.00	8.13	5.10
W1-3-1	15°	12.22	5.16	12.19	5.10	0.00	0.00
W1-3-2		12.22	5.16	11.48	5.16	0.35	0.00
W1-3-3		12.22	5.16	10.90	4.89	1.21	0.285
W1-3-4		12.21	5.16	9.68	4.11	2.42	1.11
W1-3-5		12.22	5.22	8.50	2.73	3.65	2.43
W1-3-6		12.25	5.16	7.29	1.23	4.85	3.96
W1-3-7		12.22	5.22	6.13	0.12	6.126	5.04
W1-3-8		12.22	5.22	6.13	0.00	6.41	5.1

Table B.2(a) (continued)

Test Number	θ	W_{G1} (kg/h)	W_{L1} (kg/h)	W_{G2} (kg/h)	W_{L2} (kg/h)	W_{G3} (kg/h)	W_{L3} (kg/h)
W1-4-1	30°	12.21	5.16	12.25	4.5	0.00	0.69
W1-4-2		12.21	5.16	11.53	4.14	0.60	1.02
W1-4-3		12.22	5.16	10.921	3.69	1.21	1.5
W1-4-4		12.24	5.16	9.846	2.64	2.49	2.58
W1-4-5		12.12	5.16	8.48	1.08	3.64	4.02
W1-4-6		12.22	5.16	7.33	0.42	4.84	4.74
W1-4-7		12.24	5.13	6.47	0.18	5.63	5.04
W1-4-8		12.24	5.13	6.47	0.00	5.77	5.16
W1-5-1	45°	12.21	5.16	12.21	3.00	0.00	2.01
W1-5-2		12.21	5.16	11.78	2.82	0.29	2.40
W1-5-3		12.21	5.16	11.04	1.8	0.99	3.36
W1-5-4		12.23	5.16	9.82	0.72	2.42	4.38
W1-5-5		12.23	5.16	8.46	0.30	3.63	4.92
W1-5-6		12.21	5.16	7.90	0.30	4.13	4.74
W1-5-7		12.09	5.16	7.82	0.00	4.41	5.16
W1-6-1	75°	12.23	5.16	12.16	0.48	0.00	4.68
W1-6-2		12.23	5.16	11.66	0.24	0.60	4.8
W1-6-3		12.22	5.16	10.90	0.12	1.21	5.01
W1-6-4		12.22	5.16	10.70	0.06	1.49	5.10
W1-6-5		12.22	5.16	10.77	0.00	1.56	5.10
W1-7-1	87.5°	12.23	5.16	12.16	0.00	0.00	5.10
W2-1-1	0.0°	12.30	20.70	12.15	19.5	0.00	1.5
W2-1-2		12.30	20.70	11.65	18	0.63	2.52
W2-1-3		12.30	20.70	11.07	17.4	1.20	3.48
W2-1-4		12.34	20.70	9.77	15.00	2.49	5.40
W2-1-5		12.34	20.70	9.27	14.4	3.07	6.36
W2-1-6		12.30	20.70	8.50	13.5	3.68	7.08
W2-1-7		12.30	20.70	7.44	12.0	4.82	8.52

Table B.2(a) (continued)

Test Number	θ	W_{G1} (kg/h)	W_{L1} (kg/h)	W_{G2} (kg/h)	W_{L2} (kg/h)	W_{G3} (kg/h)	W_{L3} (kg/h)
W2-1-8	0.0°	12.30	20.7	6.02	10.32	6.02	10.32
W2-2-1	5.0°	12.22	20.40	12.22	15.9	0.00	4.56
W2-2-2		12.22	20.40	11.50	15.6	0.64	4.98
W2-2-3		12.22	20.40	11.14	15.3	1.21	5.64
W2-2-4		12.30	20.70	9.71	13.2	2.41	7.20
W2-2-5		12.10	20.40	8.58	12.3	3.69	8.10
W2-2-6		12.09	20.70	7.50	10.92	4.82	9.60
W2-2-7		12.08	20.40	6.03	9.30	6.03	11.4
W2-2-8		12.32	20.70	4.83	7.50	7.53	13.5
W2-2-9		12.34	20.58	3.70	5.10	8.63	15.6
W2-2-10		12.32	20.40	2.42	0.90	9.91	19.68
W2-2-11		12.32	20.40	2.13	0.00	10.05	20.7
W2-3-1	15°	12.27	20.70	12.17	13.8	0.00	6.60
W2-3-2		12.33	20.40	11.87	13.5	0.60	7.08
W2-3-3		12.27	20.58	11.09	12.9	1.20	7.80
W2-3-4		12.08	20.70	9.72	11.4	2.48	9.00
W2-3-5		12.10	20.40	8.59	9.90	3.55	10.68
W2-3-6		12.09	20.70	7.47	8.40	4.84	12.00
W2-3-7		12.29	20.64	6.12	6.60	6.12	13.80
W2-3-8		12.32	20.70	4.83	4.92	7.53	15.84
W2-3-9		12.26	20.58	3.54	1.80	8.72	18.90
W2-3-10		12.05	20.40	3.25	0.00	8.85	20.40
W2-4-1	30°	12.13	20.40	12.23	11.10	0.00	9.00
W2-4-2		12.13	20.40	11.87	10.50	0.571	10.20
W2-4-3		12.32	20.58	11.17	9.30	1.21	11.40
W2-4-4		12.34	20.58	9.86	7.80	2.42	13.20
W2-4-5		12.31	20.48	8.48	5.64	3.70	14.88
W2-4-6		12.09	20.70	7.47	4.80	4.84	16.08
W2-4-7		12.32	20.64	6.14	3.12	6.14	17.70

Table B.2(a) (continued)

Test Number	θ	W_{G1} (kg/h)	W_{L1} (kg/h)	W_{G2} (kg/h)	W_{L2} (kg/h)	W_{G3} (kg/h)	W_{L3} (kg/h)
W2-4-8	30°	12.34	20.70	4.99	0.54	7.34	20.16
W2-4-9		12.28	20.58	4.62	0.00	7.53	20.70
W2-5-1	45°	12.25	20.58	12.14	8.40	0.00	12.24
W2-5-2		12.25	20.58	11.07	6.00	1.20	14.70
W2-5-3		12.13	21.00	9.86	3.90	2.42	16.80
W2-5-4		12.31	20.40	8.62	3.60	3.70	17.28
W2-5-5		12.09	20.70	7.47	2.82	4.84	18.30
W2-5-6		12.24	21.00	6.08	0.90	6.08	19.92
W2-5-7		12.31	20.70	5.35	0.66	6.91	20.40
W2-5-8		12.31	20.70	5.13	0.00	7.05	20.52
W2-6-1	90	12.33	20.40	12.25	5.70	0.00	15.12
W2-6-2		12.33	20.40	11.89	2.70	0.57	17.64
W2-6-3		12.31	20.58	11.07	1.92	1.20	18.60
W2-6-4		12.13	21.00	9.86	1.20	2.42	19.20
W2-6-5		12.28	20.40	8.56	1.20	3.68	19.32
W2-6-6		12.07	20.70	7.42	0.60	4.81	20.10
W2-6-7		12.32	20.70	6.09	0.30	6.09	20.40
W2-6-8		12.32	21.00	5.80	0.00	6.37	20.70
An1-1-1	0.0°	48.89	5.16	48.51	4.98	0.00	0.00
An1-1-2		48.89	5.16	47.34	5.04	2.41	0.00
An1-1-3		48.89	5.16	43.07	4.26	4.82	0.78
An1-1-4		48.99	5.16	38.95	3.60	9.65	1.50
An1-1-5		49.00	5.10	34.11	2.90	14.21	2.04
An1-1-6		49.03	5.10	29.06	2.76	19.13	2.28
An1-1-7		49.07	5.10	24.69	2.58	24.29	2.58
An1-2-1	5.0°	49.14	5.10	48.80	5.04	0.00	0.00
An1-2-2		49.14	5.10	48.00	4.98	0.72	0.00
An1-2-3		49.14	5.10	46.80	4.68	2.44	0.36

Table B.2(a) (continued)

Test Number	θ	W_{G1} (kg/h)	W_{L1} (kg/h)	W_{G2} (kg/h)	W_{L2} (kg/h)	W_{G3} (kg/h)	W_{L3} (kg/h)	
An1-2-4	5.0°	48.87	5.16	43.53	4.20	4.97	0.90	
An1-2-5		48.99	5.16	38.95	3.48	9.73	1.62	
An1-2-6		49.00	5.10	33.59	2.88	14.82	2.10	
An1-2-7		48.67	5.10	28.40	2.58	19.69	2.46	
An1-2-8		50.02	5.10	24.66	2.46	24.26	2.76	
An1-2-9		50.02	5.22	19.68	2.10	29.21	3.06	
An1-2-10		48.72	5.10	14.76	1.68	33.99	3.36	
An1-2-11		48.72	5.22	9.70	1.41	39.22	3.78	
An1-2-12		49.84	5.22	4.28	0.30	44.50	4.80	
An1-2-13		49.84	5.22	4.28	0.12	46.09	5.04	
An1-2-14		48.84	5.22	0.00	0.00	48.41	5.16	
An1-3-1		30°	48.59	5.16	48.50	4.92	0.00	0.12
An1-3-2			48.59	5.16	44.12	4.08	4.95	0.96
An1-3-3			48.59	5.22	38.73	3.30	9.59	1.80
An1-3-4	48.59		5.22	33.98	2.82	14.63	2.34	
An1-3-5	48.44		5.22	28.21	2.52	19.55	2.64	
An1-3-6	48.62		5.16	24.50	2.28	24.09	2.88	
An1-3-7	48.51		5.16	19.53	1.98	29.21	3.12	
An1-3-8	48.80		5.16	14.83	1.56	34.14	3.54	
An1-3-9	48.81		5.22	9.90	1.20	38.67	3.90	
An1-3-10	48.49		5.16	4.81	0.18	43.84	5.01	
An1-3-11	48.49		5.16	4.60	0.00	44.23	5.10	
An1-4-1	90°	48.84	5.10	48.24	4.62	0.00	0.45	
An1-4-2		48.88	5.16	44.22	3.75	4.97	1.32	
An1-4-3		48.84	5.22	38.82	2.88	9.61	2.22	
An1-4-4		48.84	5.16	34.06	2.49	14.79	2.58	
An1-4-5		48.89	5.22	29.11	2.16	19.50	2.94	
An1-4-6		48.90	5.10	24.63	1.92	24.21	3.12	
An1-4-7		48.87	5.16	19.48	1.62	29.61	3.48	
An1-4-8		48.87	5.16	14.79	1.35	34.06	3.81	

Table B.2(a) (continued)

Test Number	θ	W_{G1} (kg/h)	W_{L1} (kg/h)	W_{G2} (kg/h)	W_{L2} (kg/h)	W_{G3} (kg/h)	W_{L3} (kg/h)
An1-4-9	90°	48.83	5.10	10.02	1.02	38.76	4.02
An1-4-10		48.91	5.22	6.38	0.12	42.84	5.10
An1-4-11		48.91	5.22	5.67	0.00	43.39	5.16
An2-1-1	0.0°	48.56	20.40	48.11	18.30	0.00	1.68
An2-1-2		49.40	21.00	46.86	17.10	2.42	3.60
An2-1-3		49.24	20.70	44.44	15.60	5.00	4.92
An2-1-4		49.00	20.40	39.34	13.20	9.65	6.90
An2-1-5		49.27	20.70	33.94	12.30	14.76	8.22
An2-1-6		48.90	20.70	29.13	11.40	20.21	9.30
An2-1-7		48.77	20.70	24.04	10.32	24.40	10.35
An2-2-1	5.0°	48.95	20.70	47.98	18.00	0.00	2.52
An2-2-2		48.87	20.70	44.37	14.70	4.99	5.70
An2-2-3		48.34	20.40	39.40	13.32	9.67	7.32
An2-2-4		48.90	20.70	34.78	12.12	14.71	8.52
An2-2-5		48.79	20.70	29.41	11.10	19.71	9.48
An2-2-6		47.91	20.70	24.30	10.08	24.16	10.56
An2-2-7		48.79	20.70	19.72	9.00	29.64	11.58
An2-2-8		48.77	20.70	14.67	8.40	34.67	12.42
An2-2-9		49.23	20.70	9.70	7.02	39.42	13.56
An2-2-10		48.63	20.70	4.95	4.80	44.02	15.84
An2-2-11		49.00	20.70	2.00	0.18	46.80	20.40
An2-2-12		49.00	20.70	1.43	0.00	47.61	20.52
An2-3-1	30°	49.12	20.70	48.31	17.10	0.00	3.42
An2-3-2		49.12	20.70	46.44	15.42	2.49	4.92
An2-3-3		49.01	20.70	44.34	14.40	4.99	6.18
An2-3-4		48.81	20.40	38.79	12.90	9.61	7.56
An2-3-5		48.80	20.70	33.86	11.76	14.84	9.00
An2-3-6		48.82	20.70	29.39	10.80	19.70	9.84
An2-3-7		49.09	20.70	24.66	9.60	24.73	10.80

Table B.2(a) (continued)

Test Number	θ	W_{G1} (kg/h)	W_{L1} (kg/h)	W_{G2} (kg/h)	W_{L2} (kg/h)	W_{G3} (kg/h)	W_{L3} (kg/h)
An2-3-8	30°	48.79	20.70	19.62	8.76	30.32	11.94
An2-3-9		48.79	20.70	14.80	7.80	33.96	12.96
An2-3-10		48.93	21.00	10.01	6.90	38.81	14.04
An2-3-11		48.93	21.00	10.01	5.70	41.89	15.18
An2-3-12		48.74	20.70	4.96	2.40	44.17	18.12
An2-3-13		48.86	20.70	3.54	0.30	45.49	20.40
An2-3-14		48.86	20.70	2.84	0.00	46.05	20.40
An2-4-1		45°	49.05	20.70	48.43	16.80	0.00
An2-4-2	49.08		20.70	44.27	14.04	4.98	6.60
An2-4-3	48.91		20.40	38.97	12.66	9.67	7.92
An2-4-4	48.71		20.70	33.88	11.40	14.81	9.42
An2-4-5	48.79		20.70	29.19	10.32	19.66	10.32
An2-4-6	49.19		20.70	24.61	9.72	24.54	11.04
An2-4-7	48.86		20.70	19.71	8.40	29.77	12.30
An2-4-8	48.86		20.70	14.87	7.32	34.60	13.32
An2-4-9	48.88		21.00	9.76	6.30	39.73	14.52
An2-4-10	49.22		20.70	7.39	5.40	42.02	15.30
An2-4-11	48.94		20.70	3.91	0.42	45.21	20.10
An2-4-12	48.94		20.70	3.20	0.00	45.60	20.40
An2-5-1	90°	49.08	20.70	48.93	15.72	0.00	4.92
An2-5-2		49.09	20.70	46.31	14.40	2.42	6.12
An2-5-3		48.76	20.70	44.17	13.20	4.83	7.44
An2-5-4		48.73	20.70	38.97	11.70	9.76	8.82
An2-5-5		48.80	20.70	33.86	10.92	14.80	9.84
An2-5-6		48.79	20.70	29.19	9.96	19.66	10.92
An2-5-7		48.81	20.70	24.60	8.76	24.52	11.88
An2-5-8		48.75	20.70	19.07	7.80	30.42	12.84
An2-5-9		48.92	20.70	14.81	6.60	34.10	13.80
An2-5-10		48.72	21.00	9.92	5.88	38.95	15.00
An2-5-11		48.64	20.70	4.61	0.48	44.60	20.10

Table B.2(a) (continued)

Test Number	θ	W_{G1} (kg/h)	W_{L1} (kg/h)	W_{G2} (kg/h)	W_{L2} (kg/h)	W_{G3} (kg/h)	W_{L3} (kg/h)
An2-5-12	90°	48.65	20.70	4.61	0.48	44.61	20.10
An2-5-13		48.65	20.70	2.84	0.00	45.08	20.40
An3-1-1	0.0°	48.67	92.70	47.74	75.00	0.00	16.32
An3-1-2		48.67	92.70	47.35	66.00	1.21	26.88
An3-1-3		48.67	92.70	47.35	64.20	1.21	28.20
An3-1-4		48.90	92.70	44.18	60.48	4.87	31.98
An3-1-5		48.89	92.70	39.17	57.00	9.85	35.40
An3-1-6		48.83	92.40	34.22	54.00	14.77	38.10
An3-1-7		48.65	92.40	28.60	48.60	19.42	43.32
An3-1-8		48.73	92.70	24.21	46.20	24.42	46.50
An3-2-1	5.0°	48.80	92.70	46.39	70.20	0.00	22.20
An3-2-2		48.80	92.70	47.58	64.20	1.21	27.90
An3-2-3		48.80	92.70	46.39	61.80	2.42	30.90
An3-2-4		48.80	92.70	44.18	59.28	4.88	33.42
An3-2-5		48.89	92.70	39.17	56.10	9.79	37.20
An3-2-6		48.82	92.70	34.22	53.10	14.72	39.48
An3-2-7		48.81	92.70	28.52	49.20	19.51	43.50
An3-2-8		48.43	92.70	23.88	45.00	23.94	48.00
An3-2-9		48.76	92.70	19.08	42.00	29.59	50.40
An3-2-10		48.76	92.70	14.48	39.18	35.73	54.30
An3-2-11		48.76	92.70	9.76	34.80	38.82	57.90
An3-2-12		49.07	92.70	4.86	32.88	44.50	60.30
An3-2-13		48.83	92.70	2.50	26.40	46.85	66.00
An3-2-14		48.83	92.70	2.50	23.10	47.64	69.30
An3-2-15		48.83	92.70	0.00	1.50	48.44	91.20
An3-3-1	30°	48.90	92.7	47.98	63.6	0.00	28.8
An3-3-2		48.90	92.7	47.18	61.5	1.06	30.6
An3-3-3		48.87	92.7	44.11	54.6	4.86	37.2
An3-3-4		49.13	92.7	39.41	52.5	9.87	39.9

Table B.2(a) (continued)

Test Number	θ	W_{G1} (kg/h)	W_{L1} (kg/h)	W_{G2} (kg/h)	W_{L2} (kg/h)	W_{G3} (kg/h)	W_{L3} (kg/h)	
An3-3-5	30°	48.65	92.70	34.16	50.40	14.74	42.60	
An3-3-6		48.51	92.70	29.30	46.68	19.31	45.60	
An3-3-7		49.10	92.70	24.29	42.30	24.66	50.40	
An3-3-8		48.76	92.70	19.07	39.60	29.29	53.40	
An3-3-9		48.76	92.70	15.10	35.10	34.00	57.60	
An3-3-10		48.85	92.70	9.98	31.20	39.12	60.90	
An3-3-11		49.10	92.40	5.00	29.70	43.95	63.60	
An3-3-12		49.08	92.40	1.77	22.50	47.02	69.60	
An3-3-13		49.08	92.40	0.71	6.90	47.82	85.20	
An3-3-14		49.08	92.40	0.71	4.20	48.23	88.80	
An3-4-1		90°	49.13	92.70	44.48	60.00	4.88	31.80
An3-4-2			49.13	92.70	44.48	51.30	4.88	41.40
An3-4-3			49.33	92.70	39.68	48.00	10.06	44.40
An3-4-4			49.09	92.70	34.16	45.00	14.82	47.40
An3-4-5	48.85		92.70	30.28	41.70	19.44	51.00	
An3-4-6	49.15		92.70	24.35	39.00	24.72	53.40	
An3-4-7	48.90		92.70	19.89	36.00	30.54	57.30	
An3-4-8	48.76		92.70	15.10	31.80	34.38	60.90	
An3-4-9	48.85		93.00	9.98	29.70	39.19	63.30	
An3-4-10	49.39		92.40	4.85	25.80	44.81	66.60	
An3-4-12	49.39		92.40	1.78	10.80	47.19	81.00	
An3-4-13	48.84		92.40	1.00	0.72	47.70	91.80	
An3-4-14	48.84		92.40	1.00	0.00	48.10	91.80	

Table B.2 Mass flow rates data
(b) Short outlets

Test Number	θ	W_{G1} (kg/h)	W_{L1} (kg/h)	W_{G2} (kg/h)	W_{L2} (kg/h)	W_{G3} (kg/h)	W_{L3} (kg/h)
St1-1-1	0.0°	2.46	20.58	2.48	16.68	0.00	3.78
St1-1-2		2.43	20.58	2.35	16.08	0.14	4.38
St1-1-3		2.40	20.58	2.23	15.60	0.24	4.98
St1-1-4		2.40	20.70	1.99	14.58	0.50	6.00
St1-1-5		2.46	20.58	1.74	13.38	0.74	7.32
St1-1-6		2.45	20.70	1.48	12.0	0.99	8.76
St1-1-7		2.45	20.70	1.23	10.38	1.25	10.38
St2-2-1	0.5°	2.45	20.70	2.43	6.00	0.00	14.88
St2-2-2		2.45	20.58	2.36	4.20	0.14	16.20
St2-2-3		2.45	20.70	2.29	3.60	0.18	17.28
St2-2-4		2.45	20.58	2.22	0.00	0.21	20.40
W2-1-1	0.0°	12.30	20.70	12.16	19.50	0.00	0.96
W2-1-2		12.30	20.70	11.66	18.30	0.57	2.04
W2-1-3		12.31	20.70	11.08	17.40	1.20	3.48
W2-1-4		12.34	20.70	9.78	15.00	2.50	5.40
W2-1-5		12.30	20.70	8.51	13.50	3.69	7.20
W2-1-6		12.30	20.70	7.44	12.00	4.82	8.64
W2-1-7		12.30	20.70	6.03	10.32	6.03	10.32
W2-2-1	5.0°	12.22	20.40	12.22	16.08	0.00	4.38
W2-2-2		12.22	20.40	11.14	15.30	1.21	5.40
W2-2-3		12.31	20.70	9.72	13.20	2.41	7.20
W2-2-4		12.10	20.40	8.59	12.30	3.69	8.22
W2-2-5		12.10	20.70	7.51	10.92	4.82	9.78
W2-2-6		12.08	20.40	6.03	9.30	6.03	11.40
W2-2-7		12.32	20.70	4.84	7.50	7.54	13.32
W2-2-8		12.34	20.58	3.71	5.10	8.64	15.60
W2-2-9		12.32	20.40	2.42	0.90	9.91	19.68
W2-2-10		12.32	20.40	2.14	0.00	10.05	20.70

Table B.2(b) (continued)

Test Number	θ	W_{G1} (kg/h)	W_{L1} (kg/h)	W_{G2} (kg/h)	W_{L2} (kg/h)	W_{G3} (kg/h)	W_{L3} (kg/h)
W2-3-1	30°	12.14	20.40	12.24	11.40	0.00	9.00
W2-3-2		20.40	11.88	10.50	0.57	10.20	20.40
W2-3-3		12.32	20.58	11.17	9.30	1.21	11.28
W2-3-4		12.34	20.58	9.86	7.80	2.43	12.90
W2-3-5		12.32	20.40	8.48	5.64	3.71	14.88
W2-3-6		12.09	20.70	7.48	4.80	4.85	16.08
W2-3-7		12.33	20.64	6.14	3.12	6.14	17.40
W2-3-8		12.34	20.70	5.00	0.54	7.35	20.16
W2-3-9		12.28	20.58	4.62	0.00	7.54	20.70
An2-1-1	0.0°	48.56	20.40	48.11	19.50	0.00	1.08
An2-1-2		49.24	20.70	44.44	15.00	5.00	5.40
An2-1-3		49.00	20.40	39.34	13.50	9.65	7.20
An2-1-4		49.27	20.70	33.94	12.30	14.76	8.58
An2-1-5		48.90	20.70	29.13	10.80	20.21	9.30
An2-1-6		48.77	20.70	24.04	10.32	24.40	10.44
An2-2-1	5.0°	48.95	20.70	47.98	18.00	0.00	2.70
An2-2-2		48.87	20.70	44.37	14.70	4.99	5.70
An2-2-3		48.34	20.40	39.40	13.32	9.67	7.32
An2-2-4		48.90	20.70	34.78	12.12	14.71	8.52
An2-2-5		48.79	20.70	29.41	11.10	19.71	9.48
An2-2-6		47.91	20.70	24.67	11.22	24.67	10.56
An2-2-7		48.79	20.70	19.72	9.24	30.02	11.52
An2-2-8		48.77	20.70	14.67	8.40	34.67	12.42
An2-2-9		49.23	20.70	9.70	7.02	39.42	13.56
An2-2-10		48.63	20.70	4.95	4.86	44.02	15.72
An2-2-11		49.00	20.70	2.00	0.18	46.80	20.22
An2-2-12		49.00	20.70	1.43	0.00	47.61	20.70
An2-3-1	30°	49.12	20.70	48.31	16.80	0.00	3.78
An2-3-2		49.01	20.70	44.34	14.40	4.99	6.00

Table B.2(b) (continued)

Test Number	θ	W_{G1} (kg/h)	W_{L1} (kg/h)	W_{G2} (kg/h)	W_{L2} (kg/h)	W_{G3} (kg/h)	W_{L3} (kg/h)
An2-3-3	30.0°	48.81	20.40	38.79	13.20	9.61	7.44
An2-3-4		48.80	20.70	33.86	11.76	14.84	9.24
An2-3-5		48.83	20.70	29.39	11.04	19.70	9.72
An2-3-6		49.09	20.70	24.66	9.96	24.88	10.92
An2-3-7		48.79	20.70	19.62	9.00	29.65	11.70
An2-3-8		48.79	20.70	14.80	8.04	33.96	12.96
An2-3-9		48.93	21.00	10.01	6.90	38.81	13.80
An2-3-10		48.74	20.70	4.96	2.58	44.41	18.00
An2-3-11		48.86	20.70	3.54	0.48	45.10	20.10
An2-3-12		48.86	20.70	3.50	0.00	45.49	20.58

Table B.3 Full-separation data

(a) Long Outlets

Test Number	Inclination angle (θ)	J_{G1} (m/s)	J_{L1} (m/s)	Mass balance Error (%)	
				air	water
2.5-1	2.5°	0.10	0.115	-	-1.02
2.5-2		0.20	0.109	-	0.53
2.5-3		0.50	0.095	1.22	-0.62
2.5-4		1.00	0.060	2.09	1.89
2.5-5		1.25	0.050	0.94	0.00
2.5-6		1.95	0.025	0.84	2.33
2.5-7		2.52	0.010	-1.45	1.18
2.5-8		2.85	0.005	0.31	4.65
7.5-1	7.5°	0.10	0.127	-	-0.92
7.5-2		0.20	0.122	-	0.95
7.5-3		0.50	0.116	2.38	0.99
7.5-4		0.90	0.100	3.56	0.58
7.5-5		1.75	0.051	0.35	-1.16
7.5-6		2.00	0.040	2.09	1.45
7.5-7		2.58	0.025	1.02	0.00
7.5-8		3.30	0.010	-1.75	-1.18
7.5-9		3.70	0.005	0.95	2.32
15-1	15°	0.10	0.150	-	1.15
15-2		0.20	0.144	-	0.00
15-3		0.50	0.138	3.64	0.83
15-4		1.00	0.118	3.60	0.49
15-5		1.45	0.100	0.77	1.15
15-6		2.45	0.050	1.92	1.16
15-7		3.35	0.025	-0.59	1.40
15-8		4.01	0.010	0.28	1.16
15-9		4.50	0.005	-0.21	2.33
30-1	30°	0.10	0.180	-	0.65
30-2		0.20	0.172	-	0.68
30-3		0.50	0.168	3.90	0.69
30-4		1.00	0.145	2.09	0.80
30-5		2.20	0.100	0.89	1.15
30-6		3.20	0.050	-0.87	0.00
30-7		4.10	0.025	2.18	2.33
30-8		4.90	0.010	-0.18	2.33
30-9		5.53	0.005	0.43	4.65

Table B.3(a) (continued)

Test Number	Inclination angle (θ)	J_{G1} (m/s)	J_{L1} (m/s)	Mass balance Error (%)	
				air	water
60-1	60°	0.10	0.212	-	0.65
60-2		0.20	0.202	-	0.57
60-3		0.50	0.190	3.64	0.61
60-4		1.00	0.170	3.60	0.68
60-5		1.90	0.125	1.21	0.47
60-6		2.60	0.102	1.53	1.14
60-7		3.32	0.080	1.14	0.73
60-8		4.55	0.050	-0.21	1.16
60-9		6.56	0.025	-0.50	1.40
60-10		8.42	0.010	0.00	2.33
60-11		9.30	0.005	-0.32	6.90
75-1	75°	0.10	0.227	-	0.26
75-2		0.20	0.216	-	0.54
75-3		0.50	0.196	3.90	0.30
75-4		1.00	0.170	1.97	0.66
75-5		2.10	0.123	0.10	0.94
75-6		2.90	0.100	0.89	1.16
75-7		5.25	0.050	1.15	1.15
75-8		7.21	0.025	0.56	2.33
75-9		9.50	0.010	0.24	2.30
75-10		10.2	0.005	1.64	6.98
90-1	90°	0.10	0.250	-	0.47
90-2		0.20	0.232	-	0.25
90-3		0.50	0.208	2.29	0.56
90-4		1.00	0.189	1.97	0.62
90-5		2.42	0.128	-0.47	0.91
90-6		3.20	0.100	-0.41	1.16
90-7		5.63	0.050	-0.18	1.15
90-8		7.70	0.025	0.50	2.33
90-9		10.1	0.010	1.15	2.30
90-10		11.1	0.005	0.35	6.98

Table B.3 Full-separation data
(b) Short outlets

Test Number	Inclination angle (θ)	J_{G1} (m/s)	J_{L1} (m/s)	Mass balance Error (%)	
				air	water
2.5-1	2.5°	0.10	0.066	-	0.877193
2.5-2		0.20	0.064	-	0.90
2.5-3		0.50	0.061	1.21	0.97
2.5-4		1.01	0.050	2.08	1.05
2.5-5		1.22	0.050	-0.09	0.00
2.5-6		1.85	0.025	-0.53	2.32
2.5-7		2.44	0.010	-0.09	1.16
2.5-8		2.70	0.005	-1.51	2.33
7.5-1	7.5°	0.10	0.110	-	1.06
7.5-2		0.20	0.107	-	0.86
7.5-3		0.50	0.102	1.21	1.09
7.5-4		0.91	0.090	1.74	0.64
7.5-5		1.51	0.050	0.16	0.0
7.5-6		2.02	0.040	2.08	1.44
7.5-7		2.36	0.025	1.26	2.32
7.5-8		3.03	0.010	2.08	3.44
7.5-9		3.37	0.005	3.22	6.97
15-1	15°	0.10	0.135	-	0.00
15-2		0.20	0.125	-	0.46
15-3		0.51	0.121	-2.02	0.97
15-4		1.02	0.102	0.77	1.16
15-5		1.18	0.095	0.77	0.61
15-6		2.29	0.051	-0.21	1.16
15-7		3.19	0.025	-0.41	0.00
15-8		3.77	0.010	1.34	3.49
15-9		4.36	0.005	-0.06	4.65
30-1	30°	0.10	0.160	-	0.36
30-2		0.20	0.150	-	0.77
30-3		0.50	0.144	1.21	0.80
30-4		1.00	0.120	1.21	0.48
30-5		1.83	0.100	-1.42	0.00
30-6		3.03	0.050	2.08	1.16
30-7		3.96	0.025	1.47	2.32
30-8		4.81	0.010	0.57	4.56
30-9		5.35	0.005	-1.01	6.52

Table B.3(b) (continued)

Test Number	Inclination angle (θ)	J_{G1} (m/s)	J_{L1} (m/s)	Mass balance Error (%)	
				air	water
60-1	60°	0.10	0.190	-	0.00
60-2		0.20	0.184	-	0.62
60-3		0.50	0.170	1.45	0.68
60-4		1.00	0.130	1.43	0.44
60-5		1.90	0.086	0.16	1.35
60-6		2.60	0.070	1.00	0.00
60-7		3.26	0.059	1.87	1.96
60-8		4.52	0.045	-0.50	2.56
60-9		6.28	0.025	0.73	2.32
60-10		8.21	0.010	0.60	3.48
60-11		9.22	0.005	0.05	6.97
75-1	75°	0.10	0.202	-	0.28
75-2		0.20	0.192	-	0.00
75-3		0.50	0.175	1.43	0.33
75-4		1.00	0.142	1.42	0.82
75-5		2.01	0.088	1.52	0.66
75-6		2.60	0.075	-1.00	1.53
75-7		4.85	0.050	1.62	0.00
75-8		7.12	0.025	0.13	2.32
75-9		9.21	0.010	0.05	3.48
75-10		10.22	0.005	0.19	6.98
90-1	90°	0.10	0.220	-	0.52
90-2		0.20	0.208	-	0.56
90-3		0.51	0.180	2.29	0.00
90-4		1.01	0.145	1.97	0.80
90-5		2.43	0.080	-0.47	0.00
90-6		2.90	0.070	0.02	0.83
90-7		5.13	0.050	0.17	1.15
90-8		7.50	0.025	0.81	2.33
90-9		10.01	0.010	0.31	2.30
90-10		11.10	0.005	0.35	6.90

Appendix C

EXPERIMENTAL UNCERTAINTY

This appendix gives an overview of the steps used in the uncertainty analysis, and tabulated results of the analysis of both phase-redistribution and full-separation experiments. All uncertainties given in the current study are meant to accommodate: discrimination uncertainties in the measuring instruments, the error in fitting an equation (for computer data reduction) to the calibration data, the accuracy of the calibrating devices, and unsteadiness in the process. The method reported by Moffat (1988) was used in estimating the uncertainties in the experimental data. The “uncertainty interval” is an interval around the measured value within which the true value is believed to lie. Table C.1 shows the individual percentage uncertainties for the phase-redistribution experiments while Table C.2 shows uncertainties for the full-separation experiments.

Given a set of variables that are related by a function as follows:

$$R = f(V_1, V_2, V_3, \dots) \quad (C.1)$$

The uncertainty in the dependent variable R of $(\pm \delta R)$ can be expressed according to

the relation:

$$\delta R = \left[\sum_{i=1}^n \left(\frac{\partial R}{\partial V_i} \delta V_i \right)^2 \right]^{\frac{1}{2}} \quad (C.2)$$

Where, n is the number of variables and δV_i is the uncertainty in the independent variable V_i .

In the present study, the uncertainty was calculated based on 20 to 1 odds (95% confidence).

Table C.1 Uncertainty intervals for phase-redistribution data

Test Number	θ	J_{G1} %	J_{L1} %	W_{G1} %	W_{L1} %	W_{G2} %	W_{L2} %	W_{G3} %	W_{L3} %	F_{G3} %	F_{L3} %	x_1 %
St1-1-1	0.0°	6.39	3.88	3.73	2.50	4.07	2.38	-	-	-	-	2.04
St1-1-2		6.38	3.88	3.72	2.50	4.09	2.37	8.38	-	9.17	-	2.05
St1-1-3		6.39	3.88	3.73	2.50	4.12	2.42	5.79	3.25	5.89	4.00	2.04
St1-1-4		6.39	3.88	3.73	2.50	4.16	2.46	4.92	2.63	5.17	3.62	2.05
St1-1-5		6.38	3.87	3.72	2.49	4.27	2.50	4.56	2.43	5.89	3.48	2.04
St1-1-6		6.38	3.87	3.72	2.49	4.39	2.59	5.90	3.17	5.18	4.00	2.04
St1-1-7		6.20	3.87	3.43	2.49	4.56	2.87	4.90	2.87	5.58	3.80	2.87
St1-2-1	0.1°	6.38	3.88	3.72	2.50	4.07	2.43	-	2.91	-	3.84	2.04
St1-2-2		6.38	3.87	3.72	2.50	4.09	2.46	8.37	2.65	8.16	3.64	2.04
St1-2-3		6.39	3.87	3.74	2.49	4.12	2.48	5.84	2.54	6.54	3.56	2.06
St1-2-4		6.38	3.87	3.73	2.49	4.15	2.52	5.64	2.38	5.59	3.45	2.05
St1-2-5		6.40	3.87	3.74	2.49	4.24	2.63	5.26	2.28	5.55	3.38	2.05
St1-2-6		6.39	3.87	3.74	2.50	5.03	3.80	5.08	3.21	5.59	4.00	2.05
St1-2-7		6.39	3.87	3.74	2.50	5.26	3.95	4.99	3.18	5.30	4.00	2.05
St1-2-8		6.39	3.87	3.74	2.50	5.57	4.27	4.91	3.16	5.31	4.03	2.05
St1-2-9		6.39	4.08	3.74	2.80	6.58	5.50	5.03	3.45	5.27	4.44	2.17
St1-2-10		6.38	4.07	3.73	2.79	7.79	8.00	4.91	3.40	5.33	4.40	2.16
St1-2-11		6.39	4.08	3.73	2.80	5.57	6.33	4.87	3.38	5.14	4.39	2.17
St1-2-12		6.39	4.08	3.73	2.80	5.57	-	4.87	3.38	5.13	4.39	2.17
St1-3-1	0.2°	6.24	3.88	3.45	2.50	4.65	2.58	-	1.15	-	2.75	2.89
St1-3-2		6.38	3.97	3.73	2.50	4.65	2.55	6.18	1.37	7.22	2.85	2.04
St1-3-3		6.39	3.87	3.74	2.50	4.69	2.60	4.89	1.31	6.15	2.82	2.05
St1-3-4		6.38	3.87	3.73	2.50	4.15	2.66	4.53	2.26	5.87	3.37	2.04
St1-3-5		6.40	3.87	3.74	2.49	4.27	2.83	4.43	2.20	5.80	3.33	2.06
St1-3-6		6.39	3.88	3.74	2.50	4.44	3.08	4.37	2.18	5.75	3.31	2.06
St1-3-7		6.39	3.88	3.74	2.50	5.33	4.71	5.00	3.15	6.24	4.00	2.06
St1-3-8		6.39	3.88	3.74	2.50	5.70	7.64	5.00	3.41	6.24	4.23	2.06
St1-3-9		6.41	3.88	3.75	2.50	5.91	-	4.90	3.38	6.17	4.00	2.07
St1-4-1	0.3°	6.38	3.87	3.73	2.50	4.62	3.57	0.00	3.20	0.00	4.01	2.80
St1-4-2		6.39	3.87	3.73	2.50	4.62	3.62	7.78	3.13	8.63	4.01	2.04
St1-4-3		6.39	3.87	3.73	2.49	4.86	3.67	5.67	2.96	8.79	3.87	2.05
St1-4-4		6.38	3.87	3.72	2.49	4.97	4.01	4.87	2.68	5.14	3.66	2.04
St1-4-5		6.38	3.87	3.72	2.50	5.05	7.64	4.62	2.46	5.94	3.51	2.04
St1-4-6		6.38	3.88	3.73	2.50	5.10	-	4.56	2.44	5.89	3.49	2.04
St1-5-1	0.5°	6.39	3.87	3.74	2.50	4.78	4.22	0.00	2.62	0.00	3.62	2.05

Table C.1 (continued)

Test Number	θ	J_{G1} %	J_{L1} %	W_{G1} %	W_{L1} %	W_{G2} %	W_{L2} %	W_{G3} %	W_{L3} %	F_{G3} %	F_{L3} %	x_1 %
St1-5-2	0.5°	6.38	3.87	3.73	2.50	4.82	5.16	9.27	2.52	9.00	3.55	2.04
St1-5-3		6.38	3.87	3.73	2.50	4.84	7.64	6.90	2.47	7.84	3.51	2.05
St1-5-4		6.39	3.88	3.74	2.50	4.85	-	6.34	2.44	7.36	3.49	2.05
St1-6-1	0.6°	6.40	3.87	3.74	2.50	4.78	7.64	0.00	2.46	3.00	3.51	2.05
St1-6-2		6.39	3.88	3.74	2.50	4.85	0.00	4.82	2.43	3.10	3.49	2.06
St1-7-1	0.7°	6.39	3.88	3.74	2.50	4.84	-	-	2.44	-	3.49	2.06
St2-1-1	0.1°	6.38	3.91	3.71	2.55	4.65	2.11	0.00	2.57	0.00	3.62	2.02
St2-1-2		6.37	3.91	3.71	2.55	4.67	2.12	8.65	2.46	9.41	3.55	2.02
St2-1-3		6.37	4.00	3.71	2.68	4.44	2.90	6.19	2.38	7.21	3.59	2.09
St2-1-4		6.38	4.00	3.71	2.69	5.12	3.07	4.77	2.27	5.04	3.51	2.09
St2-1-5		6.37	3.99	3.71	2.68	5.20	3.14	4.61	2.23	5.92	3.49	2.09
St2-1-6		6.36	3.99	3.70	2.68	5.48	3.36	4.52	2.18	5.84	3.46	2.08
St2-2-1	0.2°	6.41	4.00	3.75	2.68	4.85	3.02	-	2.29	-	3.53	2.12
St2-2-2		6.40	3.91	3.75	2.54	4.63	3.09	8.69	3.88	9.40	4.63	2.06
St2-2-3		6.40	3.99	3.74	2.68	5.12	3.46	4.80	2.17	6.08	3.45	2.12
St2-2-4		6.38	3.99	3.73	2.68	5.28	3.80	5.77	2.15	6.87	3.43	2.10
St2-2-5		6.39	4.00	3.73	2.69	5.51	4.76	5.45	2.92	6.61	3.96	2.11
St2-2-6		6.39	4.00	3.73	2.69	5.84	2.68	5.21	2.82	6.41	3.89	2.11
St2-2-7		6.38	3.99	3.72	2.68	6.58	3.25	5.04	2.76	6.26	3.85	2.10
St2-2-8		6.40	4.00	3.72	2.69	7.80	8.50	4.92	2.71	6.17	3.82	2.10
St2-2-9		6.40	4.00	3.72	2.69	8.49	-	4.90	2.70	6.16	3.80	2.10
St2-3-1	0.5°	6.41	4.00	3.75	2.68	4.82	3.31	-	2.20	-	3.47	4.12
St2-3-2		6.38	3.99	3.73	2.68	4.83	2.18	8.03	3.41	8.86	3.34	4.10
St2-3-3		6.40	3.99	3.74	2.68	4.85	3.51	6.19	2.17	7.24	3.45	4.12
St2-3-4		6.40	3.99	3.74	2.68	4.97	3.74	5.09	2.15	6.32	3.43	4.12
St2-3-5		6.40	3.99	3.74	2.68	5.12	4.35	6.26	2.13	7.29	3.42	4.12
St2-3-6		6.39	4.00	3.73	2.68	5.29	3.08	5.77	2.10	5.87	3.41	4.11
St2-3-7		6.37	4.00	3.70	2.69	5.29	3.33	5.65	2.72	5.76	3.82	4.08
St2-3-8		6.39	4.00	3.73	2.68	5.29	-	5.65	2.09	5.77	3.40	4.11
St2-4-1	1.0°	6.39	4.00	3.74	2.68	4.62	2.19	-	2.19	-	3.46	2.12
St2-4-2		6.39	3.99	3.74	2.68	4.63	2.51	8.66	2.29	9.44	3.52	2.12
St2-4-3		6.40	3.99	3.74	2.68	4.88	3.62	6.19	2.16	7.24	3.44	2.12
St2-4-4		6.40	4.00	3.75	2.68	4.94	3.96	5.14	2.14	6.36	3.43	2.12
St2-4-5		6.40	3.99	3.74	2.67	5.10	5.13	6.21	2.12	7.25	3.41	2.12

Table C.1 (continued)

Test Number	θ	J_{G1} %	J_{L1} %	W_{G1} %	W_{L1} %	W_{G2} %	W_{L2} %	W_{G3} %	W_{L3} %	F_{G3} %	F_{L3} %	x_1 %
St2-4-6	1.0°	6.40	4.00	3.75	2.68	5.11	4.14	4.72	2.14	6.03	3.43	2.12
St2-4-7		6.40	3.99	3.74	2.67	5.19	-	5.84	2.09	6.94	3.39	2.12
St2-5-1	2.5°	6.40	4.00	3.75	2.68	4.61	2.66	-	2.17	-	3.45	2.12
St2-5-2		6.39	3.99	3.74	2.68	4.62	2.92	8.67	2.11	9.45	3.41	2.12
St2-5-3		6.39	4.00	3.74	2.68	4.87	3.96	5.96	3.06	7.04	3.07	2.12
St2-5-4		6.41	4.00	3.75	2.69	4.95	5.22	5.10	2.12	5.33	3.42	2.12
St2-5-5		6.41	4.00	3.75	2.69	4.98	-	5.03	2.10	5.27	3.41	2.12
St2-4-6		6.40	4.00	3.75	2.68	5.11	4.14	4.72	2.14	5.03	3.43	2.12
St2-4-7		6.40	3.99	3.74	2.67	5.19	-	5.84	2.09	5.94	3.39	2.12
St2-5-1	5.0°	6.40	3.99	3.74	2.68	4.79	4.35	-	2.96	-	3.99	2.11
St2-5-2		6.41	4.00	3.75	2.69	4.62	4.43	8.68	1.89	9.40	3.28	2.12
St2-5-3		6.40	4.00	3.74	2.68	4.84	5.92	6.61	2.84	7.59	3.91	2.12
St2-5-4		6.41	4.00	3.75	2.69	4.66	-	7.20	1.71	8.12	3.18	2.12
St2-7-1	6.5°	6.39	3.99	3.74	2.68	4.59	5.36	0.00	1.82	0.00	3.24	2.11
St2-7-2		6.39	3.99	3.74	2.68	4.59	0.00	16.6	1.70	17.04	3.18	2.11
St2-8-1	7.5°	6.39	3.99	3.74	2.68	4.61	0.00	0.00	1.70	0.00	3.17	2.11
W1-1-1	0.0°	5.84	3.87	2.68	2.49	4.26	3.37	-	-	-	-	1.09
W1-1-2		5.85	3.88	2.68	2.50	4.29	3.38	4.20	-	4.98	-	1.09
W1-1-3		5.87	3.27	2.74	1.38	4.23	3.39	4.01	6.33	4.86	6.48	0.91
W1-1-4		5.87	3.27	2.74	1.38	4.23	3.43	3.91	4.11	4.77	4.34	0.91
W1-1-5		5.87	3.26	2.74	1.37	4.36	3.38	3.85	3.71	4.73	3.96	0.91
W1-1-6		5.88	3.27	2.75	1.38	4.54	3.55	3.79	3.33	4.69	3.61	0.92
W1-1-7		5.86	3.26	2.75	1.37	4.83	3.74	3.79	3.22	4.68	3.51	0.92
W1-2-1	5.0°	5.88	3.27	2.75	1.38	4.71	3.38	-/0!	-	-	-	0.92
W1-2-2		5.87	3.27	2.74	1.38	4.15	3.38	4.95	-	5.66	-	0.91
W1-2-3		5.87	3.26	2.73	1.37	4.21	3.41	4.54	2.25	5.30	2.63	0.90
W1-2-4		5.85	3.26	2.74	1.37	4.39	3.50	4.36	2.82	5.15	3.14	0.91
W1-2-5		5.88	3.27	2.75	1.38	4.55	3.72	5.43	1.91	6.08	2.36	0.92
W1-2-6		5.87	3.26	2.74	1.37	4.76	4.08	5.10	1.66	5.79	2.16	0.91
W1-2-7		5.87	3.26	2.74	1.37	5.93	5.40	4.91	1.51	5.62	2.04	0.91
W1-2-8		5.88	3.27	2.75	1.38	6.26	10.13	4.83	1.45	5.56	2.00	0.92
W1-2-9		5.88	3.27	2.75	1.38	6.35	-	4.80	1.44	5.53	1.99	0.92
W1-3-1	15°	5.87	3.27	2.75	1.38	4.73	3.38	10.03	-	9.40	-	0.91

Table C1 (continued)

Test Number	θ	J_{G1} %	J_{L1} %	W_{G1} %	W_{L1} %	W_{G2} %	W_{L2} %	W_{G3} %	W_{L3} %	F_{G3} %	F_{L3} %	x_1 %
W1-3-2	15°	5.86	3.26	2.74	1.37	4.77	3.39	5.43	8.50	6.08	8.6	0.91
W1-3-3		5.86	3.26	2.74	1.37	4.88	3.47	4.56	2.97	5.32	3.27	0.93
W1-3-4		5.86	3.26	2.75	1.37	5.00	3.71	4.37	1.91	5.16	2.35	0.91
W1-3-5		5.86	3.26	2.74	1.37	5.22	4.58	4.27	1.56	5.07	2.08	0.90
W1-3-6		5.85	3.26	2.74	1.37	3.80	7.00	4.22	1.44	5.03	1.99	0.92
W1-3-7		5.86	3.27	2.74	1.37	3.80	-	4.21	1.44	5.03	1.99	0.92
W1-3-8												
W1-4-1	30°	5.87	3.27	2.75	1.38	4.67	3.50	//	5.26	//	5.44	0.91
W1-4-2		5.86	3.26	2.74	1.37	4.71	3.54	4.84	4.20	5.57	3.42	0.91
W1-4-3		5.86	3.26	2.74	1.37	4.76	3.60	4.46	3.50	5.24	3.76	0.92
W1-4-4		6.36	3.80	3.69	2.37	4.86	3.85	4.77	2.87	6.03	3.72	1.30
W1-4-5		6.38	3.80	3.70	2.38	5.02	5.08	4.56	2.56	5.87	3.49	1.31
W1-4-6		6.37	3.80	3.70	2.37	5.22	8.35	4.43	2.46	5.77	3.42	1.30
W1-4-7		6.37	3.80	3.69	2.38	5.41	5.33	4.39	2.12	5.74	3.19	1.30
W1-4-8		6.37	3.80	3.69	2.38	5.41	-	4.38	2.12	5.73	3.18	1.30
W1-5-1	45°	5.88	3.27	2.75	1.38	4.69	3.75	//	3.12	//	3.41	0.91
W1-5-2		5.88	3.26	2.75	1.37	4.71	3.79	5.83	2.93	6.44	3.24	1.01
W1-5-3		5.87	3.26	2.75	1.37	4.15	4.25	5.69	2.66	6.32	2.16	0.91
W1-5-4		5.87	3.26	2.74	1.37	4.23	7.12	4.70	2.50	5.44	3.03	0.91
W1-5-5		5.87	3.26	2.74	1.37	4.18	7.60	6.83	2.45	7.36	3.00	0.91
W1-5-6		5.88	3.27	2.75	1.38	5.12	10.50	4.23	2.46	5.04	2.82	0.91
W1-5-7		5.87	3.27	2.76	1.38	5.30	-	6.12	3.12	5.71	3.41	0.92
W1-6-1	75°	5.88	3.80	2.75	2.38	4.11	4.25	-	2.48	-	3.44	1.08
W1-6-2		5.87	3.80	2.74	2.37	4.13	5.50	4.71	2.45	5.45	3.41	1.07
W1-6-3		5.86	3.80	2.74	2.37	4.15	8.00	4.34	2.45	5.14	3.41	1.07
W1-6-4		5.87	3.80	2.74	2.37	4.16	13.00	4.28	2.43	5.08	3.40	1.07
W1-6-5		5.87	3.80	2.75	2.38	4.16	-	4.27	2.44	5.08	3.40	1.08
W1-7-1	87.5°	5.88	3.80	2.75	2.38	4.11	-	-	2.44	-	3.40	1.08
W2-1-1	0.0°	5.87	3.42	2.74	1.70	4.11	2.74	-	3.30	-	3.71	2.02
W2-1-2		5.87	3.42	2.74	1.70	4.14	2.80	5.37	2.77	6.03	3.25	2.02
W2-1-3		5.87	3.42	2.74	1.70	4.17	2.83	5.99	2.65	6.58	3.14	2.02
W2-1-4		5.86	3.41	2.73	1.69	4.20	2.96	5.24	2.39	5.91	2.93	2.01
W2-1-5		5.86	3.42	2.73	1.70	4.21	3.00	5.12	2.35	5.80	2.90	2.02
W2-1-6		5.86	3.41	2.73	1.69	4.26	3.06	5.03	2.31	5.73	2.84	2.01
W2-1-7		5.86	3.41	2.73	1.69	5.23	3.20	6.71	3.71	7.24	3.08	2.01

Table C.1 (continued)

Test Number	θ	J_{G1} %	J_{L1} %	W_{G1} %	W_{L1} %	W_{G2} %	W_{L2} %	W_{G3} %	W_{L3} %	F_{G3} %	F_{L3} %	x_1 %
W2-1-8	0.0°	5.87	3.42	2.74	1.70	5.55	3.40	6.25	3.40	5.82	3.80	2.02
W2-2-1	5.0°	5.87	3.42	2.75	1.71	4.08	2.91	-	5.16	-	5.43	2.02
W2-2-2		5.87	3.42	2.75	1.71	4.12	2.92	7.43	4.89	7.92	5.18	2.02
W2-2-3		5.86	3.42	2.74	1.70	4.13	2.94	5.99	4.66	6.59	4.96	2.02
W2-2-4		5.86	3.41	2.73	1.69	4.24	3.09	5.25	4.00	5.92	3.34	2.01
W2-2-5		5.88	3.42	2.76	1.70	4.21	3.17	5.02	2.27	5.73	2.84	2.03
W2-2-6		5.88	3.41	2.76	1.69	5.18	3.31	6.71	3.50	7.25	3.88	2.04
W2-2-7		5.87	3.42	2.76	1.71	5.55	3.55	6.25	3.26	6.83	3.68	2.04
W2-2-8		5.86	3.41	2.73	1.69	5.97	2.92	5.15	3.06	5.83	3.50	2.01
W2-1-8		5.87	3.42	2.74	1.70	5.55	3.40	6.25	3.40	5.82	3.80	2.02
W2-2-9		5.86	3.41	2.73	1.69	6.67	3.82	4.99	2.92	5.69	3.38	2.01
W2-2-10		5.72	3.42	2.40	1.70	4.61	3.16	4.74	2.09	5.31	2.70	1.84
W2-2-11	5.72	3.42	2.41	1.71	4.70	-	4.74	2.09	5.32	2.70	1.84	
W2-3-1	15°	6.36	4.01	3.79	2.71	4.10	3.26	-	3.58	-	4.49	2.86
W2-3-2		6.36	4.01	3.79	2.70	4.12	3.02	6.47	4.18	7.44	4.98	2.85
W2-3-3		6.35	4.01	3.78	2.70	4.08	3.06	5.48	4.00	6.60	4.82	2.84
W2-3-4		5.86	3.41	2.74	1.69	4.16	3.11	5.99	3.84	6.58	3.20	2.01
W2-3-5		5.88	3.41	2.76	1.69	4.23	3.26	5.23	3.60	5.92	3.97	2.04
W2-3-6		5.88	3.42	2.76	1.70	4.20	3.45	5.03	2.21	5.74	2.79	2.03
W2-3-7		5.87	3.41	2.76	1.69	5.20	3.71	6.72	3.20	7.27	3.62	2.04
W2-3-8		5.85	3.41	2.73	1.69	5.50	4.18	5.47	3.04	6.11	3.48	2.02
W2-3-9		5.85	3.41	2.73	1.69	5.96	5.00	5.15	2.92	5.83	3.38	2.02
W2-3-10		5.86	3.41	2.74	1.69	6.82	3.08	4.99	2.76	5.69	3.24	2.02
W2-3-11		5.71	3.42	2.41	1.70	4.49	0.00	4.76	2.09	5.34	2.70	1.85
W2-4-1	30°	6.37	4.01	3.81	2.71	4.07	3.26	-	3.60	-	4.50	2.88
W2-4-2		6.37	4.01	3.70	2.70	4.08	3.37	5.48	3.41	6.61	4.35	2.87
W2-4-3		5.86	3.41	2.73	1.69	4.12	3.54	6.00	3.26	6.59	3.67	2.01
W2-4-4		5.86	3.41	2.73	1.69	4.15	3.84	5.26	3.11	5.92	3.54	2.01
W2-4-5		5.86	3.42	2.73	1.70	4.18	4.55	5.02	2.96	5.72	3.41	2.01
W2-4-6		5.87	3.41	2.76	1.69	5.20	5.00	6.72	2.90	7.27	3.36	2.04
W2-4-7		5.85	3.41	2.73	1.69	5.49	6.61	5.45	2.82	6.10	3.29	2.01
W2-4-8		5.86	3.41	2.73	1.69	5.89	4.82	5.22	2.71	5.89	3.20	2.01
W2-4-9		5.86	3.42	2.74	1.70	4.35	-	5.16	2.70	5.84	3.19	2.02
W2-5-1	45°	5.86	4.01	2.74	2.70	4.12	2.71	-	3.18	-	4.17	2.41
W2-5-2		5.86	4.00	2.74	2.69	4.17	3.40	5.22	2.97	5.90	4.02	2.41
W2-5-3		5.87	3.41	2.75	1.68	4.15	2.57	5.26	2.85	5.94	3.31	2.04

Table C.1 (continued)

Test Number	θ	J_{G1} %	J_{L1} %	W_{G1} %	W_{L1} %	W_{G2} %	W_{L2} %	W_{G3} %	W_{L3} %	F_{G3} %	F_{L3} %	x_1 %
W2-5-4	45°	5.86	3.42	2.73	1.70	4.18	2.62	7.46	2.84	7.95	3.31	2.01
W2-5-5		5.88	3.42	2.77	1.70	5.21	2.80	5.90	2.79	6.52	3.26	2.05
W2-5-6		5.85	3.41	2.74	1.68	5.53	4.50	5.44	2.72	5.09	3.20	2.03
W2-5-7		5.87	3.42	2.74	1.70	5.75	3.95	5.29	2.71	5.95	3.19	2.02
W2-5-8		5.87	3.42	2.74	1.70	5.83	-	5.26	2.70	5.93	3.18	2.02
W2-6-1	90°	5.86	4.01	2.73	2.71	4.66	1.34	-	2.95	-	4.00	2.40
W2-6-2		5.86	4.01	2.73	2.71	4.69	1.72	5.48	2.82	6.13	3.91	2.40
W2-6-3		5.86	4.00	2.73	2.69	4.17	3.17	5.22	2.77	5.89	3.87	2.40
W2-6-4		5.87	3.41	2.76	1.68	4.85	3.87	5.26	2.75	5.94	3.22	2.04
W2-6-5		5.86	3.42	2.73	1.70	5.03	3.87	6.58	2.73	7.13	3.22	2.01
W2-6-6		5.88	3.41	2.76	1.69	5.24	3.00	5.89	2.71	6.51	3.20	2.05
W2-6-7		5.86	3.41	2.72	1.68	5.53	5.00	5.44	2.70	5.09	3.18	2.02
W2-6-8		5.86	3.41	2.72	1.68	5.61	8.00	5.37	2.69	5.02	3.17	2.02
An1-1-1	0.0°	6.04	4.81	3.10	3.79	3.86	4.82	-	-	-	-	0.46
An1-1-2		6.06	5.15	3.10	3.11	3.99	4.85	4.56	-	5.52	-	0.49
An1-1-3		6.05	5.14	3.10	3.10	4.10	5.33	4.28	4.88	5.28	5.72	0.49
An1-1-4		6.03	5.14	3.09	3.10	4.24	2.62	4.84	2.50	5.74	4.89	0.49
An1-1-5		6.32	5.16	3.21	3.13	4.47	2.77	4.54	2.10	5.56	4.72	0.50
An1-1-6		6.32	5.16	3.21	3.13	4.80	2.81	4.40	1.98	5.45	3.67	0.50
An1-1-7		6.04	5.16	3.10	4.13	3.56	2.87	4.28	1.87	5.28	3.63	0.49
An1-2-1	5.0°	6.05	4.84	3.10	3.82	3.86	4.86	-	-	-	-	0.46
An1-2-2		6.05	4.84	3.10	3.82	3.88	4.89	6.28	-	7.00	-	0.46
An1-2-3		6.04	4.83	3.10	3.82	3.90	5.00	4.55	4.66	5.50	6.03	0.46
An1-2-4		6.03	5.14	3.08	4.10	4.05	5.42	4.25	4.50	5.25	6.16	0.49
An1-2-5		6.03	5.14	3.09	4.10	4.24	2.63	4.83	2.38	5.74	4.83	0.49
An1-2-6		6.04	5.16	3.10	4.13	4.54	2.75	4.51	2.07	5.48	4.71	0.49
An1-2-7		6.02	5.16	3.08	4.13	3.54	2.83	4.37	1.91	5.35	4.64	0.49
An1-2-8		6.00	5.16	3.03	4.13	3.57	2.91	4.28	1.81	5.25	4.60	0.48
An1-2-9		6.00	5.12	3.03	4.10	3.82	3.04	5.01	1.75	5.85	4.53	0.48
An1-2-10		6.00	5.12	3.03	4.10	3.82	3.04	5.01	1.73	5.81	4.52	0.48
An1-2-11		6.05	5.12	3.11	4.10	4.27	3.59	4.53	1.59	5.50	3.47	0.50
An1-2-12		6.00	5.12	3.04	4.10	3.89	4.50	4.39	1.45	5.35	3.43	0.49
An1-2-13		6.01	5.13	3.05	4.10	3.90	7.00	4.35	1.45	5.31	3.43	0.49
An1-2-14		6.02	5.12	3.08	4.10	0.00	0.00	4.29	1.43	5.29	3.42	0.50
An1-3-1	30°	6.05	5.63	3.10	3.79	3.88	4.93	-	2.75	-	11.3	0.55
An1-3-2		6.05	5.63	3.10	3.79	3.99	5.53	4.28	4.34	5.29	6.47	0.55

Table C.1 (continued)

Test Number	θ	J_{G1} %	J_{L1} %	W_{G1} %	W_{L1} %	W_{G2} %	W_{L2} %	W_{G3} %	W_{L3} %	F_{G3} %	F_{L3} %	x_1 %	
An1-3-3	30°	6.05	5.13	3.10	3.18	4.27	2.68	4.84	2.25	5.75	4.75	0.50	
An1-3-4		6.05	4.79	3.10	3.76	4.51	2.80	4.55	1.96	5.50	4.24	0.47	
An1-3-5		6.04	5.13	3.10	3.18	4.87	2.89	4.38	1.85	5.36	4.58	0.51	
An1-3-6		6.04	5.15	3.09	3.21	3.61	2.99	4.29	1.78	5.29	3.57	0.50	
An1-3-7		6.05	5.15	3.10	3.21	3.82	3.14	5.01	1.72	5.89	3.55	0.50	
An1-3-8		6.04	5.15	3.09	3.21	3.94	3.44	4.73	1.64	5.65	3.52	0.50	
An1-3-9		6.04	5.13	3.08	3.18	4.30	3.88	4.54	2.58	5.49	3.91	0.50	
An1-3-10		6.05	5.15	3.09	3.21	3.92	6.33	4.41	1.45	5.39	3.45	0.50	
An1-3-11		6.05	5.15	3.09	3.21	3.93	-	4.40	1.44	5.38	3.45	0.50	
An1-4-1		90°	6.03	5.66	3.08	3.82	3.85	5.11	-	6.16	-	7.82	0.54
An1-4-2			6.03	5.63	3.07	3.79	3.98	5.84	5.83	3.56	6.59	5.97	0.54
An1-4-3	6.04		5.13	3.08	3.18	4.26	2.82	4.84	1.94	5.74	4.61	0.50	
An1-4-4	6.04		4.81	3.08	3.79	4.50	2.90	4.54	1.84	5.48	4.21	0.47	
An1-4-5	6.04		5.13	3.09	3.18	3.54	3.06	4.38	1.74	5.36	3.53	0.50	
An1-4-6	6.04		5.17	3.09	3.24	3.58	3.21	4.28	1.68	5.28	3.56	0.49	
An1-4-7	6.04		5.15	3.08	3.21	3.85	3.32	4.90	1.65	5.79	3.52	0.50	
An1-4-8	6.04		5.15	3.08	3.21	3.96	3.67	4.73	1.59	5.64	3.50	0.50	
An1-4-9	6.04		5.17	3.09	3.24	4.23	4.21	4.54	2.54	5.49	3.94	0.50	
An1-4-10	6.02		5.15	3.08	3.21	3.85	8.00	4.44	1.44	5.40	3.45	0.50	
An1-4-11	6.02		5.13	3.08	3.18	3.87	-	4.42	1.44	5.38	3.42	0.50	
An2-1-1	0.0°	6.07	4.01	3.12	2.71	3.86	2.72	0.00	5.00	0.00	5.69	1.22	
An2-1-2		6.04	4.00	3.08	2.69	3.90	2.84	4.56	3.63	5.50	4.51	1.22	
An2-1-3		6.04	3.91	3.09	2.55	4.02	2.96	4.26	3.67	5.26	4.47	1.19	
An2-1-4		6.04	3.92	3.10	2.56	4.23	2.17	4.84	2.92	5.75	3.88	1.18	
An2-1-5		6.32	3.91	3.20	2.55	4.48	3.17	4.53	2.75	5.55	3.75	1.21	
An2-1-6		6.04	4.01	3.10	2.70	4.80	3.26	4.36	2.60	5.35	3.75	1.22	
An2-1-7		6.05	4.01	3.10	2.70	3.73	3.40	4.29	2.39	5.29	3.60	1.22	
An2-2-1	5.0°	6.04	4.01	3.08	2.70	3.87	2.80	-	3.25	0.00	4.22	1.22	
An2-2-2		6.02	3.91	3.08	2.55	4.03	2.98	5.83	3.53	6.60	4.35	1.19	
An2-2-3		6.04	3.92	3.10	2.56	4.22	3.08	4.84	2.97	5.75	3.92	1.19	
An2-2-4		6.03	3.91	3.08	2.55	3.33	3.19	4.53	2.69	5.48	3.71	1.19	
An2-2-5		6.03	4.01	3.08	2.70	3.48	3.30	4.37	2.52	5.35	3.69	1.22	
An2-2-6		6.04	4.01	3.12	2.70	3.66	2.28	4.28	2.36	5.30	3.59	1.24	
An2-2-7		6.03	4.01	3.08	2.70	3.77	2.56	5.80	2.25	6.57	3.51	1.22	
An2-2-8		6.03	4.01	3.08	2.70	3.92	3.71	4.71	2.16	5.63	3.45	1.22	
An2-2-9		6.02	4.01	3.05	2.70	4.27	4.05	4.53	2.06	5.47	3.39	1.21	
An2-2-10		6.02	3.91	3.10	2.55	5.17	4.96	4.39	1.92	5.38	3.19	1.20	

Table C.1 (continued)

Test Number	θ	J_{G1} %	J_{L1} %	W_{G1} %	W_{L1} %	W_{G2} %	W_{L2} %	W_{G3} %	W_{L3} %	F_{G3} %	F_{L3} %	x_1 %
An2-2-11	5.0°	6.02	4.01	3.08	2.70	4.23	6.33	4.35	1.71	5.33	3.19	1.21
An2-2-12		6.02	4.01	3.08	2.70	4.55	-	4.33	1.70	5.31	3.19	1.21
An2-3-1	30°	6.02	4.01	3.07	2.70	5.28	2.80	-	2.69	-	3.81	1.21
An2-3-2		6.02	4.01	3.07	2.70	3.91	2.91	4.64	3.79	5.56	4.65	1.21
An2-3-3		6.02	3.91	3.08	2.55	4.03	3.00	5.83	3.26	6.59	4.14	1.19
An2-3-4		6.03	3.92	3.08	2.56	4.26	3.09	4.84	2.90	5.74	3.87	1.18
An2-3-5		6.03	3.91	3.09	2.55	3.42	3.22	4.53	2.56	5.48	3.61	1.19
An2-3-6		6.04	4.01	3.08	2.70	3.49	2.30	4.37	2.50	5.35	3.68	1.22
An2-3-7		6.04	4.01	3.08	2.70	3.66	2.45	4.27	2.28	5.26	3.53	1.21
An2-3-8		6.03	4.01	3.09	2.70	3.80	2.60	4.91	2.22	5.80	3.49	1.22
An2-3-9		6.03	4.01	3.09	2.70	3.95	2.79	4.75	2.11	5.66	3.42	1.22
An2-3-10		6.05	4.00	3.09	2.69	4.24	3.09	4.55	2.04	5.50	3.37	1.23
An2-3-11		6.05	4.00	3.09	2.69	4.24	3.53	4.44	1.95	5.41	3.32	1.23
An2-3-12		6.03	3.91	3.08	2.55	5.16	7.58	4.39	1.79	5.36	3.12	1.19
An2-3-13		6.02	4.01	3.08	2.70	3.99	4.43	5.15	1.71	5.00	3.19	1.22
An2-3-14		6.02	4.01	3.08	2.70	4.07	-	4.35	1.71	5.33	3.19	1.22
An2-4-1	45°	6.02	4.01	3.07	2.70	3.89	1.86	-	2.57	-	3.72	1.21
An2-4-2		6.02	3.91	3.07	2.55	4.04	3.03	5.84	3.18	6.60	4.08	1.18
An2-4-3		6.04	3.92	3.08	2.56	4.24	2.14	4.85	2.82	5.74	3.81	1.18
An2-4-4		6.02	3.91	3.08	2.55	3.43	2.26	4.53	2.53	5.48	3.59	1.19
An2-4-5		6.04	4.01	3.08	2.70	4.78	2.26	4.37	2.46	5.35	3.65	1.22
An2-4-6		6.02	4.01	3.07	2.70	3.67	2.48	4.28	2.30	5.27	3.55	1.21
An2-4-7		6.04	4.01	3.08	2.70	3.77	2.69	4.93	2.17	5.82	3.46	1.22
An2-4-8		6.02	4.01	3.08	2.70	3.92	2.89	4.71	2.08	5.63	3.41	1.22
An2-4-9		6.06	4.00	3.09	2.69	4.24	3.29	4.52	2.74	5.47	3.84	1.23
An2-4-10		6.03	3.91	3.07	2.55	4.51	4.61	4.45	1.96	5.40	3.22	1.18
An2-4-11		6.03	4.01	3.08	2.70	3.93	4.43	4.37	1.72	5.35	3.20	1.22
An2-4-12		6.03	4.01	3.08	2.70	4.00	-	4.36	1.71	5.34	3.19	1.22
An2-5-1	90°	6.03	4.01	3.07	2.70	3.86	1.92	-	2.46	-	3.65	1.21
An2-5-2		6.03	4.01	3.08	2.70	3.91	1.98	0.95	2.38	3.22	3.59	1.21
An2-5-3		6.03	3.91	3.08	2.55	4.05	3.09	5.90	2.95	6.65	3.90	1.19
An2-5-4		6.05	3.91	3.10	2.55	4.24	2.23	4.85	2.63	5.75	3.67	1.20
An2-5-5		6.02	3.91	3.08	2.55	3.43	2.32	4.53	2.45	5.48	3.54	1.19
An2-5-6		6.04	4.01	3.08	2.70	4.78	2.45	4.37	2.32	5.35	3.56	1.22
An2-5-7		6.04	4.01	3.09	2.70	3.68	2.64	4.28	2.21	5.28	3.49	1.22
An2-5-8		6.04	4.01	3.09	2.70	3.74	2.78	4.91	2.13	5.80	3.44	1.22
An2-5-9		6.03	4.01	3.07	2.70	3.95	3.07	4.73	2.04	5.64	3.38	1.22

Table C.1 (continued)

Test Number	θ	J_{G1} %	J_{L1} %	W_{G1} %	W_{L1} %	W_{G2} %	W_{L2} %	W_{G3} %	W_{L3} %	F_{G3} %	F_{L3} %	x_1 %
An2-5-10		6.06	4.00	3.09	2.69	4.28	3.45	4.54	1.98	5.49	3.34	1.23
An2-5-11		6.04	3.91	3.09	2.55	4.52	5.38	4.49	1.88	5.44	3.17	1.19
An2-5-12		6.03	4.01	3.09	2.70	3.91	3.91	4.39	1.72	5.36	3.20	1.22
An2-5-13		6.03	4.01	3.09	2.70	4.07	-	4.37	1.71	5.35	3.19	1.22
An3-1-1	0.0°	6.02	3.52	3.07	1.90	3.90	4.12	-	2.82	-	3.40	2.37
An3-1-2		6.02	3.52	3.06	1.90	3.91	4.27	5.21	2.50	6.05	3.14	2.36
An3-1-3		6.03	3.52	3.07	1.91	3.91	4.31	5.22	2.48	6.05	3.13	2.37
An3-1-4		6.01	3.55	3.05	1.95	4.03	4.38	5.90	4.76	6.64	5.15	2.37
An3-1-5		6.01	3.55	3.05	1.95	4.23	4.65	4.83	4.42	5.71	4.83	2.37
An3-1-6		6.03	3.55	3.08	1.95	4.48	4.62	4.53	4.20	5.48	4.64	2.38
An3-1-7		6.02	3.55	3.07	1.95	4.82	4.70	4.37	4.04	5.34	4.49	2.38
An3-1-8		6.01	3.55	3.07	1.95	3.68	4.81	4.28	3.90	5.27	4.36	2.38
An3-2-1	5.0°	6.02	3.52	3.06	1.91	4.68	2.20	-	4.78	-	5.15	2.36
An3-2-2		6.02	3.52	3.06	1.91	4.65	2.31	6.00	4.01	6.73	4.44	2.36
An3-2-3		6.01	3.52	3.05	1.90	4.68	2.35	5.25	3.71	6.08	4.17	2.36
An3-2-4		6.01	3.52	3.05	1.90	4.78	2.41	6.74	3.51	7.40	3.99	2.36
An3-2-5		6.02	3.52	3.05	1.90	4.99	2.49	5.57	3.25	6.35	3.77	2.36
An3-2-6		6.01	3.52	3.05	1.90	5.24	2.58	5.24	3.12	6.07	3.66	2.36
An3-2-7		6.01	3.52	3.05	1.90	5.62	2.70	5.07	2.93	5.92	3.49	2.36
An3-2-8		6.02	3.52	3.09	1.90	6.06	2.86	4.97	2.75	5.85	3.34	2.38
An3-2-9		6.02	3.52	3.06	1.90	6.73	2.93	4.92	2.70	5.79	3.31	2.36
An3-2-10		6.02	3.52	3.06	1.90	4.52	3.14	6.27	2.54	6.98	3.18	2.36
An3-2-11		6.02	3.52	3.06	1.90	4.87	3.35	6.16	2.46	6.88	3.11	2.36
An3-2-12		6.02	3.52	3.05	1.90	4.31	3.55	6.14	2.39	5.86	3.05	2.35
An3-2-13		6.03	3.52	3.07	1.90	4.82	4.11	5.15	3.27	5.99	3.78	2.36
An3-2-14		6.03	3.52	3.07	1.91	4.82	4.64	5.13	3.21	5.98	3.74	2.37
An3-2-15		6.03	3.52	3.07	1.91	-	5.07	5.10	2.92	5.96	3.49	2.37
An3-3-1	30°	6.02	3.52	3.06	1.91	4.64	2.32	-	1.49	-	2.42	2.36
An3-3-2		6.02	3.52	3.06	1.91	4.66	2.37	6.20	1.46	6.91	2.40	2.36
An3-3-3		6.01	3.52	3.05	1.90	4.76	2.45	4.91	3.39	5.79	3.89	2.35
An3-3-4		6.01	3.52	3.04	1.90	4.96	2.57	5.57	3.15	6.35	3.68	2.35
An3-3-5		6.01	3.52	3.06	1.90	5.25	2.66	5.24	3.00	6.07	3.55	2.36
An3-3-6		6.02	3.52	3.07	1.90	5.54	2.79	7.66	2.84	8.25	3.42	2.37
An3-3-7		6.02	3.52	3.05	1.91	6.03	2.99	7.00	2.67	7.64	3.28	2.35
An3-3-8		6.02	3.52	3.06	1.91	6.73	3.12	6.69	2.57	7.35	3.20	2.36
An3-3-9		6.02	3.52	3.06	1.91	7.59	3.39	6.39	2.46	7.09	3.11	2.36
An3-3-10		6.02	3.52	3.05	1.91	4.86	3.69	6.20	2.38	6.91	3.05	2.36

Table C.1 (continued)

Test Number	θ	J_{G1} %	J_{L1} %	W_{G1} %	W_{L1} %	W_{G2} %	W_{L2} %	W_{G3} %	W_{L3} %	F_{G3} %	F_{L3} %	x_1 %
An3-3-11	30°	6.01	3.53	3.05	1.91	5.87	3.83	6.15	2.32	6.86	3.01	2.35
An3-3-12		6.02	3.53	3.04	1.91	4.30	1.09	6.11	2.21	6.82	2.92	2.34
An3-3-13		6.02	3.53	3.04	1.91	4.66	1.28	6.08	1.99	6.80	2.75	2.34
An3-3-14		6.02	3.53	3.04	1.91	4.66	1.46	6.07	1.95	6.79	2.73	2.34
An3-4-1	90°	6.02	3.52	3.04	1.91	4.74	2.64	4.91	3.03	5.77	3.58	2.35
An3-4-2		6.01	3.52	3.04	1.90	4.73	2.63	4.90	3.02	5.77	3.57	2.34
An3-4-3		6.00	3.52	3.03	1.90	4.95	2.75	5.56	2.89	6.33	3.46	2.34
An3-4-4		6.02	3.52	3.05	1.90	5.25	2.86	5.24	2.77	6.06	3.36	2.35
An3-4-5		6.02	3.52	3.05	1.90	5.47	3.01	7.63	2.64	8.22	3.26	2.35
An3-4-6		6.02	3.52	3.05	1.90	6.02	3.15	7.00	2.57	7.64	3.20	2.35
An3-4-7		6.02	3.52	3.05	1.90	6.59	3.25	6.61	2.50	7.28	3.14	2.35
An3-4-8		6.03	3.52	3.06	1.90	4.07	3.64	6.37	2.37	6.07	3.04	2.36
An3-4-9		6.02	3.52	3.05	1.90	4.86	3.82	6.19	2.32	5.90	3.00	2.36
An3-4-10		6.00	3.52	3.03	1.90	4.95	4.25	6.11	2.26	5.83	2.95	2.33
An3-4-11		6.04	3.53	3.08	1.91	5.57	2.18	6.11	2.04	5.84	2.79	2.37
An3-4-12		6.04	3.53	3.08	1.91	6.39	4.71	6.08	1.92	5.81	2.70	2.37
An3-4-13		6.04	3.53	3.08	1.91	6.39	-	6.06	1.92	5.80	2.70	2.37

Table C.2 Uncertainty intervals for full-separation data

Test Number	θ	J_{G1} %	J_{L1} %	J_{G2} %	J_{L3} %	W_{G1} %	W_{L1} %	W_{G2} %	W_{L3} %	x_1 %
2.5-1	2.5°	-	3.60	-	3.60	-	2.04	-	2.04	-
2.5-2		-	3.60	-	3.60	-	2.05	-	2.04	-
2.5-3		9.29	3.61	8.44	3.60	7.71	2.05	7.1	2.05	7.08
2.5-4		7.21	3.62	7.17	3.62	5.00	2.08	5.51	2.07	5.21
2.5-5		6.85	3.63	6.96	3.63	4.48	2.10	5.23	2.09	4.66
2.5-6		6.41	3.69	6.67	3.68	3.75	2.20	4.83	2.17	3.68
2.5-7		6.23	3.88	6.55	3.84	3.44	2.51	4.67	2.44	2.65
2.5-8		6.16	4.22	6.52	4.13	3.32	3.00	4.62	2.87	1.90
2.5-9		6.13	-	6.49	-	3.27	-	4.59	-	-
2.5-10		6.10	-	6.48	-	3.20	-	4.57	-	-
7.5-1	7.5°	-	3.60	-	3.60	-	2.04	-	2.03	-
7.5-2		-	3.60	-	3.60	-	2.04	-	2.04	-
7.5-3		9.29	3.60	8.44	3.60	7.71	2.04	7.08	2.04	7.00
7.5-4		7.42	3.60	7.28	3.60	5.30	2.05	5.65	2.04	5.57
7.5-5		6.46	3.63	6.70	3.63	3.85	2.10	4.88	2.09	4.04
7.5-6		6.23	3.69	6.55	3.68	3.42	2.20	4.67	2.17	3.27
7.5-7		6.09	3.88	6.48	3.84	3.20	2.51	4.56	2.44	2.28
7.5-8		6.09	3.88	6.48	3.84	3.20	2.51	4.56	2.44	2.28
7.5-9		6.05	4.94	6.44	4.81	3.10	3.95	4.52	3.79	1.10
7.5-10		6.02	-	6.42	-	3.06	-	4.49	-	-
7.5-11		6.02	-	6.42	-	3.06	-	4.49	-	-
15-1	15°	-	3.59	-	3.59	-	2.03	-	2.03	-
15-2		-	3.14	-	4.22	-	1.03	-	3.01	-
15-3		8.92	3.14	7.48	4.22	7.26	1.03	5.90	3.01	7.00
15-4		6.37	3.14	6.50	4.22	3.71	1.03	4.59	3.01	3.78
15-5		5.97	3.14	6.25	4.23	2.96	1.04	4.23	3.01	3.03
15-6		5.66	3.15	6.08	4.23	2.27	1.08	3.97	3.02	2.25
15-7		5.55	3.18	6.00	4.25	2.00	1.15	3.88	3.05	1.75
15-8		5.51	3.27	5.98	4.30	1.88	1.38	3.84	3.12	1.19
15-9		5.85	3.45	6.74	4.39	2.72	1.76	4.94	3.24	1.03
15-10		5.48	-	6.66	-	1.78	-	4.84	-	-
2.5-11		5.82	-	5.95	-	2.64	-	3.80	-	-
30-1	30°	-	3.59	-	3.59	-	2.03	-	2.02	-
30-2		-	3.59	-	3.59	-	2.03	-	2.03	-
30-3		8.26	3.59	8.44	3.59	6.43	2.03	7.08	2.03	6.70
30-4		7.01	3.60	7.17	3.59	4.71	2.03	5.51	2.03	5.05

Table C.2 (continued)

Test Number	θ	J_{G1} %	J_{L1} %	J_{G2} %	J_{L3} %	W_{G1} %	W_{L1} %	W_{G2} %	W_{L3} %	x_1 %
30-5	30°	6.30	3.60	6.61	3.60	3.58	2.05	4.75	2.04	3.92
30-6		6.30	3.60	6.61	3.60	3.58	2.05	4.75	2.04	3.92
30-7		6.01	3.69	6.43	3.68	3.04	2.20	4.50	2.18	2.69
30-8		5.48	3.88	6.40	3.84	1.77	2.50	4.45	2.44	1.42
30-9		5.47	4.22	6.38	4.14	1.71	3.00	4.42	2.89	0.95
30-10		5.92	-	6.37	-	2.86	-	4.41	-	-
30-11		5.92	-	6.36	-	2.84	-	4.40	-	-
60-1	60°	-	3.59	-	3.59	-	2.02	-	2.02	-
60-2		-	3.13	-	4.22	-	1.02	-	3.01	-
60-3		8.92	3.14	7.55	4.22	7.26	1.02	5.99	3.01	7.20
60-4		6.37	3.14	6.50	4.22	3.71	1.02	4.59	3.01	3.80
60-5		5.78	3.14	6.15	4.22	2.57	1.03	4.08	3.01	2.67
60-6		5.63	3.14	6.07	4.23	2.20	1.04	3.95	3.01	2.30
60-7		5.55	3.14	6.01	4.23	2.00	1.05	3.88	3.01	2.05
60-8		5.36	3.15	5.97	4.23	1.37	1.08	3.82	3.02	1.44
60-9		5.77	3.18	5.94	4.25	2.55	1.15	3.77	3.05	1.73
60-10		5.42	3.27	5.92	4.30	1.57	1.38	3.75	3.12	0.70
60-11		5.41	3.45	5.92	4.39	1.55	1.76	3.75	3.24	0.43
60-12		5.40	-	5.92	-	1.53	-	3.74	-	-
60-13		5.40	-	5.91	-	1.50	-	3.74	-	-
75-1	75°	-	3.13	-	4.22	-	1.02	-	3.01	-
75-2		-	3.13	-	4.22	-	1.02	-	3.01	-
75-3		8.92	3.14	7.54	4.22	7.25	1.02	5.99	3.01	7.20
75-4		7.01	3.14	6.99	4.22	4.73	1.02	5.28	3.01	4.77
75-5		5.73	3.14	6.10	4.22	2.44	1.03	4.03	3.01	2.55
75-6		5.59	3.14	6.03	4.23	2.10	1.04	3.91	3.01	2.19
75-7		5.81	3.15	6.26	4.23	2.63	1.07	4.26	3.02	2.28
75-8		5.43	3.18	5.93	4.25	1.62	1.15	3.77	3.05	1.18
75-9		5.41	3.27	5.92	4.30	1.54	1.37	3.74	3.12	0.64
75-10		5.40	3.45	5.92	4.40	1.52	1.76	3.74	3.25	0.40
75-11		5.70	-	5.91	-	2.38	-	3.74	-	-
75-12		6.21	-	6.49	-	3.42	-	4.60	-	-
90-1	90°	-	3.13	-	4.23	-	1.02	-	3.02	-
90-2		-	3.13	-	4.22	-	1.02	-	3.01	-
90-3		8.21	3.13	7.54	4.22	6.37	1.02	5.99	3.01	6.41
90-4		6.40	3.14	6.49	4.22	3.76	1.02	4.59	3.01	3.85
90-5		5.66	3.14	6.06	4.22	2.28	1.03	3.97	3.01	2.39

Table. C2 (continued)

Test Number	θ	J_{G1} %	J_{L1} %	J_{G2} %	J_{L3} %	W_{G1} %	W_{L1} %	W_{G2} %	W_{L3} %	x_1 %
90-6	90°	5.57	3.14	6.01	4.23	2.04	1.04	3.89	3.01	2.13
90-7		5.46	3.15	5.95	4.23	1.71	1.07	3.79	3.02	1.60
90-8		5.42	3.18	5.93	4.25	1.60	1.15	3.76	3.05	1.14
90-9		5.40	3.27	5.92	4.30	1.53	1.37	3.74	3.11	0.61
90-10		5.40	3.45	5.91	4.39	1.51	1.76	3.74	3.23	0.37
90-11		5.39	-	5.91	-	1.49	-	3.73	-	-
90-12		5.39	-	5.91	-	1.48	-	3.73	-	-